Copyright Warning & Restrictions

The copyright law of the United States (Title 17, United States Code) governs the making of photocopies or other reproductions of copyrighted material.

Under certain conditions specified in the law, libraries and archives are authorized to furnish a photocopy or other reproduction. One of these specified conditions is that the photocopy or reproduction is not to be "used for any purpose other than private study, scholarship, or research." If a, user makes a request for, or later uses, a photocopy or reproduction for purposes in excess of "fair use" that user may be liable for copyright infringement,

This institution reserves the right to refuse to accept a copying order if, in its judgment, fulfillment of the order would involve violation of copyright law.

Please Note: The author retains the copyright while the New Jersey Institute of Technology reserves the right to distribute this thesis or dissertation

Printing note: If you do not wish to print this page, then select "Pages from: first page # to: last page #" on the print dialog screen

ABSTRACT

ASSESSING THE EFFECTIVENESS OF MANAGED LANE STRATEGIES FOR THE RAPID DEPLOYMENT OF COOPERATIVE ADAPTIVE CRUISE CONTROL TECHNOLOGY

by
Zijia Zhong

Connected and Automated Vehicle (C/AV) technologies are fast expanding in the transportation and automotive markets. One of the highly researched examples of C/AV technologies is the Cooperative Adaptive Cruise Control (CACC) system, which exploits various vehicular sensors and vehicle-to-vehicle communication to automate vehicular longitudinal control. The operational strategies and network-level impacts of CACC have not been thoroughly discussed, especially in near-term deployment scenarios where Market Penetration Rate (MPR) is relatively low. Therefore, this study aims to assess CACC's impacts with a combination of managed lane strategies to provide insights for CACC deployment. The proposed simulation framework incorporates 1) the Enhanced Intelligent Driver Model; 2) Nakagami-based radio propagation model; and 3) a multi-objective optimization (MOOP)-based CACC control algorithm. The operational impacts of CACC are assessed under four managed lane strategies (i.e., mixed traffic (UML), HOV (High Occupancy Vehicle)-CACC lane (MML), CACC dedicated lane (DL), and CACC dedicated lane with access control (DLA)).

Simulation results show that the introduction of CACC, even with 10% MPR, is able to improve the network throughput by 7% in the absence of any managed

lane strategies. The segment travel times for both CACC and non-CACC vehicles are reduced. The break-even point for implementing dedicated CACC lane is 30% MPR, below which the priority usage of the current HOV lane for CACC traffic is found to be more appropriate. It is also observed that DLA strategy is able to consistently increase the percentage of platooned CACC vehicles as MPR grows. The percentage of CACC vehicles within a platoon reaches 52% and 46% for DL and DLA, respectively. When it comes to the impact of vehicle-to-vehicle (V2V), it is found that DLA strategy provides more consistent transmission density in terms of median and variance when MPR reaches 20% or above. Moreover, the performance of the MOOP-based cooperative driving is examined. With average 75% likelihood of obtaining a feasible solution, the MOOP outperforms its counterpart which aims to minimize the headway objective solely. In UML, MML, and DL strategy, the proposed control algorithm achieves a balance spread among four objectives for each CACC vehicle. In the DLA strategy, however, the probability of obtaining feasible solution falls to 60% due to increasing size of platoon owing to DLA that constraints the feasible region by introduction more dimensions in the search space.

In summary, UML or MML is the preferred managed lane strategy for improving traffic performance when MPR is less than 30%. When MRP reaches 30% or above, DL and DLA could improve the CACC performance by facilitating platoon formation. If available, priority access to an existing HOV lane can be adopted to encourage adaptation of CACC when CACC technology becomes publically available.

ASSESSING THE EFFECTIVENESS OF MANAGED LANE STRATEGIES FOR THE RAPID DEPLOYMENT OF COOPERATIVE ADAPTIVE CRUISE CONTROL TECHNOLOGY

By
Zijia Zhong

A Dissertation
Submitted to the Faculty of
New Jersey Institute of Technology
in Partial Fulfillment of the Requirements for the Degree of
Doctor of Philosophy in Transportation

John A. Reif, Jr. Department of Civil and Environmental Engineering

May 2018

APPROVAL PAGE

ASSESSING THE EFFECTIVENESS OF MANAGED LANE STRATEGIES FOR THE RAPID DEPLOYMENT OF COOPERATIVE ADAPTIVE CRUISE CONTROL TECHNOLOGY

Zijia Zhong

Dr. Joyoung Lee, Dissertation Advisor — Date
Assistant Professor of Civil and Environmental Engineering, NJIT

Dr. Steven I-Jy Chien, Committee Member — Date
Professor of Civil and Environmental Engineering, NJIT

Dr. Lazar Spasovic, Committee Member — Date
Professor of Civil and Environmental Engineering, NJIT

Dr. Guiling Wang, Committee Member — Date
Professor of Computer Science, NJIT

Dr. Parth Bhavsar, Committee Member — Date
Assistant Professor of Civil and Environmental Engineering, Rowan University

BIOGRAPHICAL SKETCH

Author: Zijia Zhong

Degree: Doctor of Philosophy

Date: May 2018

Undergraduate and Graduate Education:

- Doctor of Philosophy in Transportation,
  New Jersey Institute of Technology, Newark, NJ, 2018

- Master of Science in Civil Engineering,
  New Jersey Institute of Technology, Newark, NJ, 2011

- Bachelor of Engineering in Environmental Engineering,
  Jinan University, Guangzhou, P. R. China, 2009

Major: Transportation

Publications:

Z. Zhong, L. Joyoung, and L. Zhao, “Multiobjective Optimization Framework for Cooperative Adaptive Cruise Control Vehicles in the Automated Vehicle Platooning Environment,” *Transp. Res. Rec. J. Transp. Res. Board*, vol. 2625, pp. 32–42, 2017.

J. Lee, Z. Zhong, J. Singh, B. Dimitrijevic, S. Chien, L. Spasovic, “Real-time performance measure monitoring system for long-term freeway work zone,” in *Intell. Transp. Syst. World Congress 2017*, Montreal, Canada

J. Lee, S. Gutesa, Z. Zhong, B. Dimitrijevic, L. Spasovic, J. Singh, “Evaluation of freeway merging assistance system using driving simulator,” in *Intell. Transp. Syst. World Congress 2017*, Montreal, Canada

Z. Zhong, L. Joyoung, and L. Zhao, “Evaluations of managed lane strategies for arterial deployment of cooperative adaptive cruise control,” in *96th Transp. Res. Board Annu. Meeting*, Washington, DC, USA, 2017.

J. Lee, Z. Zhong, B. Du, S. Gutesa, and K. Kim, “Low-cost and energy-saving wireless sensor network for real-time urban mobility monitoring system,” *J. Sensors*, vol. 2015, pp. 1–8, 2015.

Z. Zhong and J. Lee, “Development of CID-free hardware-in-the-loop simulation framework,” in *96th Transp. Res. Board Annu. Meeting*, Washington, DC, USA, 2017.

J. Lee *et al.*, “WIMAP: work zone interactive monitoring application,” in *94th Transp. Res. Board Annu. Meeting*, Washington, DC, USA, 2015, no. 15–4257.

J. Lee, Z. Zhong, K. Kim, B. Dimitrijevic, B. Du, and S. Gutesa, “Examining the applicability of small quadcopter drone for traffic surveillance and roadway incident monitoring,” in *94th Transp. Res. Board Annu. Meeting*, Washington, DC, USA, 2015, no. 15–4184.

Z. Zhong, and J. Lee, “Estimation of real-time origin-destination flow using mobile sensor network," in *21st Intell. Transp. Syst. World Congress*, Detroit, MI, USA, 2014

Awards:

2017 Outstanding Graduate Student, Intelligent Transportation Society NJ Chapter

2015 The Future of ITS Award, Intelligent Transportation Society NJ Chapter

This dissertation is dedicated to my family:

Father, Fazhi Zhong

Mother, Yanmei Lai

Wife, Liuhui Zhao

for all their love and support

僅以此文獻給我的親人

父親，鍾發枝

母親，賴燕媚

妻子，趙劉慧

ACKNOWLEDGMENT

First and foremost, I would like to express my sincere gratitude to my dissertation advisor, Dr. Joyoung Lee, without whom this dissertation would not be possible. I am genuinely impressed by his dedication to research and his patience in guiding me through my doctoral study for the past five years. I am privileged to become his first Ph.D. student and to call him a friend.

I would also like to express my appreciation to Dr. Steven I-Jy Chien, Dr. Lazar Spasovic, Dr. Guiling Wang, and Dr. Parth Bhavsar for accepting to serve on my committee and for their invaluable suggestions in shaping my dissertation. Their guidance undoubtedly sublimates my knowledge in transportation, particularly in the area of intelligent transportation systems.

Lastly, I am grateful for the research team in the Intelligent Transportation System Resource Center at NJIT, in particular, Mr. Slobodan Gutesa, Mr. Branislav Dimitrijevic, Dr. Bo Du, Dr. Haifeng Yu, Mr. Chaitanya Pathak, and Mr. Ravi Jagirdar. I am indebted for their constant encouragement and support in helping me overcome setbacks and keeping me stay focus in the pursuit of my doctoral degree.

TABLE OF CONTENTS

Chapter		Page
1	INTRODUCTION	1
	1.1 Background	1
	1.2 Problem Statement and Research Motivation	4
	1.3 Research Scope and Objectives	6
	1.4 Dissertation Organization	6
2	LITERATURE REVIEW	8
	2.1 Cooperative Adaptive Cruise Control	8
	2.2 CACC Field Experiment	15
	2.3 CACC Simulation	16
	2.4 Measure of Effectiveness for CACC	24
	2.5 Communication Simulation for CACC	26
	2.6 Summary	29
3	MANAGED LANE STRATEGY	31
	3.1 Managed Lane Strategy	31
	3.2 CACC Near-term Deployment	35
	3.3 CACC String Formation and Dissolution	37
	3.4 Equity Issue in Managed Lane	39
4	MULTI-OBJECTIVE OPTIMIZATION-BASED CACC CONTROL ALGORITHM	41
	4.1 Non-Dominated Sorting Genetic Algorithm II	43
	4.2 Multi-objective Optimization-based CACC Control Algorithm	45
	4.2.1 Headway Objective	48

TABLE OF CONTENTS
(Continued)

Chapter **Page**

4.2.2 Vehicular Jitter Objective……..……..... 48

4.2.3 Emission and Fuel Consumption Objectives…….....…... 49

4.2.4 Constraints……..……..……. 50

4.3 Numerical Simulation ……..……..…… 52

5 DEVELOPMENT OF MICROSCOPIC SIMULATION FRAMEWORK 61

5.1 Simulation Framework Architecture……..... 61

5.2 Vissim Traffic Simulator……..……..……..... 62

5.3 Vissim External Driver Model API ……..……. 64

5.4 Vissim COM Interface ……...……..……...… 68

5.5 Wireless Communication Module……..……..……..... 70

6 SIMULATION STUDY……..……..……..…… 75

6.1 Simulation Network…….……... 75

6.1.1 Network Calibration…..…….. 75

6.1.2 Managed Lane Strategy…….……...…….. 76

6.2 Simulation Results……..…… 79

6.2.1 Traffic Flow Performance Measure……..……..… 79

6.2.2 Platoon Performance Measure…….…….…. 87

6.2.3 Wireless Communication Performance Measure……..… 92

6.2.4 Optimization Performance Measure……..…. 96

6.3 Discussion……...…. 99

TABLE OF CONTENTS
(Continued)

Chapter **Page**

7 CONCLUSION AND FUTURE RESEARCH……..…… 103

7.1 Conclusions……...….. 103

7.2 Future Research…….……..….. 105

APPENDIX A NUMERICAL SIMULATION RESULTS……...… 106

APPENDIX B I-66 SIMULATION NETWORK CALIBRATION……..…… 112

REFERENCES……... 123

LIST OF TABLES

Table		Page
2.1	SAE International Level of Automation…….……	13
2.2	Comparison of Mostly-used Microscopic Simulation Packages……	19
3.1	A Non-inclusive List for Managed Lane Implementation in the U.S.….	33
4.1	Comparison of SOOP and MOOP…….…….	42
4.2	MOOP-CACC Parameters……..	52
4.3	Eight Control Algorithms for Testing…….…….....	53
4.4	Initial Conditions for Testing……..……..	55
4.5	Average Medians Over Ten Trajectories …….	60
5.1	EDM Longitudinal and Lateral Control Parameters……..……..	66
6.1	Managed Lane Strategies for Testing……	77
6.2	Simulation Configuration…….……	78
6.3	Relationship of Platoon Variables…….…….	90
6.4	Evaluation Score Assignment…….……	99
B.1	RTMS Trailer Locations……	114
B.2	TMC Information……...	117

LIST OF FIGURES

Figure		Page
1.1	Supply versus demand of public road mileage……	2
2.1	Relationship of overall driving and DDT…….…….	12
2.2	Use case sequence at level 3 of DDT fallback…….……..…	14
3.1	Managed lane implementation strategies……..…...…	32
3.2	Suitability of managed lane strategy……..…..…	36
3.3	Deployment roadmap for CACC vehicles…..……..…	36
4.1	Non-dominated solutions and Pareto frontier……...……	42
4.2	Non-dominated sorting and crowding distant sorting……..…..	45
4.3	Illustrate of platoon-wide objectives.……	46
4.4	Speed profiles for leading GP vehicle…….……..…	54
4.5	Comparison of control algorithms…..……..…..…….	57
4.6	MOOP Platoon dynamic comparison. ……..……	59
5.1	Simulation framework architecture…….……..	61
5.2	Wiedemann car-following model……..	63
5.3	Vissim EDM Functions ……..……	65
5.4	CACC platooning algorithm ….…….	67

LIST OF FIGURES
(Continued)

Figure		Page
5.5	Pipelining for salability…….…..…	69
5.6	Killat's wireless communication model ……..….....	72
5.7	DSRC communication testing procedure……..……	74
6.1	I-66 testbed……..……..	75
6.2	Observed speed-flow diagram……..	81
6.3	Network-wide performance measure……..	83
6.4	Network mainline travel time…….....	85
6.5	Mainline travel time for all vehicles……..	85
6.6	Speed variance…….…….……	86
6.7	Percentage of CACC vehicles in platoons…….	88
6.8	Average total number of platoons in the network……	89
6.9	Weaving activity of leftmost/managed lane…….	91
6.10	Transmission density for CACC vehicle……..	94
6.11	Probability of successful reception of V2V packet…….	95
6.12	Feasible solution ratios among strategies……...	96

LIST OF FIGURES
(Continued)

Figure **Page**

6.13 Objective values for each vehicle between SOOP and MOOP..... 98

6.14 Evaluation scores…… 100

6.15 Managed lane recommendations. ……..… 102

A.1 Comparisons of ten trajectories…… 106

B.1 I-66 network……..…… 112

B.2 Flow-speed diagram comparison…….. 114

B.3 TMC travel time calibration……..……. 118

LIST OF ACRONYMS

Acronym	Definition
ACC	Adaptive Cruise Control
ADAS	Advanced Driver-Assistance System
ADS	Automated Driving System
API	Application Programming Interface
AVCS	Advanced Vehicle Control System
CACC	Cooperative Adaptive Cruise Control
CAH	Constant Acceleration Heuristic
CHEM	Comprehensive Modal Emissions Model
COM	Component Object Model
DDT	Dynamic Driving Task
DL	Dedicated Lane
DLA	Dedicated Lane with Access Control
DLR	German Aerospace Center
EDM	External Driving Model
FAST	Flexible Agent-based Simulator of Traffic
FCC	Federal Communication Commission
FHWA	Federal Highway Administration
GA	Genetic Algorithm
GKT	Gas-kinetic Traffic
GP	General Purpose
GUI	Graphical User Interface
HIA	Here-I-Am
HOT	High-Occupancy Toll
HOV	High-Occupancy Vehicle
IDM	Intelligent Driver Model
MAC	Media Access Control
MML	Mixed Managed Lane

MOBIL	Minimizing Overall Braking Induced By Lane Change
MOE	Measure of Effectiveness
MOOP	Multi-objective Optimization
MOVES	Motor Vehicle Emission Simulator
MPR	Market Penetration Rate
NHTSA	National Highway Transportation Safety Administration
NS	Network Simulator
NSGA	Non-Dominated Sorting Genetic Algorithm
ODD	Operational Design Domain
PATH	California Partner for Advanced Transportation Technology
PET	Post Encroachment Time
RTMS	Remote Traffic Microwave Sensor
SAE	Society of Automotive Engineer
SARTRE	Safe Road Trains for the Environment
SDK	Software Development Kit
SOOP	Single-objective Optimization
SSAM	Safety Surrogate Assessment Model
SUMO	Simulation for Urban Mobility
TCP	Transmission Control Protocol
TET	Time Exposed Time-to-Collision
TIT	Time-integrated Time-to-Collision
TMC	Traffic Management Channel
TNO	Netherlands Organization for Applied Scientific Research
TS	Traffic Simulator
TTC	Time-to-Collision
UDA	User-defined Attribute
UML	Unmanaged Lane
USDOT	United States Department of Transportation
USDOT	United States Department of Transportation

V2I	Vehicle-to-infrastructure
V2V	Vehicle-to-vehicle
VAD	Vehicle Awareness Device
VANET	Vehicular Ad Hoc Network
VHT	Vehicle Hour Traveled
VMT	Vehicle Mile Traveled
WAVE	Wireless Access in Vehicular Environment
WiMax	Worldwide Interoperability for Microwave Access
XML	Extensible Markup Language

CHAPTER 1

INTRODUCTION

1.1 Background

In 2014, 6.9 billion hours and 3.1 billion gallons of fuel were wasted by traffic congestion, totaling a staggering bill of $160 billion. Increase in traffic congestion was observed in 95 out of 100 America's largest metro areas. It was also estimated that on average an urban commuter in 2014 spent extra 42 hours per person on roads due to congestion [1]. The total congestion among U.S. cities has exceeded the pre-recession level, as the economy of the United States regains millions of jobs. However, roads have not been built to accommodate the increasing demand. According to the Highway Statistics 2013, the Vehicle Miles Traveled (VMT) has been increased by 1.4 trillion vehicle-mile from 1980 to 2013 [2]. During the same period, however, the public road mileage has only increased by 0.25 million miles in the United States, as shown in Figure 1.1. Such a spike in demand has been left unfulfilled over the years, resulting in chronic congestion in major corridors throughout the country.

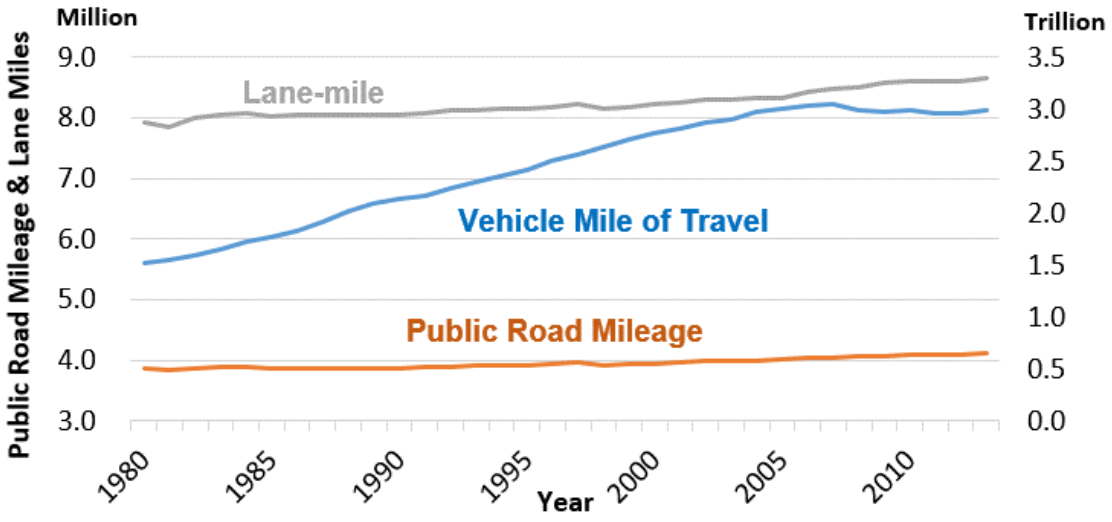

Figure 1.1 Supply versus demand for public road mileage.

Besides congestion, there are approximately 1.6 billion crashes, 1.3 deaths per ten-thousand registered vehicles in the United States[3]. In Europe, more than 40,000 causalities and 1.4 million injuries are caused by vehicle-related accidents [4]. According to the U.S. National Highway Traffic Safety Administration (NHTSA), three dominant causes for vehicle crashes are: 1) control loss without prior vehicle maneuver, 2) sudden stop of a lead vehicle, and 3) road edge departure without prior vehicle maneuver [5]. NHTSA also conducted a survey which indicated that 9.48 out of 10.2 million car crashes in the US were caused by driver mistakes [6].

Necessary steps making the surface transportation smarter, safer, and greener have to be taken. Since its inception in the early 2000s, Connected and Automated Vehicle (C/AV) technologies have been expected to revolutionize the

way a vehicle is operated. It has gained an increasing amount of attention from the automobile industry, which has been projecting their visions and roadmaps about C/AV technologies for the next decades. Ford announced its Smart Mobility Plan with initial 25 global experiments for C/AV in the 2015 Consumer Electronic Show [7][13]. General Motor projected the sales of its autonomous Cadillac CT6 Sports Utility Vehicle in 2017. Mercedes-Benz, Nissan, and Volvo also planned to offer autonomous vehicles to the mass market for customers by 2020 [8]. C/AV technology is also identified as one of the thrust areas by government agencies and academia all around the world in improving mobility, environment, and more importantly safety. The U.S. Department of Transportation (USDOT) has estimated that the Dedicated Short Range Communication (DSRC)-based vehicle-to-vehicle (V2V) communication can address up to 82% of all crashes in the United States [9]. Cooperative Adaptive Cruise Control (CACC) is one of the game-changing solutions in improving mobility as well as safety among C/AV technologies. CACC can be considered as an evolution of Adaptive Cruise Control (ACC) by adding an extra layer of wireless communication under the C/AV environment. The benefits of CACC include:

- Enhancing driver safety considerably by reducing or even eliminating human error
- Increasing carrying capacity of regular highways owing to short intra-platoon following headway
- High-performance driving under restricted driving conditions where human driving is generally deemed unsafe

Field experiments of CACC technology have been accelerated due to technological maturation and governmental encouragement in recent years. The highlights of the deployment, to name a few, include the USDOT-approved C/AV test sites [10], PATH (the California Partner for Advanced Transportation Technology) program [11]–[13], the Energy ITS Project[14], SARTRE (Safe Road Trains for the Environment) [15], KONVOI [16], and CityMobil [17]. Despite policy encouragements from government agencies and progress that have been made in academic research, large-scale field deployment is still considered premature at the current stage in terms of safety, technology, and budgetary concerns. Simulation is one of the best approaches to bridge the gap between prototyping C/AV technologies and evaluation of their large-scale deployment.

1.2 Problem Statement and Research Motivation

Numerous state-of-the-art research efforts have been focusing on the vehicle dynamic aspect of CACC, studying the mechanical aspect of CACC manipulations, for instance, how the acceleration was achieved by analyzing each subcomponent (e.g., throttle position, sensor gain, and vehicle powertrain). Such aspect is vitally important in bringing CACC to fruition; yet, it provides very limited insights into the impacts of CACC to the overall traffic and transportation network. Studies of CACC from traffic engineering standpoint so far are either using simple, hypothetical network or overly simplified traffic flow characteristics, not to mention the operational aspect of deployment. Due to the inherent difference of CACC vehicles in comparison to human-driven vehicles, potential deployment strategies

(e.g., policy encouragement, roadway adjustment) need to be derived based on quantifiable network-level evaluations.

With the DSRC-powered V2V communication in real-time, it is certainly possible to implement platoon-wide cooperative manipulations to maintain a platoon. That is, all the CACC vehicles within a platoon actively negotiate, and make necessary concessions to overall platoon goals (e.g., reducing emission, increasing riding smoothness, or facilitate merging traffic form ramps). In this sense, a platoon-wide multi-objective optimization (MOOP)-based control algorithm for platooning sounds not only logical but also is necessary to harness the benefits of CACC. However, the deployment of CACC technology into mixed traffic in the near future has not been actively researched thus far. It has been proven that managed lane strategy can encourage new travel behaviors (e.g., car-pool lane, High Occupancy Vehicle (HOV) lanes) or promote new technologies (e.g., low-emission vehicle). As an additional benefit, using managed lane can increase the density of CACC vehicles in a particular lane, even when the market penetration rate (MPR) is low. Moreover, V2V communication, an essential aspect of real-world deployment, is rarely considered for the evaluation of CACC technologies due to computational burden.

This research proposes a MOOP-based CACC control algorithm. The algorithm was evaluated in an integrated microscopic traffic simulation framework with an analytical wireless communication module. Besides, CACC implementation with managed lane strategies was studied, aiming to provide

insights when it comes to near-term CACC deployment on public roads alongside regular traffic.

1.3 Research Scope and Objectives

The primary goal of this study was to evaluate the impacts of introducing CACC into the existing roadway and the effectiveness of using managed lane strategies with CACC. Toward this goal, the following objectives have been addressed.

- To develop a simulation testbed for evaluation of large-scale operational strategies of CACC
- To develop a platoon-wide MOOP-based CACC control algorithm that can accommodate various operational objectives.
- To assess a variety of available managed lane strategies for CACC.
- To investigate the suitable performance measures for CACC traffic.
- To evaluate the performance of CACC under imperfect wireless communication environment (e.g., packet drop)

1.4 Dissertation Organization

This dissertation is organized as follows: in Chapter 1, background, motivation, and the scope of this dissertation are presented. In Chapter 2, a comprehensive literature review regarding the major tasks is conducted, including 1) CACC vehicles control, 2) CACC simulation framework, 3) measures of effectiveness (MOEs), and 4) V2V communication impact of CACC platoons. Chapter 3

discusses the operational perspective of CACC vehicles in real-world traffic. Chapter 4 goes into details of the development of the MOOP for CACC control algorithm, followed by the proposed versatile microscopic simulation framework in Chapter 5. Chapter 6 presents the simulation results and discussion and Chapter 7 offers conclusions and discussion of the future research.

CHAPTER 2

LITERATURE REVIEW

2.1 Cooperative Adaptive Cruise Control

Advanced Vehicle Control Systems (AVCS) refers to a subclass of Advanced Driver Assistance System (ADAS) that provides drivers with safety warnings or assistance in controlling their vehicles, to the extension of the full control of vehicle motions [18]. AVCS can be divided into four key aspects: 1) lateral control, 2) longitudinal control, 3) sensors and communication, and 4) safety and fault tolerance [19]. From traffic engineering perspective, the CACC control could be classified into three levels: 1) the global control between CACC platoons, 2) the local control among vehicles within a platoon, and 3) the physical control between consecutive vehicles [20]. The primary objective of vehicular lateral control is to keep the vehicle on the desired trajectory, usually in the center of a lane, from wind gust disturbance, road surface condition, or even unintentional lane-drifting by a human driver [21]. Longitudinal control is responsible for the forward movement of a vehicle, which needs to satisfy requirements in safety and performance. CACC system, with the extra layer of communication, maintains a proper following distance of a leading vehicle. Furthermore, cooperation among CACC vehicles within a platoon is made possible by V2V communication.

Bart et al. [22] proposed the Intelligent Transport Systems-Integrated Full-Range Speed Assistant to support the development of ADAS regarding the

assessment of technical functionality. Three ADAS models were derived from the model: 1) an ACC controller, 2) a time headway CACC controller, and 3) average speed CACC controller. In the time headway CACC controller, the acceleration of a CACC vehicle was determined by the minimum acceleration of its preceding vehicles. In the average speed controller, the acceleration of a CACC vehicle is determined by the minimum acceleration of all the preceding vehicles as well as the error feedback of the average velocity. Safety, string stability, and comfort measure were applied to the evaluation.

Yu and Shi [23] proposed an improved cooperative car-following model by taking into consideration of multiple instantaneous vehicular gaps and the historical gaps with memory. The memory is a variable in traffic hysteresis theory [24] for the motion of a vehicle after sufficient time steps. In essence, the model determined the position of each vehicle at any time interval by considering all the vehicular gaps in a platoon as well as speed information. Four different combinations of the weight coefficients of the two preceding vehicles were proposed. Based on the numerical examples, the authors concluded that the traffic flow becomes most stable and safer when taking into account the change of three preceding vehicular gaps with memory steps of two.

Wang et al. [25], [26] proposed a rolling horizon CACC control framework, under which different control objects were optimized for the consideration of predictive behaviors of other vehicles. An enhanced predictive ACC controller with an explicit safety mechanism and a fuel consumption objective were proposed. To improve the control framework for cooperative systems, the authors also proposed

two multi-anticipative controllers (MACCs): CACC-MP (i.e., perfect knowledge of human follower simulated by Hally's [27] car following model) and CACC-MI (imperfect knowledge of the human follower by incorporating Intelligent Driver Model (IDM) [28]). Experiments were designed to examine the performance of Multi-anticipative ACC and CACC in terms of reactions to the disturbance, oscillation of gap, speed, and acceleration. The authors reported that the cooperation between equipped vehicles and human drivers were able to dampen traffic disturbances in acceleration and increase queue-discharging rate.

Li et al. [29] had extended the IDM by incorporating cooperation of the immediately preceding vehicle. Linear stability analysis showed that the consideration of power output of a receiving vehicle improves the traffic flow stability. Montanaro et al. [30] put forward an extended CACC controller, under which the communication was asymmetrical. The objective of the algorithm was to make the controlled vehicle attain the velocity of the leading vehicle and the predetermined gap. Ge and Orosz [31] performed a vehicle dynamic with delayed acceleration feedback of a CACC platoon system.

Lee et al. [32] evaluated the impact of CACC on mobility using a Vissim simulation testbed. Compared to most of the aforementioned studies, Lee's study focused on assessing the potential benefits for both mobility and safety under a wide range of traffic scenarios. To tackle the CACC vehicles operating under mixed traffic environment, a CACC algorithm, which included rear-, front-, and cut-in join, was proposed. Among all the scenarios tested, Lee et al. concluded that at MPR of 30%, the promising mobility benefits of CACC were shown. Similar to Lee's

effort, Wang et al. [33] proposed a linear distributed consensus-based CACC protocol for lateral control, which handles four types of platoon maneuvers: 1) free-agent-to-free-agent lane change, 2) free-agent-to-platoon lane change, 3) platoon-to-free-agent lane change, and 4) platoon-to-platoon lane change. Arnaout and Bowling [34] constructed a simulation testbed to evaluate three different CACC deployment strategies: 1) no CACC vehicles as the base case, 2) CACC vehicles scattered on all the lanes, and 3) CACC vehicles with priority access to HOV lane in mixed traffic. The authors concluded that potential benefits of CACC could be realized by placing CACC vehicles on HOV lanes when the MPR is below 40%; when the MPR is above 40%, the benefit of CACC could be realized in the absence of CACC-HOV lanes.

The safety aspect of CACC has also been studied. Safety Surrogate Assessment Model (SSAM) was typically used. Lee et al. [32] used time-to-collision (TTC) and post-encroachment time (PET) to conduct a safety assessment of CACC on a freeway setting and concluded that 0.9-second headway yielded safer roadway condition than 0.6-second headway regarding total conflicts and PETs. TTC, time exposed time-to-collision (TET), and time-integrated time-to-collision (TIT) were used by Li et al. [20] to evaluate the reduction of rear-end collision risks for CACC on freeways. It was found that the TET and TIT could be reduced by more than 90% with the proper setting of desired time headway and engine time delay, whilst the TTC remained at the same level regardless of the platoon size.

NHTSA has adopted the standard of Levels of Vehicle Automation of Society of Automotive Engineers (SAE) International recently. Starting from Level 0 (zero) being a human driver does all the driving tasks, the standard designates additional five automation levels as summarized in Table 2.1. CACC is considered as a Level 3 automation. The Dynamic Driving Task (DDT) and Operational Design Domain (ODD) are two of the essential concepts defined by SAE. DDT encompasses all of the real-time operational and tactical functions that are required to operate a vehicle in on-road traffic. ODD defines the condition in which the designed function is intended to operate with respect to a variety of factors (e.g., roadway types, speed range, lighting condition). The relationship among strategies functions, tactical functions, and operational functions are illustrated in Figure 2.1.

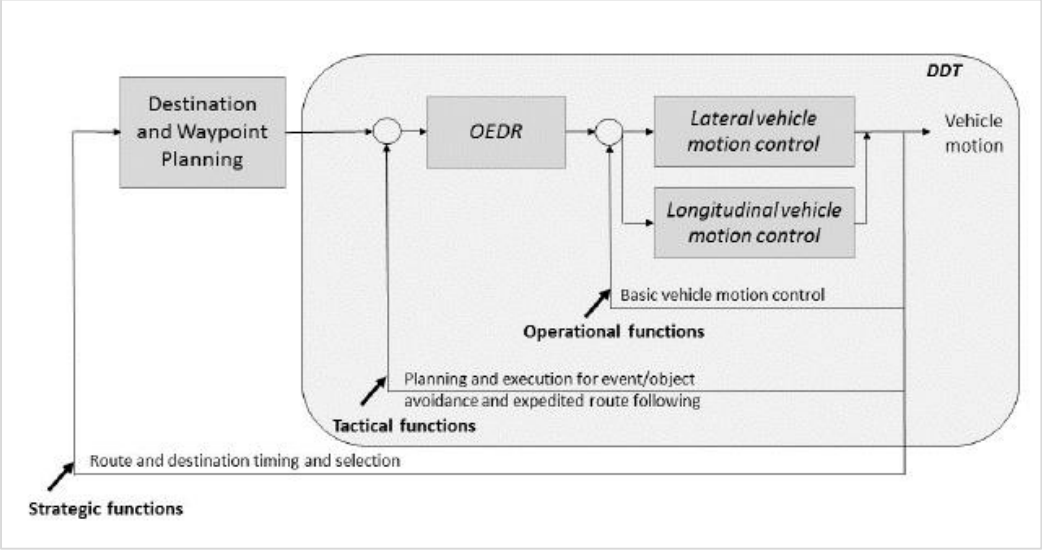

Figure 2.1 Relationship between overall driving and DDT [35].

As required by NHTSA, an automated vehicle has to return to minimal risk condition, which is defined as a low-risk operating condition that an automated driving system (ADS) resorts to automatically in the event of system failure or human driver fails to respond to a request appropriately. Figure 2.2 shows the execution of DDT fall back or exiting for a Level 3 ADS.

Table 2.1 SAE International Level of Automation [35]

Level	Automation	Description
0	No Automation	Drivers handle all aspects of dynamic driving tasks
1	Driver Assistance	One or more specific automation control function are independent of each other (e.g., automatic braking system)
2	Partial Automation	Integration of braking, throttle, and steering control
3	Conditional Automation	Automated driving systems (ADS) fully execute functions of DDTs, within a specific driving environment. Users act as DDT fallback
4	High Automation	DDTs are handled by ADS, but a driver need to resume control with reasonable warning time should be operated with operational design domain. ADS acts as DDT fallback
5	Full Automation	ADS executes entire DDTs in an unconditional and sustainable way (all ODDs)

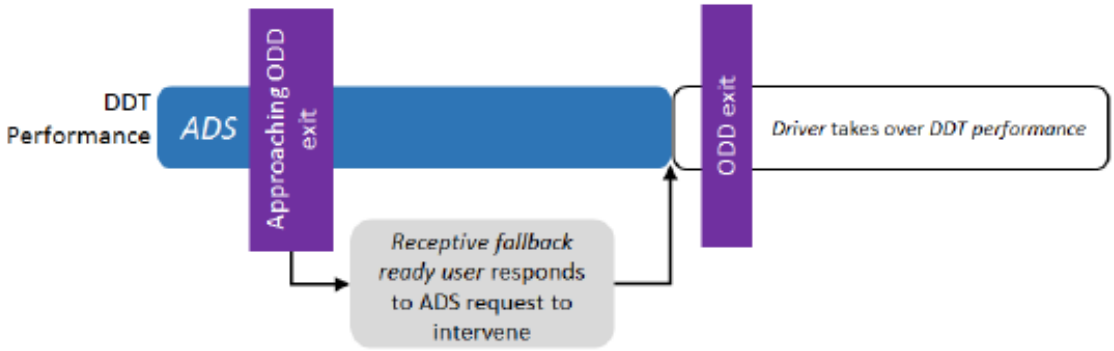

Figure 2.2 Case sequence at Level 3 of DDT fall back [35].

The USDOT makes the distinction between Level 0-2 and Level 3-5, based on the entity (e.g., human operator or ADS) which is responsible for monitoring the driving environment [36]. Different from Level 0 to 2, ADSs are responsible for monitoring the driving environment at Level 3-5. Besides the level of automation, the difference between automated system and connected (cooperative) system should not be confused. Automated vehicle system relies entirely on their onboard sensors and intelligence/software to execute all driving functions. On the other hand, connected vehicle system not only utilizes sensor and intelligence but also more distinctively rely on communication to cooperate with other systems (e.g., vehicles, infrastructures) [37]. CACC with automated lateral control for platoon formation is considered as a Level 3 ADS, which requires DDT fallback-ready drivers. Therefore, a control algorithm should have the mechanism built-in to allow driver get ready to take over the DDT.

2.2 CACC Field Experiment

The PATH program [38] integrated the V2V communication capability to Adaptive Cruise Control (ACC) system and experimented with longitudinal control of eight vehicles on a closed highway segment[11]. SARTRE, funded by European Union, developed a solution that allows a platoon of vehicles led by a truck that was driven by a professional driver. The occupants, including drivers, in the following vehicles, were permitted to do non-driving related tasks. The SARTRE concept was successfully demonstrated on a conventional highway under mixed traffic environment without the necessity of changing existing roadway infrastructure. In the U.S., Bu et al. [12] proposed a generic process of formulating a real-world application with multiple constraints in the control problem. Then they modified a commercially available ACC system of Infinity FX45 vehicles and had them retrofitted with the CACC system designed by PATH. The field test concluded that CACC equipped vehicles could operate at time gaps between 0.6 seconds and 1.1 seconds. For reference, ACC typically operates at a time gap between 1.1 to 2.2 seconds.

Omae et al. [39] proposed an inter-vehicle control scheme for implementing CACC-enabled heavy trucks. The contents and format of the V2V message were summarized. Four slightly different CACC control algorithms tailored to different vehicles were proposed. Field experiments constituted by four heavy trucks equipped with the proposed algorithms were carried out. The focuses of the field experiment were: 1) formation of a platoon by vehicles based on the CACC controller, 2) vehicle exiting of a platoon, and 3) the proper switching among CACC,

ACC, or manual modes in the event of communication failure. The experiment proved that the CACC controller successfully overcame communication failure by switching to the proper control mode.

Milares et al. [13] conducted field experimentation of CACC using commercially available vehicles that were retrofitted with V2V communication capability. With the incorporation of the gap regulation and gap closing controller, three tests: 1) gap setting change test, 2) cut-in and cut-out test, and 3) a comparison test between stock ACC and augmented CACC were conducted. Based on the field experiment, the authors stated that the knowledge about the preceding vehicles was significant in improving string stability. Similar CACC field implementations can also be found in [40]–[44].

2.3 CACC Simulation

Field-testing CACC has numerous advantages, but there are three main drawbacks. First of all, field test requires a relatively high level of automation (Level 3 or above) and technological maturation. Testing the technology on public roadway imposes much more stringent requirements than on closed course, as potential liability issue still a major concern at the current developmental stage of CACC. Secondly, the field testing of CACC requires not only the CACC vehicles, but it also requires testing infrastructure (e.g., test site, data collection devices), all of them could incur a significant amount of cost, something that could be afforded by limited entities. Lastly, the proven effectiveness of a small number of CACC vehicles may not be able to scale when it comes to network-wide implementation

linearly. Because of this, support for operational policies is desired at the initial release of the technology for the public.

The standard of CACC is still being shaped as the technology progresses. One of the common assumptions is that the CACC car-following behavior should resemble with that of the human's. By the extension of this assumption, it is acceptable to modify relevant parameters of human-based car-car following model, such as Wiedemann-99. The Department for Transport of the United Kingdom published a report [45] regarding assessing the impact of C/AV on traffic flow by which the default car-following parameters of the Wiedemann-99 model were changed in order to simulate CACC vehicles. However, the psychophysical aspect of the Wiedmnann-99 model, which may not be part of the CACC behaviors, was still in effect during the simulation. During our calibration of the test network (i.e., the I-66 network), it was discovered that overly aggressive braking occurs more frequently when the desired headway of Vissim get lower. Mathematically, smaller following headway yielded closer car following and therefore increased throughput. Realistically, as a result of short following distance, more shockwave could be generated. This has been proved to make the traffic flow more susceptible to shockwave and yield even lower throughput.

In [45], it was also argued that the capability of CACC is likely dependent on user preference in using the technology more assertively or otherwise. As such, the user choice was a crucial determinant of CACC performance as well. The four types of drivers in Level 3 automation were Cautious, Normal Cautious, Normal Assertive, and Assertive. Four of them were implemented by a unique set of car-

following parameters in Vissim. The role of user preference regarding C/AV was also studied in [46]. Hence, it is crucial to realize that the presence of CACC vehicles on the roadway does not necessarily mean enhancement in mobility, network performance, and road capacity.

Microscopic traffic simulation is the preferred type of testbed for studying CACC because it provides high-definition vehicle movements and interactions in automated longitudinal and lateral control. There is traffic simulation software that is available commercially or publically as a form of open-source collaboration. Some packages use discretization time and space cellular automata (CA) theory, whereas others use space-continuous, time-discrete approach or space and time-time continuous approach. Three of the widely-used simulation packages (i.e., PTV Vissim, Aimsun, and SUMO) for simulating CACC are briefly reviewed.

Vissim is a commercial simulation package develop ty PTV Group. It adapts the Wiedemann psychophysical driver behavior model [47] that accounts for the influence of driver's perception of velocity control. It uses a rule-based lane selection model that originated from the research of Wiedemann as well. VISSIM replaces the conventional representation of road network (typically by vertices and links) with a structure of one-way link connected to a connector, making it capable of modeling nearly any roadway structure. Also, VISSIM offers excellent options for adjusting vehicle properties with serval Application Programming Interfaces (APIs) for instance, Driver Model API, Signal Control API, etc.

Aimsun is a microscopic simulation software package that has recently been rebranded as Aimsun Next (Aimsun was used in this dissertation for

simplicity). Aimsun is able to conduct microscopic or hybrid simulations. The software package implements Gipps-based [48] car-following model. Furthermore, modifications were made on the Gipps model to simulate vehicle movement under congested condition. The lane change modeling is based on Gipps lane changing model [48]. Aimsun provides a Microsimulator Software Development Kit (microSDK) by which new car-following or lane-changing model can be used to replace the default model of Aimsun.

Table 2.2 Comparison of Widely-used Microscopic Simulation Packages

	Vissim	**SUMO**	**Aimsun**
Space domain	Continuous	Continuous	Continuous
Vehicle dynamic realism	High	Medium	High
Vehicle behavior adjustments	9 parameters (Wiedemann)	5 parameters (Kraus)	Modified Gipps
Modeling different vehicle type	Yes	Yes	Yes
Pedestrians simulation	Yes	Not support	Not support
Network representation	High precision	Medium precision	High precision
External control	COM interface, Driver model API	Traffic Control Interface (TraCI)	microSDK, platformSDK, API
Model edition	GUI	XML files	GUI
Simulation speed	Medium	Fast	Fast
Visualization	2D, 3D	2D only	2D, 3D
License	Commercial	General Public License (GPL)	Commercial

The Simulation for Urban Mobility (SUMO) is a free microscopic traffic simulator developed by German Aerospace Center (DLR) [49]. It utilizes the Krauss model [50], which is considered as an extension as Gipps model [48], for car-following and the Krajzewicsz model [51] for lane changing. SUMO is able to simulate various types of vehicles with good scalability, owing to its command-line-based simulation. It is reported that other car-following models were implemented in SUMO, but they are still in developmental stage and their reliability is not guaranteed [52]. SUMO has been evolving continuously, due to its active open-source development community. Table 2.2 presents a comparison among these three simulation packages.

Moreover, a wider range of simulation tools along with its application besides the aforementioned three simulation package is summarized for the remainder of this chapter. Nikolos et al. [53] proposed a macroscopic approach to examine the impact of ACC and CACC by incorporating traffic dynamics into gas-kinetic traffic (GKT) flow model [54]. The GKT model handles the behavior of a group of vehicles, specified by their location (X), speed (V) and desired speed (V_0) at any instant (t), and phase space density (p). The framework was applied for the evaluations of ACC and CACC under mixed traffic conditions. Two simulation scenarios have been tested: 1) a 6-mile long basic freeway segment with homogenous traffic and 2) an 18-mile long freeway segment with an on-ramp. Spatiotemporal change of density for manually driven vehicles and CACC vehicles could be obtained. Taking into consideration the length of the test segment, the model appears suitable for evaluating the impact of CACC technologies in a large-

scale area. However, it is challenging for their model to deal with the effectiveness under various MPR scenarios.

Smith et al. [55] proposed an analytical modeling framework for assessing the benefits of automated vehicle operations. The proposed framework is a comprehensive approach for the quantitative assessment of the wide-ranging impacts of various automation scenarios (or levels). Given these scenarios serve as inputs to the framework, the outputs of the framework are intended to help inform policy decisions. The framework is designed to facilitate the comparison of multiple scenarios: the degree of V2I (vehicle-to-vehicle) and V2V (vehicle-to-infrastructure) connectivity, as well as the different level of automation. To this end, the framework incorporates several sub-models to assess the impacts regarding safety, mobility, energy/environment, transportation system utilization, accessibility, land use, and economic. The framework is designed to evaluate the following C/AV applications: 1) Collision Avoidance, 2) Traffic Jam Assistance, 3) Cooperative Adaptive Cruise Control (CACC), 4) Automated Platooning, and 5) Full Automation in a Controlled Environment.

Shladover et al. [14] developed a microscopic simulation model to evaluate the performance of ACC and CACC on highway capacity under various MPR conditions. Utilizing Aimsun and its microSDK, the authors constructed an evaluation platform to handle the various scenarios reflected by the MPR of ACC and CACC. In addition to ACC and CACC, the authors introduced a “Here-I-Am (HIA)” vehicle group, which is equipped with a Vehicle Awareness Device (VAD) to provide adjacent equipped drivers with real-time position

information. While it is unable to conduct automated operations, the information disseminated from the HIA vehicles will be helpful for the operation of CACC under low MPR that would represent an early stage of CACC deployment. A 4-mile long single-lane hypothetical freeway segment without any on- and off-ramps was modeled using Aimsun to assess the impacts of various combinations of HIA, ACC, and CACC on roadway capacity. The longitudinal control algorithms for both ACC and CACC were obtained from empirical data. Both algorithms were simplified to be modeled into Aimsun driving behavior model Application Programming Interface (API). The car-following behaviors for both manually-driven and HIA vehicles are controlled by an oversaturated freeway flow model developed by Yeo [56] and Yeo et al. [57], which are based on Newell's [58] linear model. The desired target headway of the ACC or CACC vehicles were selected based on field test observations.

MICroscopic model for Simulation of Intelligent Cruise control (MIXIC) is a microscopic traffic simulator developed by the Netherlands Organization for Applied Scientific Research (TNO) for the assessment of the impacts of C/AV applications [59]. With a simulation resolution of 0.1 seconds, the MIXIC model estimates various performance measures covering mobility (e.g., travel time, delay), safety (e.g., time to collision), and environmental impacts (e.g., noise, exhaust-gas emission, and fuel consumption). Based on a modular structure, MIXIC is flexible to customize vehicle models for handling longitudinal and lateral maneuvers. With this flexibility, the authors conducted the assessment of Advanced Driver Assistance Systems (ADAS) such as ACC, automated platooning,

special lane for intelligent vehicles, cooperative following and merging, V2V communications (a.k.a., CarTalk), and CACC [60].

Flexible Agent-based Simulator of Traffic (FAST) [34] is an agent-based microscopic traffic simulation model extended from the two-lane microscopic traffic simulation model initially developed by Treiber [61]. FAST uses the microscopic simulation approach to mimic the behavior of individual driver's longitudinal and lateral driving maneuvers and macroscopic approach to deal with collective dynamics of traffic flow (e.g., density, flow, shockwaves) to analyze the traffic performance. Employing the IDM and MOBIL as a primary car-following and lane-changing model, respectively, FAST is well suited for simulating complex traffic patterns developing over time. It is also flexible in allowing simple calibration of different parameters to conduct different scenarios depending on the parameter's value. With agent-based modeling structure, FAST handles thousands of agents to represent individual vehicles at the microscopic level, but at the same time, collects measures of effectiveness at the macroscopic level. Pursuing open source policy, FAST allows modelers to customize the source codes and share them with other modelers. While pursuing realistic traffic conditions to generalize CACC performance, their experiments were somewhat limited as 1) only a single fixed on-ramp traffic volume was used, 2) no CACC vehicles from on-ramp were assumed, and 3) only one CACC headway case was explored.

The CACC add-on package developed by Lee et al. [62] is comprised of three major modules: The Vissim Network module, the Simulation Manager

module which was written via Vissim COM Interface [63], and the External Driver Model (EDM) API module of Vissim [64]. Lee et al. [32] used Vissim to evaluate the potential benefits of CACC for mobility and safety under mixed traffic conditions. The performance of CACC in signalized corridors was evaluated by Zhong et al. using Vissim and its EDM [65]. Additionally, Zhong et al. [66] integrated the multi-objective optimization framework into Vissim simulation for CACC. Pareto optimality of the platoon maneuvering was explored.

2.4 Measures of Effectiveness for CACC

This section describes the typical MOEs for assessing the performance of CACC. A vast majority of the MOEs for CACC is related to evaluation from control theory and the proper execution of the intended functionality of a CACC controller. The MOEs from the traffic engineering, however, are different in comparison. Flow rate is the most straightforward performance measure for mobility. Arnaout and Bowling [34] used flow rate to assess the mobility improvement of CACC in their FAST microscopic simulation framework. To show a more comprehensive evaluation, Lee et al. [32] used the segment travel time, system throughput, and average speed as MOEs for CACC.

When it comes to the safety aspect of CACC, SSAM has been widely adopted. Traffic stability is commonly accepted as a surrogate safety indicator, and it can be measured by speed or acceleration variations. Greater variation typically indicates less stable traffic flow and vice versa. Songchitruksa et al. [67] used the 85^{th} percentile speed, the standard deviation of speed, root mean square

of acceleration, and standard deviation of acceleration to measure the CACC traffic flow. Lee and Park [32] captured the dangerous conditions that could potentially result in crashes by two surrogate measures: the TTC and PET. The type of conflicts was classified into three categories: 1) rear-end conflict, 2) lane change conflict and 3) crossing conflict that is only applicable to the arterial setting. However, research pointed out that the pitfall for SSAM is that the assumption regarding driver's response to longitudinal disturbances has become much less relevant under CACC control.

The third type of MOEs is environmental sustainability. Due to the microscopic level interaction of CACC vehicles, emission model that utilizes second-by-second vehicle trajectory data is preferred. The VT-Micro Model [68] calculated both carbon dioxide and fuel consumption using the instantaneous acceleration and speed of a vehicle. Its usage has been reported in freeway and arterial settings[32], [66]. In addition, MOVES [69] and Comprehensive Modal Emissions Model (CHEM) [70] has been adapted for microscopic-level evaluation as well.

The platoon characteristic MOEs started emerging. Because of the short intra-platoon headway among CACC vehicles, a higher flow rate can be achieved by a higher number of CACC platoons in the network. Platoon length and its deviation were used in [67] as indicators of the stability of platoons. Additionally, the number of platoons and variation of the platoon number were also investigated. The platoon characteristics MOEs and their impacts on network level deployment

are still in their very early stage, and it is worth exploring for assessing the benefits of CACC.

2.5 Communication Simulation for CACC

When it comes to vehicular communication, the DSRC, based on 802.11p, is designed to use for vehicle-to-vehicle (V2V) communication and vehicle-to-infrastructure (V2I) communication (V2V and V2I are often jointly referred as V2X). “Dedicated” refers to the 75-MHz licensed spectrum in the 5.9 GHz band assigned by U. S. Federal Communications Commission (FCC). The term “short range” represents that the communication taking places is only over hundreds of meters, a distance that is shorter than cellular and Worldwide Interoperability for Microwave Access (WiMAX) service. Wireless Access in Vehicular Environment (WAVE) message (defined in SAE J2735 standard) is broadcasted via DSRC for safety-critical application, whereas the non-safety-critical application can use either DSRC protocol stack or other wireless communications. The 5.9 GHz band is further divided into several 10MHz channels with 5-MHz guard bands at the low end. The most critical channel among all is the Channel 172, which is designated for safety application [71]. The DSRC protocol stacks include Physical (PHY) layer, Data Link layer, Network/Transport layer, and Application layer.

Wireless communication in vehicular environment is a technological challenging due to: 1) limited communication channels are assessed by multitude of communication nodes (e.g., vehicles); 2) aforementioned communication nodes are travelling at high speed (e.g., 120 km/h); and 3) the metallic exterior of a vehicle

increases the reflection of radio, creating a more complicated communication environment. Direct experiment DSRC communication on public roadways is expensive, and doing the experiment at scale is costly prohibited. Simulation is still one of the most cost-effective ways to study CACC communication.

There are two major types of simulations when approaching CACC technology. In the transportation engineering side, simulation focuses on high-level vehicular interactions. A traffic simulator (TS) with a realistic car-following model is of the center of the simulation, and perfect wireless communication is typically assumed. Whereas on the electrical engineering standpoint, a packet-level network simulator (NS) is typically used. Efforts in combining NSs and TSs have been reported. The majority of the works attempted to couple an NS and a TS by using an external synchronizing module. Eichler at al. [72] used standard Transmission Control Protocol (TCP) connection to synchronize CARISMA and ns-2 [73]. A retrospective updating schema is adapted to utilize the vehicle movements from the TS to remedy the inadequate node trajectory modeling of ns-2. This framework improved the degree of realism in simulating CACC technology under realistic networking environment. Segata et al. [74] presented PLEXE, an extension for the Veins simulation framework, for CACC simulation. Vieins [75] is an open source framework for running VANET simulation by interlinking SUMO [49] and OMNeT++ [76] via the Traffic Control Interface. Unfortunately, most of the experiments do not function efficiently at scale.

Hybrid simulation is believed to be a viable approach, which can achieve a significant reduction in the number of scheduled events by the use of statistical models. As in most scenarios, the key question is whether the subject vehicle successfully receives the messages from another vehicle. The rest of the data traffic can be treated as background data traffic. Hence, the transmission scenarios are simplified during runtime. Jiang et al. [77] proposed the concept of communication density, which serves as a metric for channel load in vehicular communication. The communication density is defined as the number of sensible events per unit of time, and it is the product of vehicle density, message generation rate, and communication range.

Data reception rate is determined at a particular communication density level with a particular transmission power. Channel assess delay is an important aspect in vehicle safety communication, and it is defined as the duration between arrival of a frame at the median access controller (MAC) layer to the point of transmission over the air. Jiang et al. [77] proved that the average channel stays the same in cases where communication density levels are the same. Further developing from Jiang et al.'s concept of communication density level, Killat and Hartenstein [78] proposed an analytical model derived from ns-2. The model is based on Nakagami Distribution [79] m=3 model. The Levenberg-Marquardt method [80] was used to construct a two-dimensional polynomial curve fitting. The model assumed 382-byte packet size (128 bytes for certificate, 54 bytes for signature, and 200 bytes of available payload). Within the highest data transmission rate of 27Mbit/s, the maximum communication density that can be handled is 4400 in theory. The

probability of one-hop broadcast reception in Wireless Access in Vehicular Environment (WAVE) [81] can be computed.

2.6 Summary

Based on the literature review, CACC controllers have been extensively studied from the electrical engineering aspect. Limited field implementations of CACC in closed courses have been reported. Due to cost and safety constraints, large-scale CACC deployments and subsequent evaluations are almost non-existent. Traffic simulation is still one of the best ways to study the benefits of CACC at traffic operation level. Simulation is able to investigate the effectiveness of implementing CACC under various managed lane strategies, traffic conditions, and control algorithms systematically. Simulation is also able to improve the quality of the test by expanding the test scope to the realm where testing in the real world could be deemed unsafe for test operator (e.g., communication failure, extremely short following distance, DDT fallbacks). With the advantages of simulation, currently available simulation frameworks still left a lot to be desired. A qualified framework should be able to control vehicle movements in high-resolution and provide realistic vehicular interaction at the microscopic level.

Furthermore, the wireless communication aspect should be factored into the vehicle operation during simulation, as its reliability is vitally important for CACC platoon, especially under congested traffic condition. The tradeoff among managed lane strategies and effectiveness of the CACC is worth studying as well. Lastly, A MOOP-based control algorithm is able to take full advantage of

cooperative nature of CACC. The progression of a CACC platoon should be able to select a preferred objective intelligently according to roadway conditions. For example, in the heavy merging area, the jittering objective may be prioritized for ease of merging for the incoming vehicles, whereas the fuel consumption objective could be as preferable objective during free-flow condition.

CHAPTER 3

MANAGED LANE STRATEGY

This chapter discusses the traffic operation aspect of deploying CACC vehicles in the general traffic. The key discussions include managed lane strategy, deployment roadmap, and CACC vehicle string operation in traffic.

3.1 Managed Lane Strategy

According to the definition set forth by the Federal Highway Administration (FHWA), managed lanes are freeway lanes that are set aside and operated under a variety of fixed and/or real-time strategies responding to local goals as well as objectives (e.g., improving traffic operations, promoting air quality, enhancing safety) [82]. Three primary factors for managed lanes are pricing, eligibility, and access, all of which are illustrated in Figure 3.1.

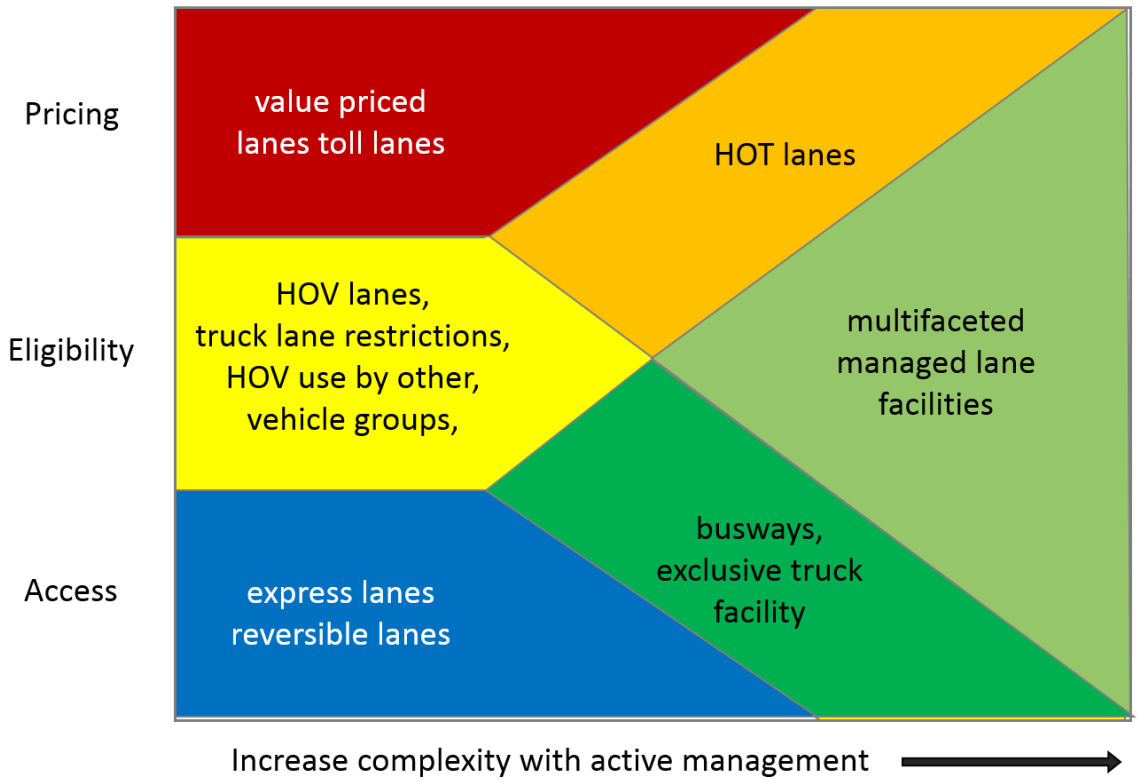

Figure 3.1 Managed lane implementation strategies [84].

One of the common managed lane policies in the U.S. is HOV lane, which was first implemented in the Henry G. Shirley Memorial Highway in Virginia in 1969. Since then, significant growth of HOV lanes has been observed from the mid-1980s to the late 1990s [83]. An HOV lane typically allows vehicles with no less than two occupants to travel. Some roadways also impose stricter policy by requiring a vehicle with no less than three occupants [84]. Table 3.1 is a non-inclusive list of the managed lane strategies that have been implemented in the U.S.

Table 3.1 A Non-inclusive list for Managed Lane Implementation in the U.S.

Managed Lane Case	State	Functionality
I-66 Corridor	VA	HOV lane
		Hard shoulder use
US-101 Corridor	CA	HOT express lane
I-680 Corridor	CA	HOT express lane
I-10 HOT Conversion	CA	HOT express lane
I-80 Express Lanes	CA	HOV lane
I-35 MnPASS Lane Extension	MN	HOT express lane
I-57/I-575 Northwest Corridor Project	GA	Express lane
I-285 Corridor	GA	Express lane
I-95 Express Toll Lanes	MD	HOT lane
I-495 Long Island Express	NY	HOV lane
Pulaski Skyway Rehabilitation	NJ	Hard shoulder as a travel lane
New Jersey Turnpike/I-95	NJ	Dual-dual roadway, Dedicated passenger car lane, HOV lane
I-5 Corridor	WA	HOV lanes, Reversible lane

When it comes to operation, the layers of managed lane could be flexible and complex. The California Clean Air Vehicle Decal program [25], [85] is designed to promote user adoption of energy-efficient and low-emission hybrid vehicles by allowing them to drive on HOV lanes without even meeting the occupancy requirement. Toll facility could also be incorporated into an HOV facility, making it a HOT (high occupancy toll) lane facility. One of the benefits of HOT lane is that it could dynamically change the lane use eligibility for either HOV or Single

Occupancy Vehicle (SOV), when appropriately designed. The I-15 express lane [86], employs a dynamic tolling practice where the toll is determined by the congestion level. The I-10 (i.e., Katy Freeway) HOV lane in Taxes is designed as HOV 3+ facility, but it allows HOV 2+ to utilize the unused capacity of the HOV lane by paying the toll, making it a HOT lane for HOV2+ vehicles [87]. Dahlgren [88] created a model to determine the proper improvements to existing freeway among the three options of HOV lane, HOT lane, or a new mixed-flow lane. The analysis showed that mixed flow lane is viable when the initial maximum delay is no more than 30 minutes, and no significant growth in traffic demand is expected. On the other hand, HOT lane become more suitable when the initial delay is not significant, and when there is a high initial HOV proportion. Managed lane policy can improve safety as well. With a dual-dual configuration separating trucks traffic from general traffic, the New Jersey Turnpike achieved clear benefits in safety: the percentage of crashes per 100 million vehicle miles was reduced by 20 % from 1994 to 1998, compared roadway without the dual-dual configuration[89].

Nonetheless, managed lane policy is not without its problems. Lessons have been learned from improper implementation of managed lane policies. Underutilization of managed lane (a.k.a. Empty Lane Syndrome) is one of the most common pitfalls. In certain occasions, such underutilization was detrimental in public support for the managed lane. In 1998, two HOV lanes in New Jersey had been decommissioned due to insufficient public support. The legislative bodies of Minnesota, New York, and Virginia had raised questions about the effectiveness

of HOV lanes[90]. Conversion of HOV lanes to either mixed flow or HOT lanes in certain roadways was being considered in these states.

3.2 CACC Near-term Deployment

The provision of CACC lane could provide users with a strong incentive to either purchase the vehicles that meet the minimum functional requirements or factor in the option of retrofitting certified aftermarket CACC systems to a possible extent. Figure 3.2 demonstrates, as an example, the suitability of managed lane in near-term deployment. Depending on the geometry and traffic flow characteristics (e.g., origin-destination (O-D) pattern, MPR) of a network, the internal boundary of Figure 3.2 could vary. As such, simulation of a large-scale network is necessary to obtain the baseline of the suitability for a broad spectrum of managed lane strategies.

The phasing in of CACC with managed lane provision is likely to be a three-phase process as envisioned in Figure 3.3. At first, the adoption of CACC vehicles could be incentivized by allowing the use of a managed lane free of charge. As the demand of CACC for the managed lane increases, shorter vehicle gap could be implemented to increase the carrying capacity of the managed lane further. Lastly, when the CACC vehicles reach a critical MPR, the transition to CACC lane could be made and the high-performance driving made possible by CACC technology can be achieved.

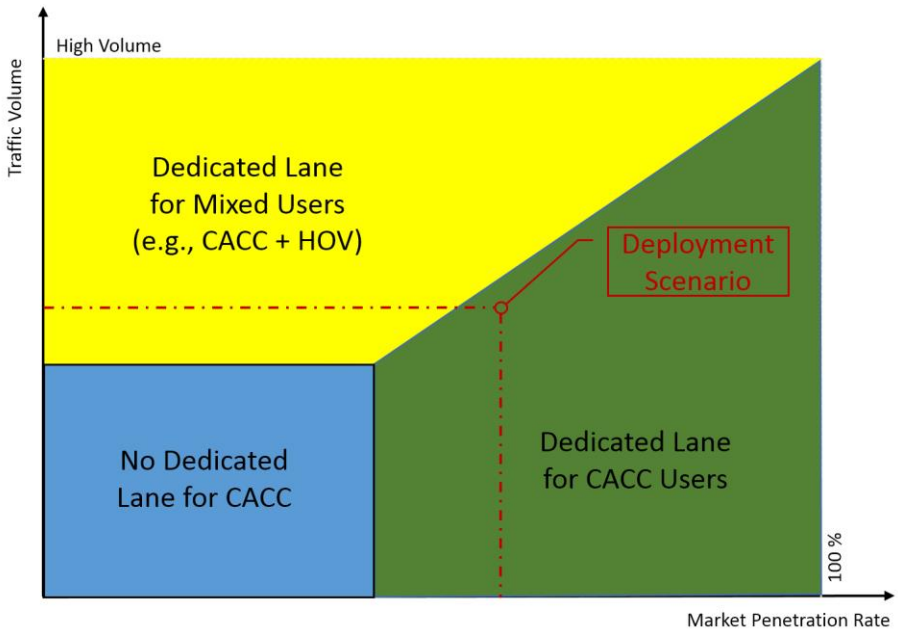

Figure 3.2 Suitability of managed lane strategy.

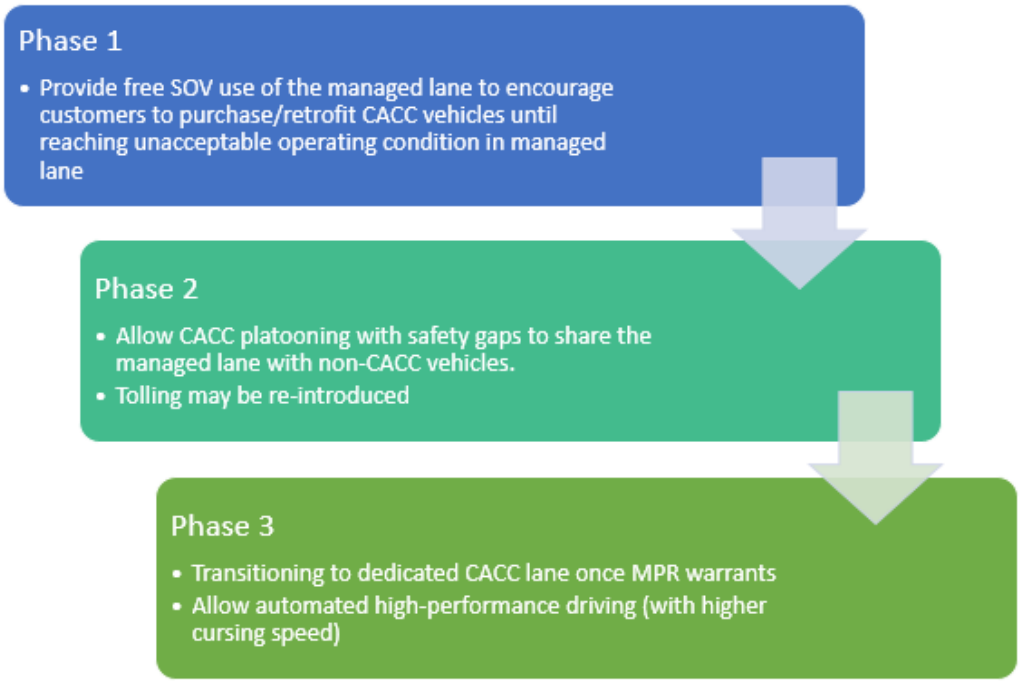

Figure 3.3 Deployment roadmap for CACC vehicles.

3.3 CACC String Formation and Dissolution

Shladover et al. [91] made the distinction between CACC and platooning. CACC refers to CACC vehicle string uses constant-time-gap car following. Platooning, however, refers to using tightly coupled, constant-clearance, vehicle following strategies. Because CACC vehicles require communication with adjacent vehicles, especially with its immediate predecessor. Clustering CACC vehicles, therefore, becomes a crucial factor in operation. Mainly three types of clustering strategies could be expected in operation: 1) ad hoc clustering, 2) local coordination, and 3) global coordination.

Ad hoc clustering assumes the vehicles arrive in random sequence and the CACC vehicles do not actively seek clustering opportunities. Hence, the probability of driving around another CACC vehicles is highly correlated to MPR. As such, its improvement in mobility (e.g., throughput) is expected to be negligible under low MPR. The ad hoc clustering has been adopted in most of the studies so far because of its simplicity of implementation. Local coordination could be employed to help with clustering, as a CACC vehicle intentionally drive closer to an existing CACC cluster or a CACC vehicle to form a new cluster. This approach of clustering has been discussed in [32], [92], [93]. The most prominent challenges to local coordination are the determination of the relative position of the entire vehicle with sufficient accuracy and reliability. Solutions have been proposed to aid the localization of CACC, for instance, infrastructure lane identification by using radio frequency identification; vehicle-based lane identification by using GPS, inertial measurement unit, and camera; vehicle-based confirmation of the predecessor by

using visual or infrared-camera-visible markings; and lastly, driver visual confirmation. The global coordination uses advance planning to coordinate vehicle traveling from similar origins to similar destinations even before the CACC vehicles entering the highway [94], [95]. However, this type of coordination is accompanied by significant logistical challenge due to the uncertainty of traffic conditions. Moreover, extensive long-range communication is required. The most likely application would be long-haul trucking or lengthy commute trip on congested highways.

Besides CACC string formation, attention should be paid to the dissolution of CACC strings. The most common reason for dissolution is exiting of a vehicle within a CACC string when its destination is reached. New traffic problem could be potentially be created from CACC string dissolution. When multiple consecutive CACC vehicles leave at the same exit, maintaining as a CACC string while performing a fully synchronized lane change is the most space efficient operation. However, finding a sufficiently large gap in the adjacent lane may be difficult under congested traffic. In addition, the switching from CACC to ACC mode prior to leaving a platoon by multiple CACC vehicles may not be desirable as well, because the traffic flow may not be able to accommodate the larger separation of the new ACC string. Shockwave is likely to be created under this circumstance. A simple lane change in the direction of the off-ramp is the most straightforward and most efficient way to deal with string dissolution. If the lateral control is not automated, a CACC string with manually driven leader could be created as the driver manual adjust acceleration for lane changing. Once a CACC vehicle has departed from a

platoon, the CACC string behind it has to decide if it should rejoin the former CACC string by closing what may be a long gap or become a new CACC string itself. Global network coordination for traffic redirection may also be required if a substantial amount of CACC vehicles depart at one exit (e.g., the one serving the football stadium). This is also an important operational aspect of CACC, which only has been studied by very limited studies.

3.4 Equity Issue Related to Managed Lane

Equity issues is a crucial factor for managed lane strategy, and it has to be appropriately addressed, due to its vital role in gaining public support. The perception of exclusivity for different road users could be a sensitive matter. The Victoria Transport Policy Institute conducted extensive research [96] regarding the equity and social justice in quantifying traffic impact analysis. The study identified that dedicated lane for CACC scenarios is considered vertical equity type in terms of income and social class [97], as not too many people is able to afford CACC. The issue becomes more pronounced when more speed limit privilege (e.g., higher speed limit) is assigned to CACC lane. Hence, the impacts of a CACC lane among users and non-user need to be quantified. More mobility option could be provided, such as access to transit, vanpool with CACC vehicle, to gain the benefits of CACC managed lane for different user groups. Valuable lessons can be learned from existing managed lane policy (e.g., HOV lane, road pricing, passenger-car lane). The possible considerations include:

- Cost incentives available to make CACC assess for all via tax deduction, subsidies, etc.
- Possible shared mobility for CACC vehicles
- Availability of alternative routes for road users

It is believed that managed lane strategy is essential in the near-term deployment of CACC, where MPR is still low. Managed lane strategy could provide technical accommodation, economic incentive, and mobility improvement for motorists who would decide whether to purchase CACC-equipped vehicles.

CHAPTER 4

MULTI-OBJECTIVE OPTIMIZATION-BASED CACC CONTROL ALGORITHM

Optimization is the procedure of finding the best feasible solutions in terms of one or multiple objectives. In multi-objective optimization (MOOP), more than one conflicting objectives are optimized simultaneously. MOOP has been proposed to deal with complex optimization problems in transportation engineering. Wu et al. [98] used MOOP for business processes of infrastructure management. Additionally, a multi-objective binary nonlinear programming model was proposed by Wu et al. [99] to prioritize the transit stops improvement for American Disability Association (ADA) compliance. An ideal fair ramp metering problem was formulated by Meng and Khoo [100]. In their study, the Pareto-optimality of ramp metering was explored using Non-Dominated Sorting Genetic Algorithm (NSGA) under dynamic traffic flow pattern. Both system efficiency and equity were addressed by Meng's MOOP. Abdelgawad et al. [101] proposed optimal evacuation strategies using mass transit by solving the MOOP with GA.

The majority of reported MOOP methods linearly transforms the MOOP problem into pseudo MOOP or single-objective optimization (SOOP) by using some user-defined parameters (i.e., weight factors) for simplifications. Deb [102] proved that, in a preference-based pseudo MOOP, a change of the preference vector does not necessarily result in a change among trade-off optimal solutions, meaning the other optimal solutions could be potentially overlooked in spite of the

change of preference vector. Admittedly, the majority of real-world optimization problems in their nature require obtaining as many trade-off solutions as possible; then a selection is made based on the high-level information. The output of a MOOP is a Pareto frontier, which is consisted of multiple equally good (i.e., non-dominated) solutions. Table 4.1 shows a comparison of SOOP and MOOP.

Table 4.1 Comparison of SOOP and MOOP

	SOOP	MOOP
Goals	• Search for an optimal solution	• Search for a Pareto frontier • Maintain diversity of solutions in the Pareto frontier
Search Space	• Decision variable space	• Decision variable space and objective space
Artificial Approximation	• Need to construct a composite objective by fix-ups (e.g., weighted sum, scaling) • Outcomes can be altered by the chosen methods (e.g., different weights)	• the set of optimal solutions can be obtained without applying fix-ups

The introduction of some non-classical stochastic evolutionary algorithms (EAs), which use the evolutionary principles of nature to drive the search toward an optimal solution set, have reshaped the landscape of optimization over the last

decades. Among all the EAs, GA has been widely adopted. GA's ability in finding multiple solutions by using a population makes it effective in solving MOOP problems. Besides its stochastic search allows optimization algorithms to locate globally optimal solution more reliably than the deterministic search (e.g., gradient, heuristic search). In a MOOP context, it is crucial to find a set of solutions sparing as far as possible in the Pareto frontier before selecting one based on high-level information. By far, very few applications had truly explored the Pareto-optimality for designing CACC control algorithm. Hence, this study aims to fill this very gap.

4.1 Non-Dominated Sorting Genetic Algorithm II

As mentioned previously, EAs are advantageous in searching for Pareto frontier with their population-based iteration approach. Within the wide spectrum of GA variants, the Non-Dominated Sorting Genetic Algorithm II (NSGA-II) has proven records for providing a good spread of solutions and convergence near the true Pareto frontier[103]. It was a significant improvement from the NSGA-I by addressing three major criticisms: 1) high computational complexity of non-dominated sorting, 2) lack of elitism, and 3) the necessity for a sharing parameter. In MOOP, the rank of a solution is determined by the dominance: X_1 dominates X_2, if 1) X_1 is no worse than X_2 in all objectives, and 2) X_1 is strictly better than X_2 in at least one objective. If X_1 is strictly better than solution X_2, one can say X_1 is strong dominates X_2. A demonstration of the Pareto frontier is shown in Figure 4.1.

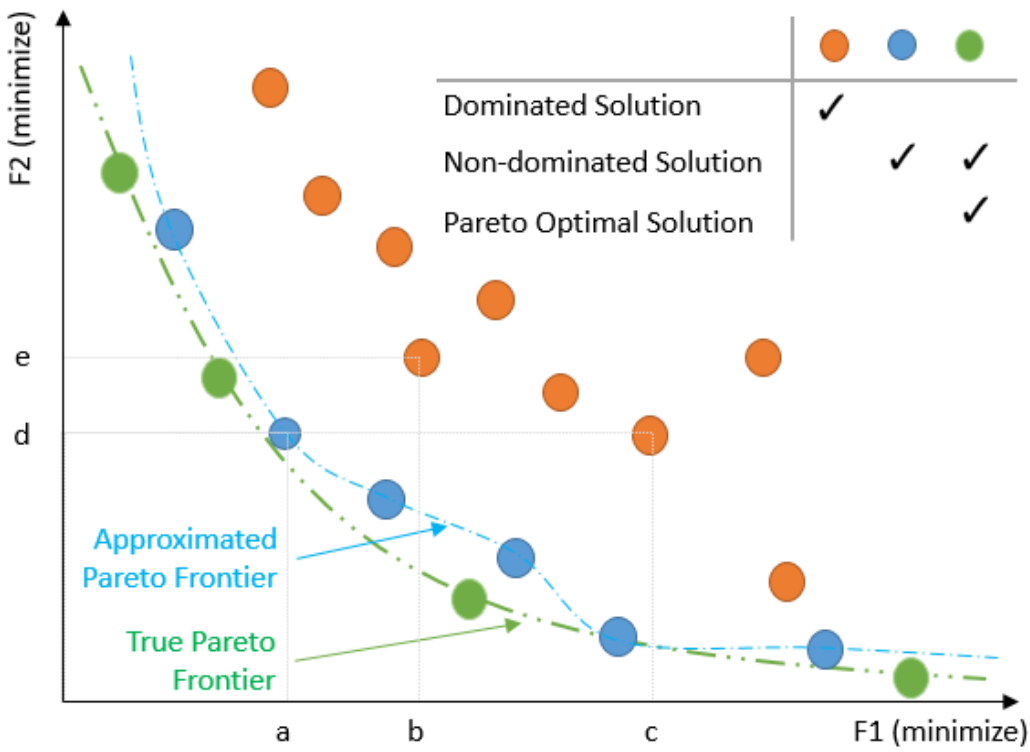

Figure 4.1 Non-dominated solutions and Pareto frontier.

The GA selects individuals based on both non-dominated rank (i.e., fitness value) and diversity of the individual in the current generation (shown in Figure 4.2). After each iteration, a set of optimal solutions are obtained from the Pareto frontier that comprised of non-dominated solutions. Among them, one optimal solution based on pre-determined preferred objective has to be chosen from the Pareto frontier.

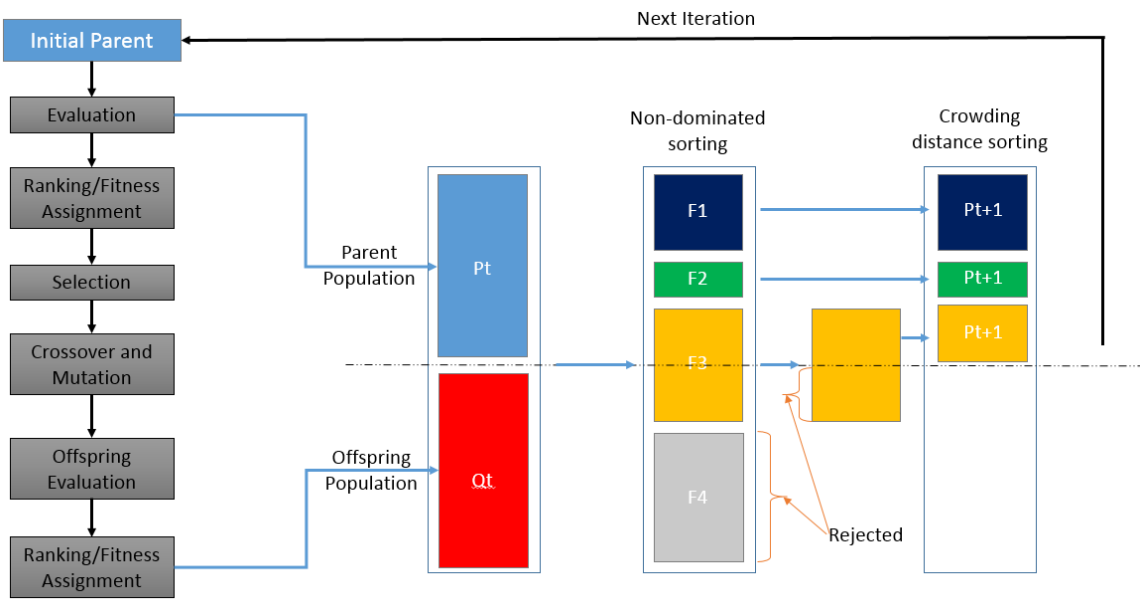

Figure 4.2 Non-dominate sorting and crowding distant sorting.

4.2 Multi-objective Optimization-based CACC Control Algorithm

The proposed MOOP-CACC framework is comprised of four objectives. As being revealed in [53], the lack of vehicle longitudinal control model occasionally yields acceleration that may not be within the powertrain constraint of a vehicle, because of the stochastically search of GA [66]. Hence, the Enhanced Intelligent Driver Model (E-IDM) [104] is used to constraint GA to find feasible solutions that also reflect vehicle powertrain limitation. The IDM proposed by Treiber et al. [28] shows a crash-free collective dynamics, and it implements an intelligent braking strategy aiming to smooth the transitions between acceleration and deceleration. The E-IDM incorporates a new constant acceleration heuristic (CAH) to determine whether a given situation is mildly critical at most or is seriously critical. The mathematically express of the E-IDM can be expressed as below in Equation (4.1).

Under the MOOP-CACC framework, each CACC vehicle has two headway-related variables (i.e., desired time gap and minimum distance) to be optimized. Each pair of the variables can be mapped to acceleration based on the mathematical relationship of the E-IDM model. During each updating interval *t*, the MOOP-CACC control algorithm optimizes the decision above variables for each vehicle for the next time interval. Figure 4.3 illustrates a high-level concept of the objectives to be minimized during the CACC vehicles operations within a platoon.

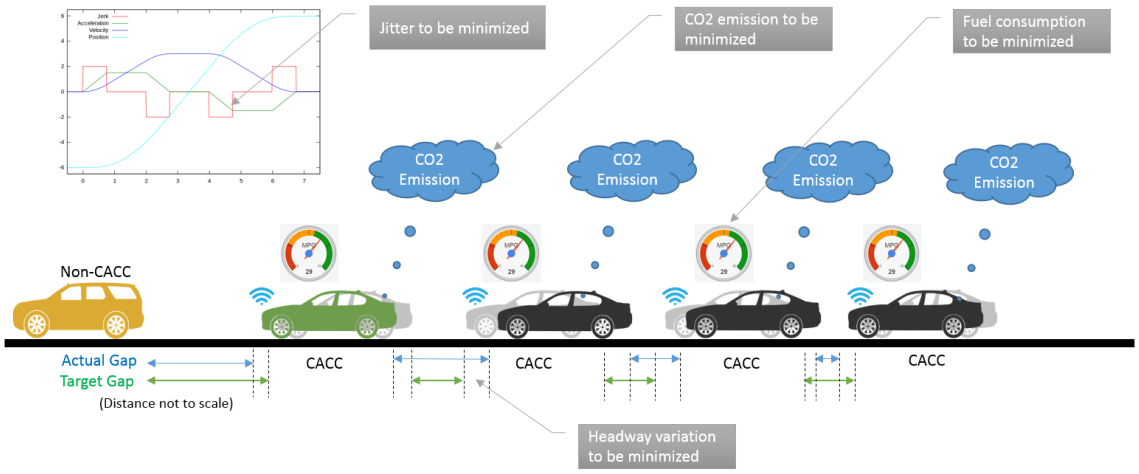

Figure 4.3 Illustrate of platoon-wide objectives.

An overview of the platoon system to be optimized is shown in Figure 4.3. The remainder of this section is to discuss each component of the framework.

$$\ddot{x} = \begin{cases} a\left[1-\left(\frac{\dot{x}}{\dot{x}_{des}}\right)^{\delta}-\left(\frac{s^*(\dot{x},\dot{x}_{lead})}{s_0}\right)^2\right], \ddot{x}_{IDM} \geq \ddot{x}_{CAH} \\ (1-c)\ddot{x}_{IDM} + c\left[\ddot{x}_{CAH} + b\tanh\left(\frac{\ddot{x}_{IDM}-\ddot{x}_{CAH}}{b}\right)\right], \text{ otherwise} \end{cases} \quad (4.1)$$

where

$$\ddot{x}_{CAH} = \begin{cases} \frac{\dot{x}^2 \square \min(\ddot{x}_{lead}, \ddot{x})}{\dot{x}_{lead}^2 - 2x \square \min(\ddot{x}_{lead}, \ddot{x})}, & \dot{x}_{lead}(\dot{x}-\dot{x}_{lead}) \leq -2x\min(\ddot{x}_{lead}, \ddot{x}) \\ \min(\ddot{x}_{lead}, \ddot{x}) - \frac{(\dot{x}-\dot{x}_{lead})^2 \Theta(\dot{x}-\dot{x}_{lead})}{2x}, & \textit{otherwise} \end{cases}$$

$$s^*(\dot{x},\dot{x}_{lead}) = s_0 + \dot{x}T + \frac{\dot{x}(\dot{x}-\dot{x}_{lead})}{2\sqrt{ab}}$$

$\ddot{x}$ – acceleration of ego vehicle, m/s^2

$\ddot{x}_{IDM}$ – acceleration calculated by IDM model, m/s^2

$\ddot{x}_{CAH}$ – acceleration calculated by CAH component, m/s^2

$\ddot{x}_{lead}$ – accleration of leading vehicle, m/s^2

$\dot{x}_{lead}$ – current speed of leading vehicle, m/s

$\dot{x}$ – current speed of ego vehicle, m/s

$\dot{x}_{des}$ – desired speed of ego vehicle, m/s

x – gap between the ego and leading vehicle, m

s_0 – minimum distance, m

s^* – effective minimum gap, s

Θ – Heaviside step function

a – maximum accleration, m/s^2

b – desired deceleration, m/s^2

c – coolness factor

T – desired time gap, s

δ – free accelration exponent

4.2.1 Headway Objective

The Headway objective represents the deviation from target headway and reflects the consistency of a CACC vehicle in adhering to the pre-set headway. This objective function only considers the absolute value of the deviation, which means either positive or negative value of deviation is the same in the view of the objective function. The safety aspect regarding the positive deviation will be addressed by the minimum safe headway constraint below. The objective function of target headway deviation to be minimized can be expressed as Equation (4.2).

$$\sum_{i=1}^{n} \left| H_i - h_i(\mathrm{t}+1) \right| \tag{4.2}$$

where

H_i – target headway for vehicle i within a platoon, s

$h_i(t+1)$ – headway of vehicle i at time interval t+1, s

n – the total number of vehicles within a platoon

4.2.2 Vehicular Jitter Objective

Vehicular jitter is defined as the switch between acceleration and deceleration. The magnitude of change of acceleration should not be overlooked. The comfort threshold is also a dependent of speed, because 2 m/s^2 deceleration yields a significant difference in riding comfort at high speed (e.g., 110 km/h), compared to that at much lower speed (e.g., 40 km/h). Therefore, a coefficient that represents

acceleration effect in different vehicle speeds was adopted. The vehicular jitter to be minimized can be formulated as Equation (4.3).

$$\sum_{i=1}^{n} \beta \bullet \frac{\left|\ddot{x}_i(t+1) - \ddot{x}_i(t)\right|}{\ddot{x}_{comfort}} \tag{4.3}$$

where

$\beta -$ adjustment coefficient for speed

$\ddot{x}_i(t+1) -$ acceleration of vehicle i at t+1, $\mathrm{m/s^2}$

$\ddot{x}_i(t) -$ acceleration of vehicle i at t, $\mathrm{m/s^2}$

$\ddot{x}_{comfort} -$ comfortable threshold for acceleration, $\mathrm{m/s^2}$

4.2.3 Emission and Fuel Consumption Objectives

The third and fourth objectives to be minimized are carbon dioxide emission and fuel consumption, respectively. Due to the microscopic nature of CACC control, an operation-level emission model is desired. Rakha *et al.* [68] proposed a microscopic emission model which is capable of estimating accumulated carbon dioxide and fuel consumption for individual vehicles. Instantaneous vehicle speed and acceleration are used for the models which yield second-by-second estimation objectives above, as shown in Equation (4.4).

$$\begin{cases} \exp(\sum_{i=0}^{3}\sum_{j=0}^{3}(L_{i,j}^{e}\times\dot{x}_i\times\ddot{x}_j)) & \text{for } \ddot{x}\geq 0 \\ \exp(\sum_{i=0}^{3}\sum_{j=0}^{3}(\mathrm{M}_{i,j}^{e}\times\dot{x}_i\times\ddot{x}_j)) & \text{for } \ddot{x}<0 \end{cases} \tag{4.4}$$

Here, $L_{i,j}^{e}$ and $\mathrm{M}_{i,j}^{e}$ are regression coefficients for emission and fuel consumption.

4.2.4 Constraints

The constraints for the decision variables (i.e., desired time gap, and minimum distance) are shown in Equations (4.5) and (4.6). These two types of constraints jointly play a crucial role in determining the range of the gap headway in E-IDM.

$$T_{\mathrm{i,min}} \leq T_i \leq T_{\mathrm{i,max}} \tag{4.5}$$

$$s_{\mathrm{i,min}} \leq s_{0,i} \leq s_{\mathrm{i,max}} \tag{4.6}$$

A minimum headway constraint for each following vehicle is proposed as safety constraint. The collision avoidance constraint for each vehicle is expressed as Equation (4.7). For the leader of a platoon, a longer time headway may be necessary for safety, assuming the vehicle gap is detected by the onboard sensors and that the preceding vehicle is not a CACC vehicle.

$$\frac{x_i(t+1)}{\dot{x}_i(t+1)} \geq h_{\mathrm{i,min}} \tag{4.7}$$

Where,

$h_{i,\min}$ – user-defined minimum headway for vehicle *i*, s

$x_i\ (t+1)$ – bumper-to-bumper distance for vehicle *i* to preceding vehicle at time interval t+1, m

$\dot{x}_i(t+1)$ – speed for vehicle i at time interval *t+1*, $\mathrm{m/s}$

A realistic range of acceleration for modern vehicles should be applied. It is assumed that such powertrain information for each vehicle would be disseminated within platoon under C/AV environment. In actual deployment on the roadway, it is very likely that a heterogeneous vehicle platoon is controlled and individual vehicle powertrain constraint can be expressed as Equation (4.8).

$$\ddot{x}_{\mathrm{i,min}} \le \ddot{x}_i \le \ddot{x}_{\mathrm{i,max}} \tag{4.8}$$

$\ddot{x}_{\mathrm{i,min}}$ – minimum acceleration of vehicle *i*, $\mathrm{m/s^2}$

$\ddot{x}_{\mathrm{i,max}}$ – maximum acceleration of vehicle *i*, $\mathrm{m/s^2}$

The last constraint is the speed limits, as displayed in Equation (4.9). This information is made available via V2I under C/AV environment.

$$\dot{x}_{\min} \le \dot{x}_i \le \dot{x}_{\max} \tag{4.9}$$

$\dot{x}_{\min}$ – minimum allowable speed on a particular roadway, $\mathrm{m/s}$

$\dot{x}_{\max}$ – maximum allowable speed on a particular roadway, $\mathrm{m/s}$

4.3 Numerical Simulation

The goal of the numerical simulation is to evaluate the platoon dynamic and its interactions with GP vehicle of the improved MOOP-CACC control algorithm at small scale with only one platoon. The proposed algorithm has been improved upon the previous study [66] with the introduction of the E-IDM longitudinal control and removal of the safety objective, which is considered redundant along with other constraints. The following behavior of each vehicle is analyzed in MATLAB environment with its multi-objective GA solver available in its Optimization Toolbox [105] . The parameters of the proposed MOOP-CACC are listed in Table 4.2. The four types of control algorithms with eight variations (shown in Table 4.3) are compared.

Table 4.2 MOOP-CACC Parameters

Parameter	Value	Parameter	Value	Parameter	Value
T_i	Decision variable	$T_{\mathrm{i,max}}$	6 s	$T_{\mathrm{i,min}}$	0.5s
$s_{i,0}$	Decision variable	$s_{\mathrm{i,max}}$	0.5m	$s_{\mathrm{i,min}}$	2m
a	2 ms^{-2}	H_i	0.6	$\ddot{x}_{\mathrm{i,max}}$	-6 ms^{-2}
b	2 ms^{-2}	$h_{\mathrm{i,min}}$	1 s	$\ddot{x}_{\mathrm{i,min}}$	3 ms^{-2}
c	0.99	β	1.1	$\dot{x}_{\max}$	125 km/h
δ	4	$\ddot{x}_{comfort}$	1 ms^{-2}	$\dot{x}_{\min}$	30 km/h
$\dot{x}_{des}$	120 km/h	$L^e_{i,j}$, $\mathrm{M}^e_{i,j}$	same as[68]		

Ten randomly generated trajectories of the leading GP vehicle (Figure 4.4), which cover a wide range of conditions (e.g., acceleration out of a low-speed area, rapid deceleration, or regular cursing), are used to demonstrate the behavior of each control algorithm. Each combination of the initial condition of the scenarios is described in Table 4.4.

Table 4.3 Eight Control Algorithms for Testing

Control Algorithm	Short Designation	Note
Human	H	Vehicles behaviors are controlled by the Vissim Wiedemann car-following model. It yields realistic human driving behaviors.
E-IDM	E	The CACC vehicles are controlled by the E-IDM, which is a representation of ACC vehicle behaviors.
SOOP-HW	S-1	The CACC vehicles are controlled by SOOP for Headway objective only.
SOOP-Jitter	S-2	The CACC vehicles are controlled by SOOP for Jittering objective only.
SOOP-CO2	S-3	The CACC vehicles are controlled by SOOP for CO2 emission objective only.
MOOP-HW	M-1	The CACC vehicles are controlled by MOOP with Headway objective preferred.
MOOP-Jitter	M-2	The CACC vehicles are controlled by MOOP with Jittering objective preferred.
MOOP-CO2	M-3	The CACC vehicles are controlled by MOOP with CO2 emission objective preferred.

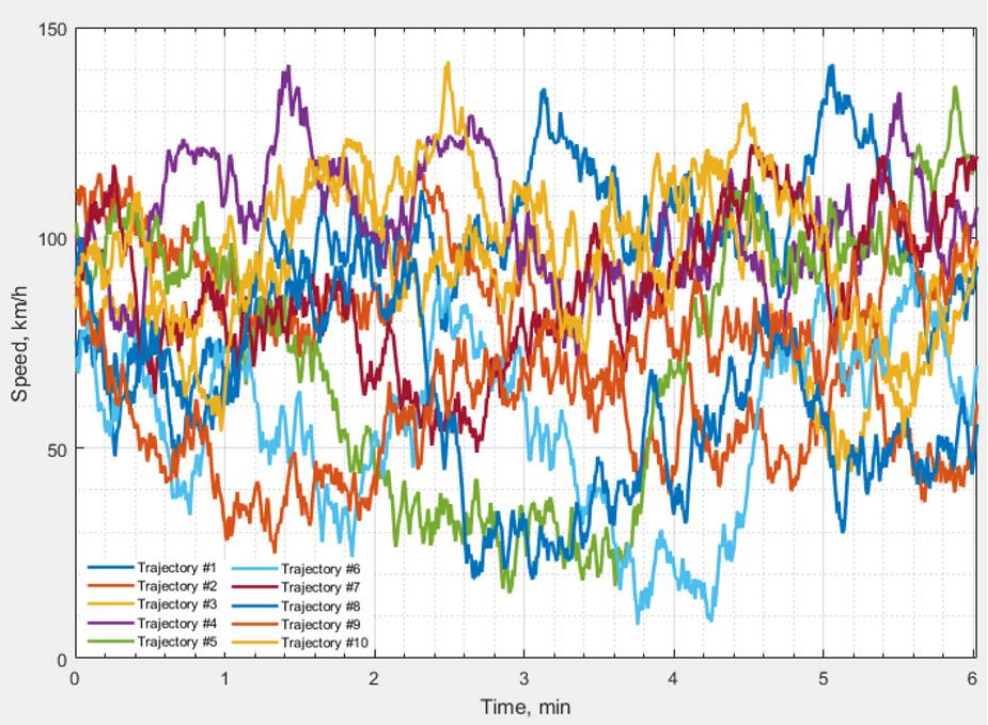

Figure 4.4 Speed profiles for leading GP vehicle.

The case study aims to demonstrate the vehicle behaviors and platoon dynamics of all the CACC control algorithms. The test network is a 15-km hypothetical roadway with one lane configuration. Each scenario consisted of seven vehicles with a GP vehicle that operates in accordance with one of the ten predetermined trajectories in the front, followed by six CACC vehicles with different control algorithms. For the human drivers, the testing was conducted in Vissim with the same predetermined initial conditions of the traffic flow (e.g., spaces, initial speed, etc.). The GP vehicle's speed was controlled by Vissim Common Objective Model (COM) Interface, and the rest was controlled by Vissim's Wiedemann car-following model. The rest of the control algorithms were tested with the same initial conditions.

Table 4.4 Initial Conditions to Be Tested

(a) Initial vehicle position, m

Trajectory ID	GP	CACC	CACC	CACC	CACC	CACC	CACC
1	278.6	230.9	148.8	130.0	31.0	19.2	0.1
2	412.4	340.7	243.6	195.7	118.4	47.3	0.1
3	299.6	271.2	233.0	136.8	101.5	72.5	0.1
4	381.5	292.5	220.2	162.2	81.2	47.3	0.1
5	261.6	249.2	160.3	88.0	68.7	14.5	0.1
6	322.6	252.3	161.7	123.3	73.0	58.2	0.1
7	360.2	312.6	295.0	223.2	131.4	69.7	0.1
8	274.9	214.6	201.1	116.0	79.5	56.3	0.1
9	253.5	230.9	205.6	194.0	158.1	95.0	0.1
10	351.8	324.0	235.0	157.5	135.8	62.8	0.1

(b) Initial vehicle acceleration, m/s^2

Trajectory ID	GP	CACC	CACC	CACC	CACC	CACC	CACC
1	0.81	0.77	-0.77	-0.35	-0.66	-0.96	0.17
2	-0.73	0.25	0.90	0.05	-0.73	-0.95	0.94
3	-0.72	0.50	-0.10	0.77	0.87	-0.94	0.12
4	0.61	-0.30	0.16	-0.29	0.39	-0.51	-0.96
5	-0.20	-0.46	-0.18	0.82	-0.87	0.72	0.60
6	-0.67	0.79	-0.53	0.25	0.51	0.08	-0.53
7	0.86	-0.14	0.81	-0.97	0.51	0.11	0.61
8	-0.30	0.93	0.15	0.86	0.85	0.68	-0.22
9	0.50	0.33	-0.99	0.38	0.42	-0.75	0.73
10	0.45	0.24	0.23	0.99	-0.75	-0.44	0.49

(c) Initial vehicle Speed, km/h

Trajectory ID	GP	CACC	CACC	CACC	CACC	CACC	CACC
1	73	64	74	79	98	76	117
2	109	118	90	119	73	64	93
3	81	94	97	95	105	104	115
4	99	72	110	83	64	106	98
5	102	75	69	93	76	114	83
6	69	105	61	105	108	116	89
7	87	72	64	100	72	61	96
8	89	95	89	76	98	74	93
9	84	118	96	64	91	97	116
10	89	111	94	82	115	117	115

The following shows 3 out of 10 trajectories, which the author believes present a wide range of car-following conditions. However, the results for the 10 trajectories are shown in the Appendix A. The boxplots in Figure 4.5 provide side-by-side comparison among eight controlling algorithms in terms of six performance measures: 1) average headway for all six following vehicles, 2) the platoon length, 3) objective value for Headway objective, 4) objective value for Jitter objective, 5) objective value for Emission objective, and 6) objective value for Fuel Consumption objective. Among all three cases, the human drivers have the highest average platoon headway for 7.5s and highest median objective value for CO_2 emission. However, it is worth noting that the human drivers are excel at achieving the lowest value for Jitter. The E-IDM controlling algorithm exhibits the least variation in the Headway objective. Nevertheless, both S-1 and M-1 are able to achieve even lower Headway objective value than those of E-IDM, but with higher variance. S-2 and M-2 are having difficulty in maintaining a short platoon as the objective function deters vehicle accelerate rapidly to keep up with the platoon.

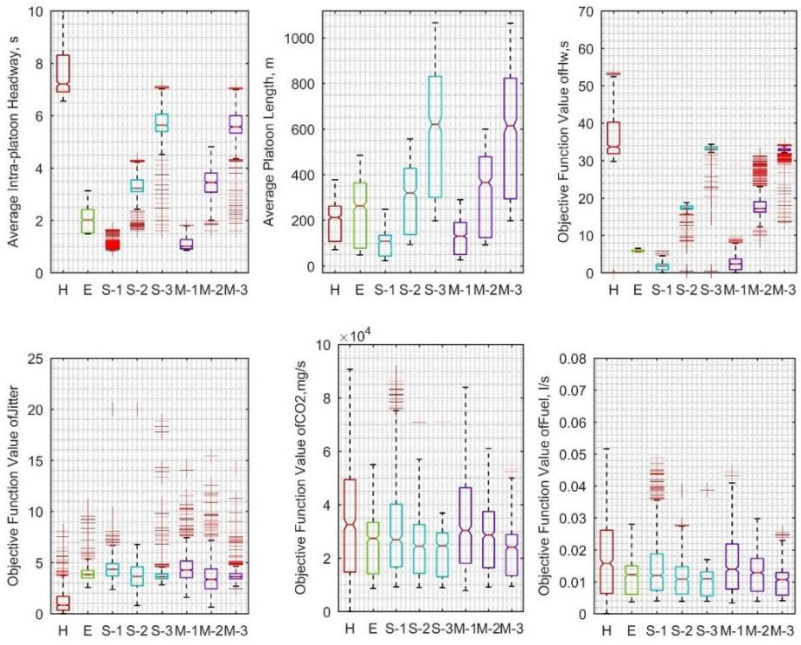

(a) Comparison of trajectory #5

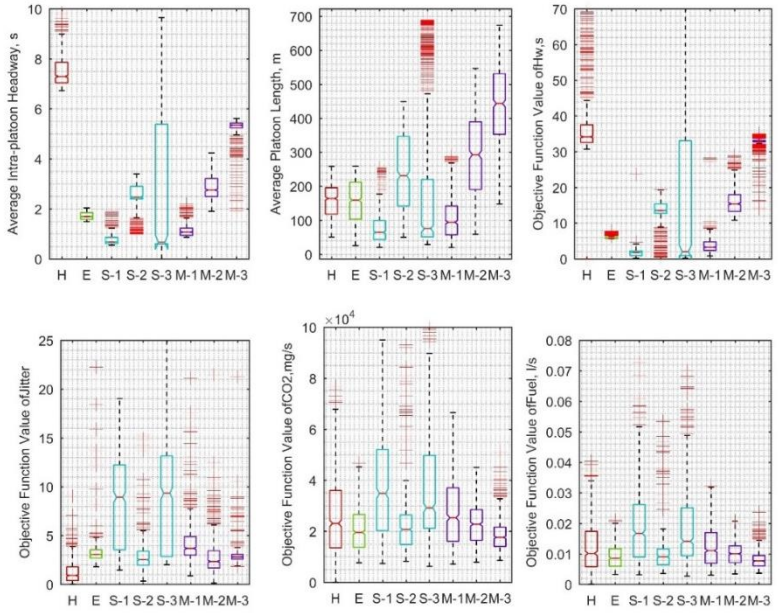

(b) Comparison of trajectory #6

Figure 4.5 Comparison of control algorithms. (H: Human; E: Enhanced IDM; S-1: SOOP for Headway; S-2 SOOP for Jitter, S-3: SOOP for Emission; M-1: MOOP for Headway; M-2 MOOP for Jitter; M-3: MOOP for Emission). (Continued)

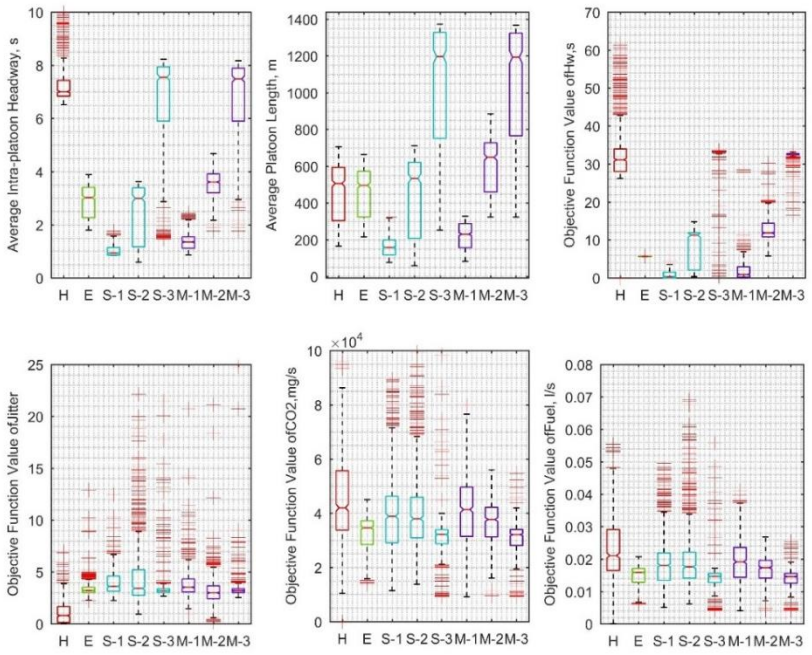

(c) Comparison of Trajectory #10

Figure 4.5 (Continued) Comparison of control algorithms. (H: Human; E: Enhanced IDM; S-1: SOOP for Headway; S-2 SOOP for Jitter, S-3: SOOP for Emission; M-1: MOOP for Headway; M-2 MOOP for Jitter; M-3: MOOP for Emission).

Figure 4.6 shows the dynamics of vehicle behavior of the control algorithm and the impact of the preferred objective when conducting MOOP. Figure 4.6(a) is MOOP-based on Headway objective, whereas in Figure 4.6(b) the preferred objective is set as Jitter. In the latter case, it is evident that the CACC platoon is dissolved into two platoons, judging from the gap shown in the Time-space (T-S) diagram and the Actual Headway. The Jitter objective prevents the vehicle from applying excessive change of acceleration, which in some case is necessary to make adjustments based on traffic turbulence and maintain a closely spaced platoon.

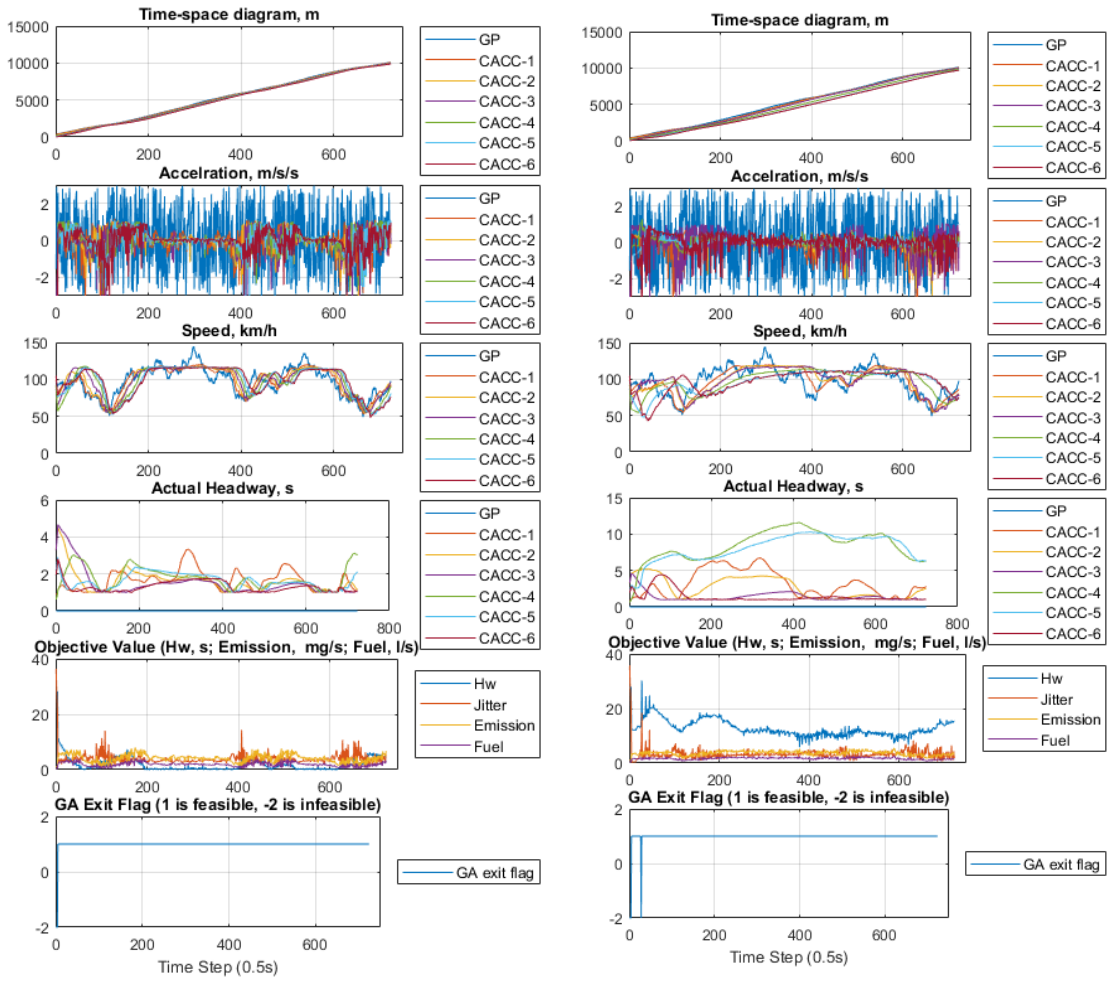

(a) MOOP (Headway as Preferred Objective)

(b) MOOP (Jitter as Preferred Objective)

Figure 4.6 MOOP Platoon dynamic comparison.

The average value of the medians over 10 trajectories are summarized in Table 4.5. As shown, the headway-, optimization-based control algorithms are able to gain significant improvement in mobility, because the shorter the length of a platoon for the same amount of vehicles, the more a given roadway segment could accommodate CACC platoons. The S-1 and M-1 reach 0.85s and 1.07s average

intra-platoon headway among all tested trajectories. The high platoon length values of S-3 and M-3 are due to platoon dissolution because of having CO2 emission as the preferred objective in the optimization. Human drivers produce the least jitter. When comparing S-1 and M-1, the MOOP approach achieves a better balance by accounting for the optimality of the remaining three objectives. M-1 also produces much less variation of the objective value.

Table 4.5 Average Medians over Ten Trajectories

	Hw, s	**Platoon Length, m**	**Obj-HW, s**	**Obj-Jitter**	**Obj-CO2, l/s**	**Obj-Fuel, mg/s**
Human	7.14	278	32.7	0.88	3.42	16.37
E-IDM	2.23	305	5.68	3.48	2.72	12.2
S-1 (Headway)	0.85	116	1.22	5.46	3.57	16.86
S-2 (Jitter)	2.83	389	12.88	4.33	3.16	14.62
S-3 (CO2)	5.14	640	26.87	4.39	2.75	12.48
M- 1 (Headway)	1.07	145	1.98	3.94	3.5	15.94
M-2 (Jitter)	3.27	466	14.51	3.1	3.03	13.67
M-3 (CO2)	6.12	785	32.78	3.38	2.53	11.31

CHAPTER 5

DEVELOPMENT OF MICROSCOPIC SIMULATION FRAMEWORK

5.1 Simulation Framework Architecture

The proposed simulation framework is comprised of Vissim, Vissim COM interface, and Vissim EDM (External Driver Model). The wireless communication module is implemented in EDM. The overall architecture of the framework is shown in Figure 5.1. The detail descriptions of each component are presented in the subsequent sections.

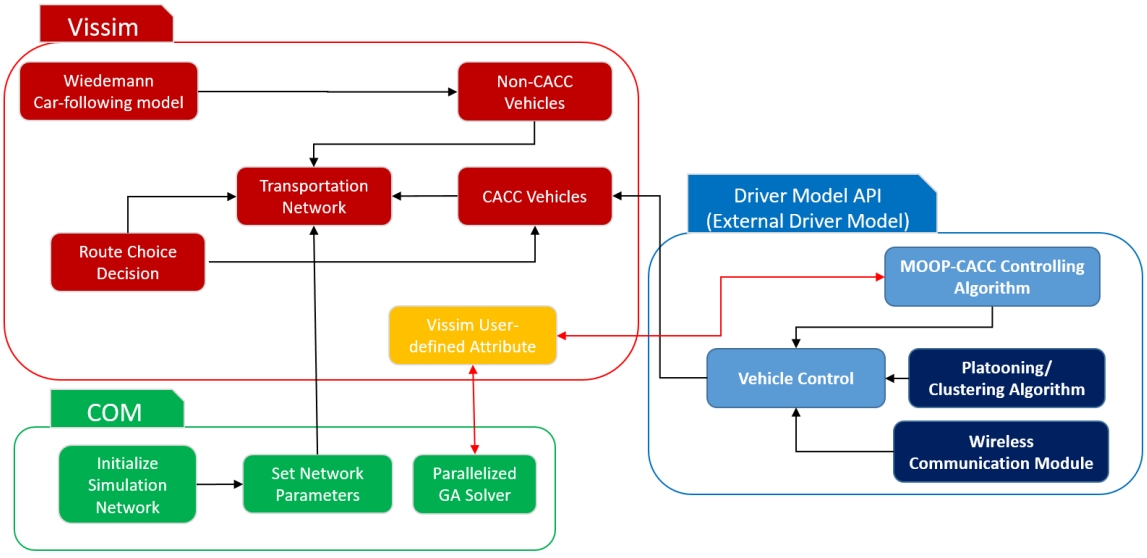

Figure 5.1 Simulation framework architecture.

5.2 Vissim Traffic Simulator

Vissim is a multimodal microscopic traffic simulation software, where each entity (e.g., car, train, pedestrian) is simulated individually. Such capability is one of the most crucial elements of CACC simulation. Vissim implements the Wiedemann psychophysical spacing model [106], which is a long-term evolution of the psychophysical spacing models initially developed by Michaels [107] to address two challenges of the GM-style [108] car-following models: 1) drivers would not allow long gaps to the leading vehicles, and 2) drivers would not be able to capture small differences in relative speeds between the leading vehicle and the subject vehicle. In the psychophysical spacing model, “perceptual threshold" defines a relative speed threshold which is a function of the gap between leading and subject vehicles. The threshold is smaller at low space headways and gradually increases with space headway. A driver only reacts to the stimulus and the relative speed, when the stimulus exceeds the perceptual threshold. In case of long gaps, the threshold becomes infinity, thereby resulting free flow conditions for subject vehicles [109]. Figure 5.2 shows the mechanism of the Wiedemann model. Before going into details for the model, the definitions of the key variable are listed as follows:

- Δ**V:** the difference of velocity
- **AX:** Desired distance between the fronts of two successive vehicles in a standing queue. $AX = Veh_L + MinGap + Rnd \cdot AX_{mult}$ with normally distribution N (0.5, 0.15).
- **BX:** Desired minimum following distance which is a function of AX, a safety delta distance BX, and the speed with $BX = AX + BX * v$.

- **SDV:** Action point where a driver consciously observes that he or she approaches as lower speed leading car. (Compared to the initial work of Wiedemann (1974), an additional threshold CLDV (closing delta velocity) is applied to model additional deceleration by usage of the brakes with a larger variation than SDV).

- **OPDV:** Action point where the following driver notices that he or she is slower than the leading vehicle and starts to accelerate again. The variation of OPDV is large compared to CLDV.

For instance, when the subject vehicle approaching a leading vehicle and ΔX decreasing due to higher subject vehicle's speed shown by a positive ΔV, a driver enters a perception area by crossing the curve of *SDV*. As ΔX reduces further to *CLDV* curve where the driver reacts further to enter an unconscious reaction car-following (the white area bounded by *OPDV*, *SDX*, and *SDV* curves).

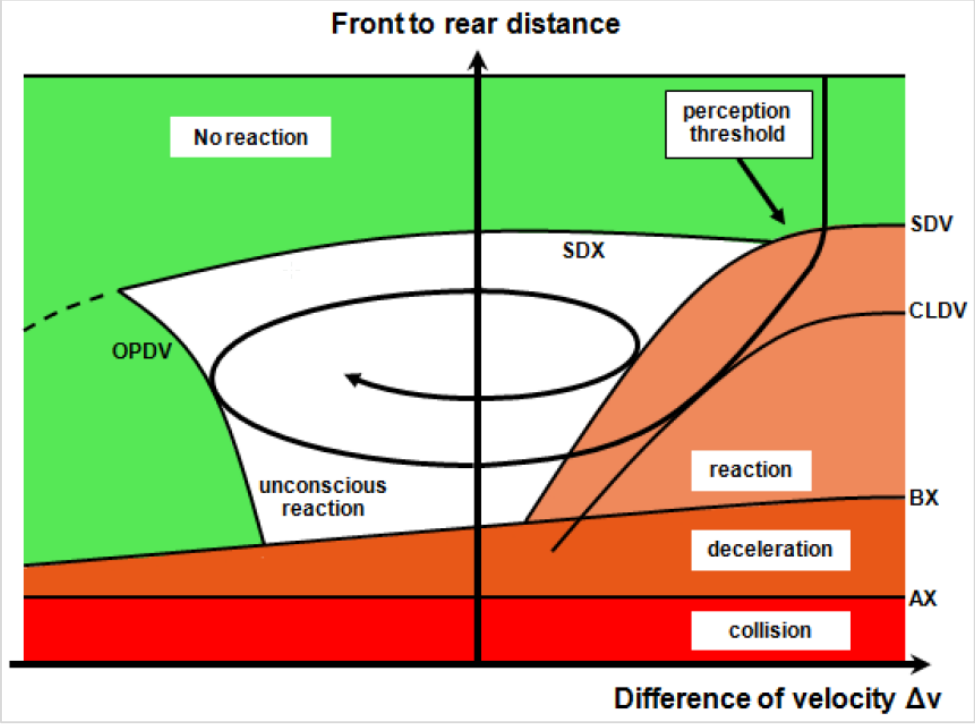

Figure 5.2 Wiedemann car-following model[110].

5.3 Vissim External Driver Model API

In the simulation of CACC, it is crucial for a vehicle to execute the lateral and longitudinal movements suggested by the CACC control algorithms, and to communicate with its surrounding vehicles. The EDM is an add-on from Vissim to fulfill the aforementioned requirements. The EDM allows users to replace the internal Wiedemann car-following model with a custom one. Furthermore, multiple EDMs can be associated with different vehicle types and executed simultaneously. During each simulation time step, the current state of a vehicle and its surrounding traffic information are passed to the EDM which computes the next time step movements (e.g., acceleration, desired lane angle for turning, and target lane) based on the user-defined algorithm. The new CACC control instructions about the vehicle movement are eventually sent back to Vissim as a subset of the overall vehicle movements for the next time step. The EDM contains three functions that are sequentially called by Vissim as shown in Figure 5.3. The variables representing the longitudinal and lateral control of a subject vehicle are shown in Table 5.1.

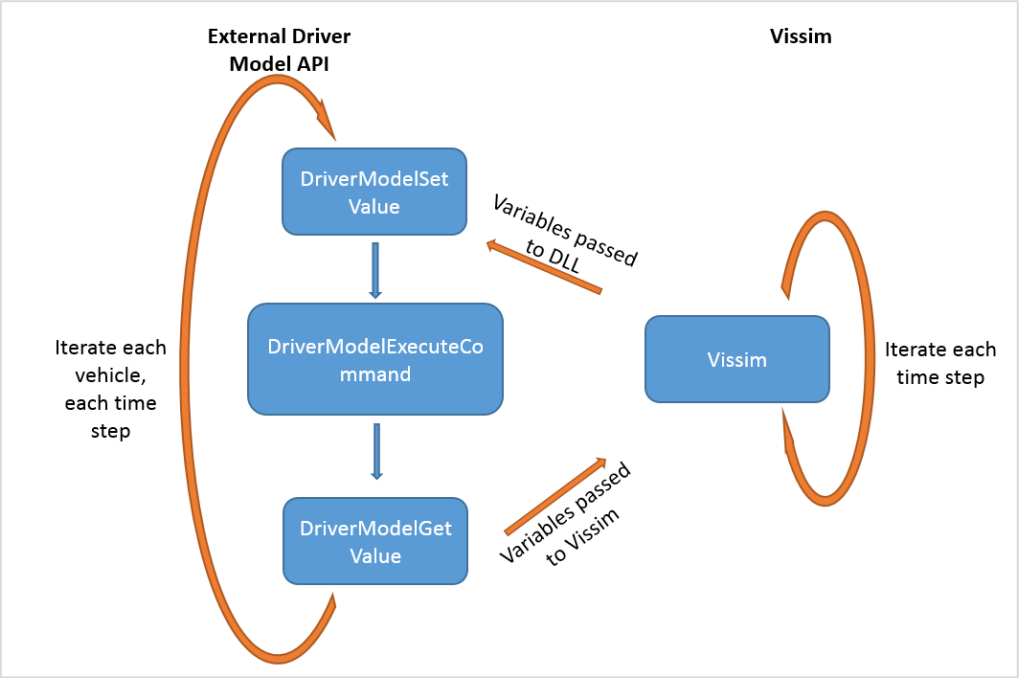

Figure 5.3 Vissim EDM functions.

Adding a stand-alone CACC vehicle into an existing CACC platoon would be of importance for successful operation. An algorithm with respect to platoon seeking and lane changing is also developed and implemented in the EDM, as shown in Figure 5.4. In each iteration, a stand-along CACC starts actively scanning its surrounding traffic and looking for existing platoons that accept a new vehicle. Once a target CACC platoon is identified, the subject CACC vehicle adjusts its following distance for joining the platoon. When a target platoon is in the adjacent lane, a lane change is instructed by the algorithm. Only back-join is allowed in the simulation.

Table 5.1 EDM Longitudinal and Lateral Control Parameters

Object ID	Short Description	Values
Lateral Vehicular Control		
DRIVER_DATA_SIMPLE_ LANECHANGE	Should the EDM or Vissim control the lateral movement	1 to the left, 0 current lane, -1 to the right
DRIVER_DATA_WANTS_ SUGGESTION	Should the EDM allow Vissim initiate a lane change	1 or 0 (logical value)
DRIVER_DATA_DESIRED_ LANE_ANGLE	The angle a vehicle steered in relation to the centerline of a lane	>0 turning left, <0 turning right
DRIVER_DATA_ACTIVE_ _LANE_CHANGE	Initiate a lane change in EDM	1 to the left, 0 no lane change, -1 to the right
DRIVER_DATA_REL_ TARGET_LANE	The intended lane relative to the current lane, rad	1 to the left, 0 no lane change or lane change has completed, -1 to the right
Longitudinal Vehicular Control		
DRIVER_DATA_DESIRED_ ACCELERATION	New acceleration in next time step, m/s^2	Continuous range
DRIVER_DATA_VEH_ DESIRED_VELOCITY	Desired speed, m/s	Continuous range

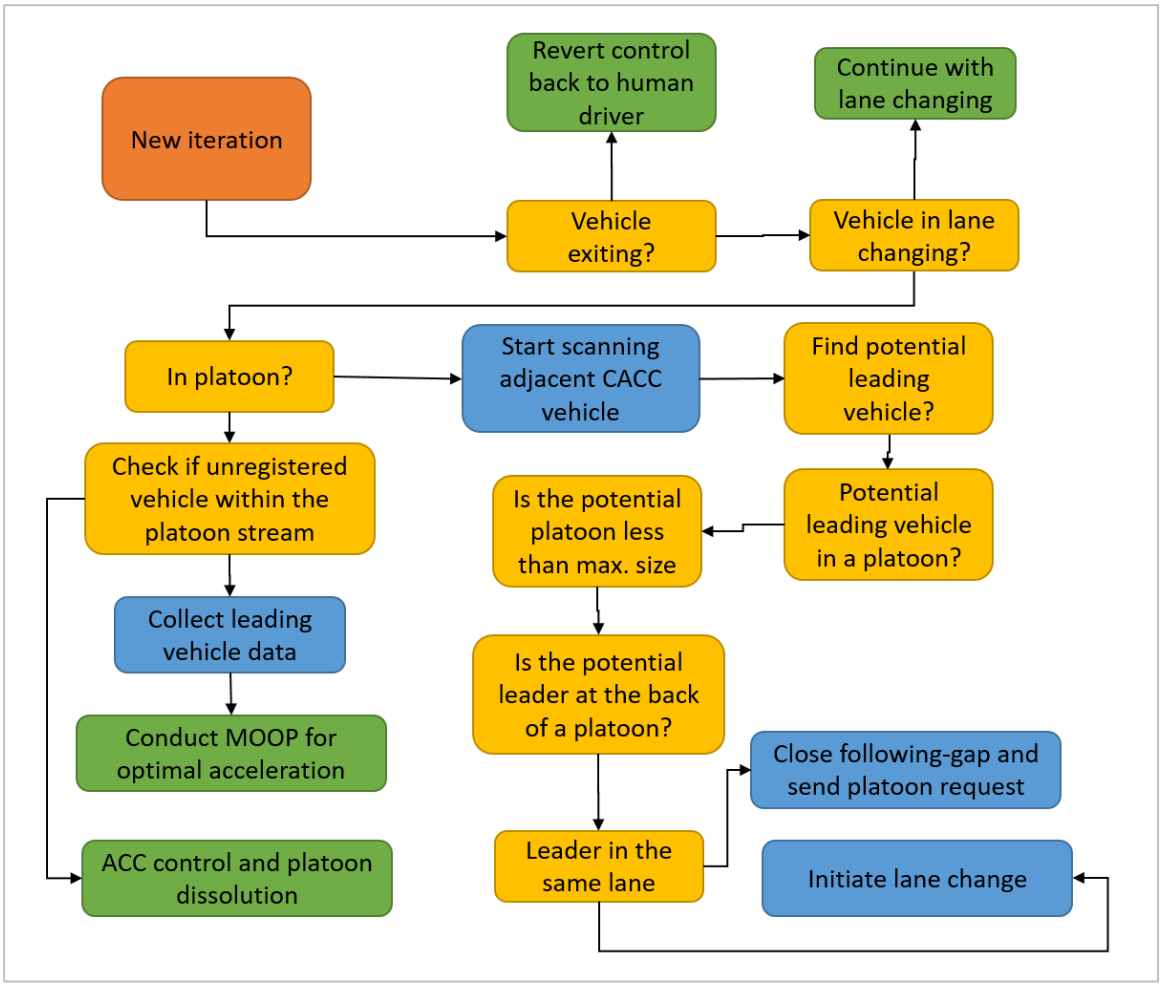

Figure 5.4 CACC platooning algorithm.

5.4 Vissim COM Interface

The Vissim COM Interface allows access to data and objects of the simulation network prior and during simulation. The COM Interface is valuable for simulation automation for hundreds or even thousands of simulation runs. Users can perform the COM Interface programming either in Vissim or via an external program. In addition, COM Interface is able to automate the change of parameters (e.g., MPR, vehicle volume) after each simulation, thus enable continuous run of simulation, which significantly increases the efficiency of the simulation. Python is chosen to manage COM Interface object attributes (e.g., vehicle type, vehicle route) during simulation runtime. A Python-based, open-source NSGA-II solver, Platypus, is adopted for the scaled-up simulation. Furthermore, to tackle the computational complexity of NSGA-II (complexity of $O(MN^2)$, where M is the number of objectives and N is the population size [103]), pipelining was implemented by using Joblib [111], another open-source pipelining package for Python.

The mechanism of implementing vehicular longitudinal control in this study utilizes the user-defined value (UDA) of Vissim. According to the COM interface manual of Vissim, the speed of a vehicle is not an editable object in COM since Vissim 6.0 release. The EDM is the only viable way to implement acceleration from EDM. Fortunately, Vissim allows its API and COM to access the same memory location of the vehicle object via its UDA, which is highly customizable. Hence, a UDA regarding optimal acceleration is created as an intermediate between COM where the optimization is conducted and API where the optimal acceleration is implemented. Additionally, by moving the optimization in COM, the simulation is

able to circumvent the limitation when using EDM API where only one core of a CPU can be used, a restruction of Vissim. As mentioned above, the Joblib Python package is used to accelerate the computation. As shown in Figure 5.5, the time used to conduct optimization for the same amount of platoons is drastically decreased with the aid of pipelining computing. With increased scalability, the simulation testbed is able to implement MOOP-based control algorithm at large transportation network.

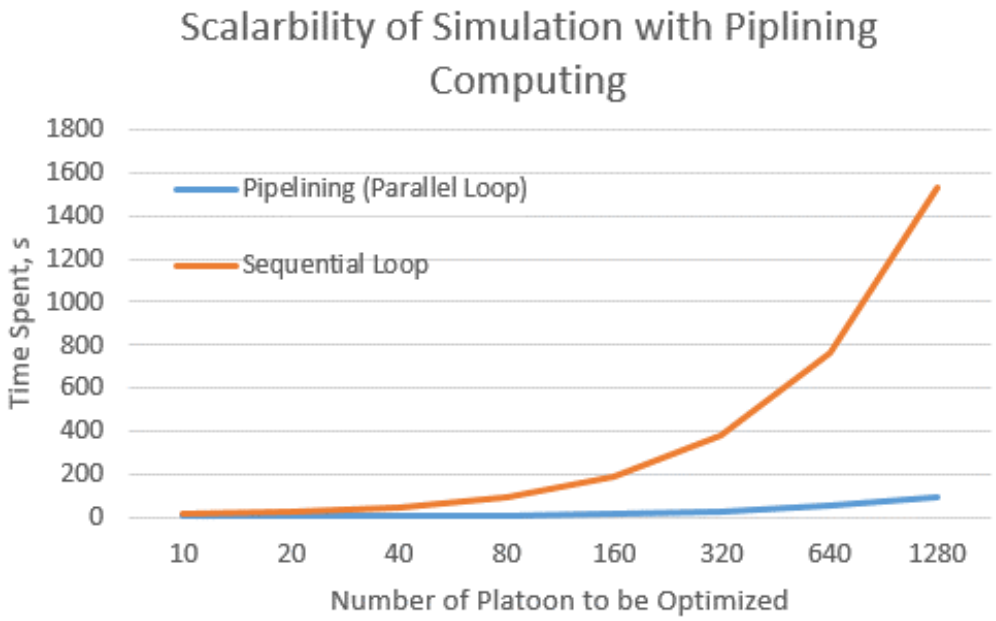

Figure 5.5 Pipelining for scalability.

5.5 Wireless Communication Module

In traffic simulation, the majority of the studies has been conducted under the assumption of perfect V2V or V2I communication, due to the difficulty and scalability of integrating a microscopic TS and a packet-level NS. However, the communication impact when it comes to actual CACC implementation could be significant. A following vehicle could respond to the change of acceleration event before its predecessor's speed has changed measurably because of V2V communication, but small communication delays in the real world can accumulate from one vehicle pair to the next, yielding unstable traffic string. Researchers found that the communication delays along for relaying the beacon message from the first to the fourth vehicle for CACC would be in the order of 400 to 800ms, which is still a significant improvement from the 5 seconds observed from ACC from the first to the fourth vehicle [91].

Data reception rate is determined at a particular communication density level with certain transmission power in wireless communication. It is computationally unsound to conduct packet-level network assessment with thousands of vehicles [78], a typical scale which traffic engineers are accustomed to. Killat et al. [78] prove that the number of scheduled events in ns-2 increases drastically as the traffic density increase within a network, resulting in time-consuming simulation and poor scalability. As such, Killat and Hartenstein [112] proposed an analytical model built from an empirical packet-level networking simulator (i.e., ns-2). The model is developed upon Jiang et al.'s concept of communication density level [77], which is a metric of representing channel load in

vehicular communication in the form of the sensible transmission per unit of time and per unit of the road.

The Killat's model yields the probability of one-hop broadcast reception under DSRC communication. For a single sender, the model is a combination of Nakagami m-distribution fast fading model and the Friis/TRG(two-ray-ground) path loss model [113]. For multiple senders, a statistical model is derived from scenarios of a single sender with the Levenberg-Marquardt method. Compared to pure ns-2-based approach, the hybrid approach is more computationally tractable (e.g., 500 speedup factor in a network of 2500 to 3000 vehicles) with similar characteristics of transmission simulated by ns-2. The probability of successful packet reception by the receiving vehicle can be calculated by Equation (5.1). The communication density is calculated as shown in Equation (5.2).

$$P_R(x,\delta,\psi,f) = e^{-3(x/\psi)^2}(1+\sum_{i=1}^{4} h_i(\xi,\psi)(\frac{x}{\psi})^i) \quad (5.1)$$

$h_i(\xi,\psi)$ -two-dimensional polynomial

ξ - communication density

ψ - transmission power, m

$$\xi = \delta \square \psi \square f \quad (5.2)$$

δ - vehicles per kilometer that periodically broadcast messages, veh/km

f - transmission rate, Hz

ξ, ψ as previously defined

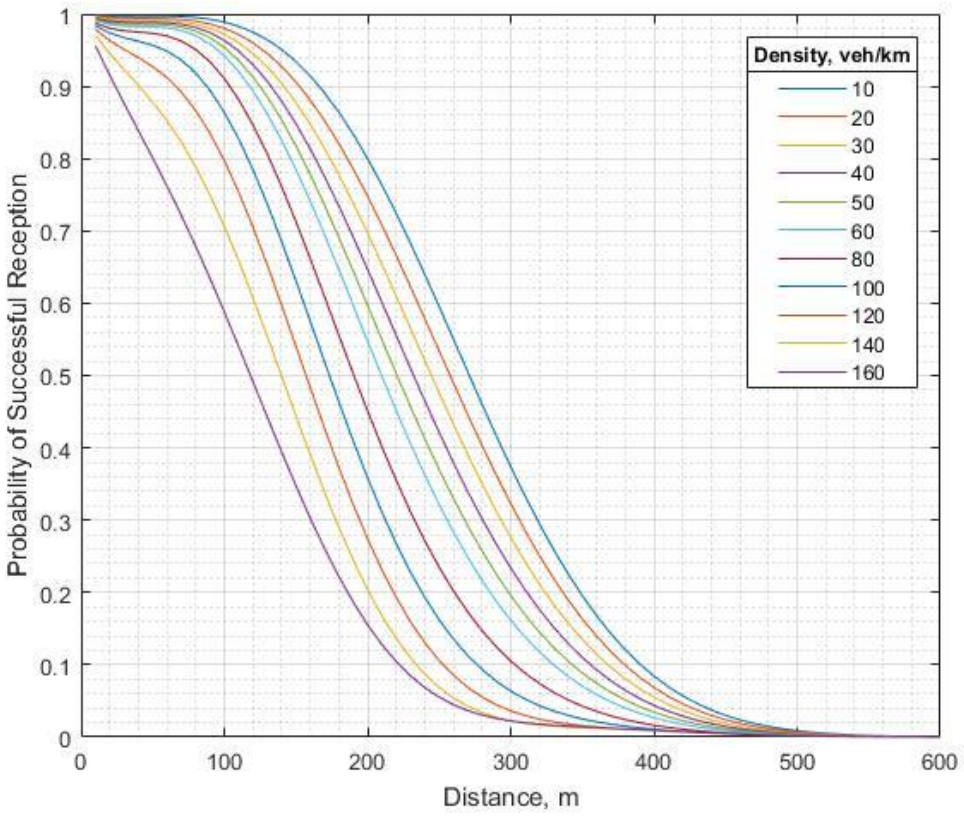

Figure 5.6 Killat's wireless communication model.

Figure 5.6 shows the probability density curve of the DSRC wireless communication model under different communication densities, with the power range of 300m [91] and the transmission frequency of 10Hz [54]. It is worth pointing out the assumptions made for the wireless communication module: 1) the channel access, defined as the delay between the arrival of a frame at the MAC layer and

the transmission over the air, is assumed zero. 2) high data rate in this simulation has the same level of countering noise and interferences of using low data rate, which may not be the case under certain circumstances.

With all the modules developed, the proposed framework is capable of assessing the potential network-level benefits, such as total travel time, total throughput, total delay, and average speed, under a wide range of traffic scenarios. Moreover, the framework can also evaluate localized impacts of CACC (e.g., specific O-D travel time, headway distribution).

Figure 5.7 illustrates the communication test based on the Nakagami fading channel model. It is assumed that for each simulation time step, a CACC vehicle is able to have a total of five attempts to transmit the vehicle status message. Each attempt is considered as an independent experiment. If the latest packet is not available, a CACC vehicle will use the 2^{nd} latest packet to conduct the optimization. Hence, as long as a packet is successfully transmitted within the five attempts, the wireless transmission is deemed successfully for communicating vehicle status. The reception probability is computed for each platooned CACC vehicle based on Equation (5.1). Then a random number with the range of [0, 1] is generated. If the number if less than the current reception probability, a transmission attempt is considered successful.

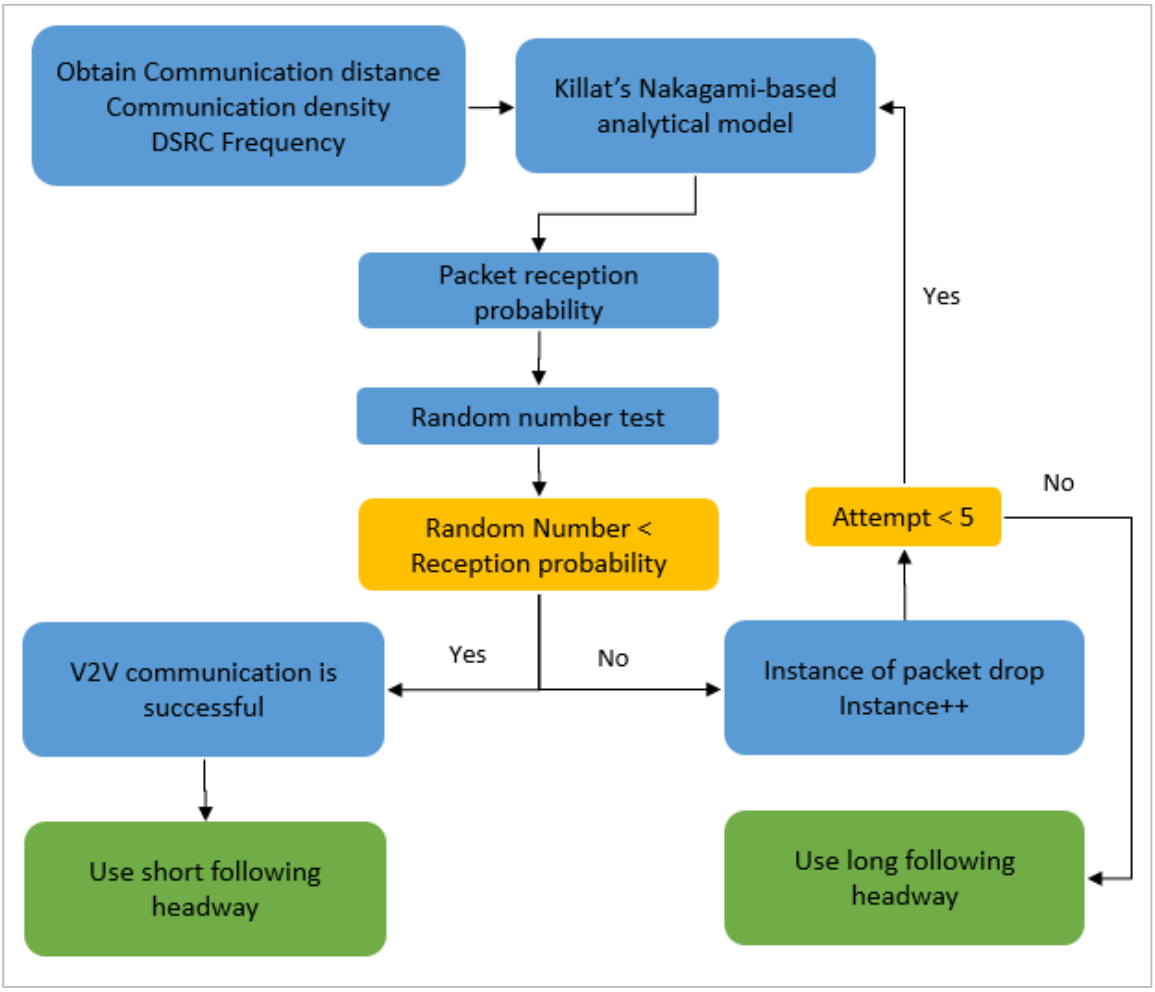

Figure 5.7 DSRC communication testing procedure.

CHAPTER 6

SIMULATION STUDY

6.1 Simulation Network

6.1.1 Network Calibration

An 8-km (5-mile) segment of Interstate Highway I-66 outside of the beltway (I-495) of Washington D.C. is selected as the freeway testbed, as shown in Figure 6.1. The roadway is a major east-west commuter corridor with four lanes in each direction. This freeway segment has recurring congestions during weekdays, specifically in eastbound direction in the morning and westbound direction in the afternoon. The leftmost lane is an HOV lane, and it has unrestricted access to the adjacent lanes. Network calibration has been completed by using two independent data sources (i.e., INRIX TMC travel time and RTMS volume) for the I-66 network and the result is summarized in Appendix B. There are two RTMS located before the exits of the freeway as marked on Figure 6.1.

Figure 6.1 I-66 testbed.

6.1.2 Managed Lane Strategy

Four managed lane strategies were proposed to test the operational impacts of CACC deployment. A break-down list of the managed lane strategy is shown in Table 6.1.

- **Base case (BASE):** This scenario serves as the base condition of the I-66 segment for this study. As stated, an HOV lane is implemented in the leftmost lane of the roadway and the network has been calibrated.
- **Unmanaged lane (UML):** In this strategy, the HOV lane was revoked, and current HOV vehicles are treated as GP vehicles. CACC vehicles are not given priority use of any lane, and they operate along with GP vehicles/human-driven vehicles.
- **Mixed managed lane (MML):** This strategy aims to utilize the current lane use layout of the network and to provide priority usage of HOV lane for CACC vehicles. It investigates the effectiveness of CACC when mixed with HOV traffic.
- **Dedicated CACC lane (DL):** The exclusive access to the leftmost lane for CACC vehicles are studied. A homogenous CACC traffic is believed to be beneficial for the CACC operation. The merging impact of CACC vehicles to the leftmost lane can be studied as well. Like in UML, the HOV vehicles are treated as GP vehicles in this strategy.
- **Dedicated CACC lane with Access Control (DLA):** This strategy is essentially a dedicated CACC lane mentioned above but with access control where a CACC vehicle is only able to merge out of the managed lane at designated locations when its destination is reached. Therefore, the weaving activities are aggregated at certain locations of the segment. It is formulated to insulate the CACC platoon form the potential impacts of weaving activities.

Table 6.1 Managed Lane Strategies for Testing

Strategy	4th (leftmost)	3rd	2nd	1st (rightmost)	Access Control
BASE	HOV	GP	GP	GP	N
UML	GP+ CACC	GP+ CACC	GP+ CACC	GP+ CACC	N
MML	CACC + HOV	GP	GP	GP	N
DL	CACC	GP	GP	GP	N
DLA	CACC	GP	GP	GP	Y

An overview of the simulation environment is shown in Table 6.2. The simulation period for one replication is set as 3900s, with 300 seconds of a warm-up period to load traffic to the network. For each combination of managed lane strategy and MPR, five random replications are run to capture the variability of the traffic flow. The simulation resolution is set as two, which means the vehicle trajectory is calculated for every 0.5s. The optimization is conducted in every five time steps of the simulation, which is 2.5s. The simulation is run on a dual-Xeon computer with 32 logical cores and 96 GB RAM with the following assumptions:

- Calibrated vehicle behaviors in Vissim realistically represent the road users' driving behaviors.
- The vehicle controller is free of control errors.

- The lateral control for platoon formation is conducted by human drivers with recommendations for lane change from the CACC system.
- Human-driven vehicles treat CACC vehicles as another human-driven vehicle. There are no indications whether a vehicle is equipped with CACC system.

Table 6.2 Simulation Configuration

Parameter	**Value**	**Parameter**	**Value**
Simulation Period	3900s	CPU	Dual Xeon E5-2670, 16 logical cores per CPU
Network loading/warm-up period	300s	RAM	96 GB
Simulation Replication	5	Optimization Interval	2.5s (5 simulation time step)
Simulation Resolution	2		

6.2 Simulation Results

6.2.1 Traffic Flow Performance Measure

This section focus on the conventional traffic flow performance measures. The speed-flow diagrams for RTMS 1 and 2 are shown in Figure 6.2 respectively. The speed-flow diagram has two different qualities of traffic flow for the same traffic volume, separated by the maximum value of volume. The stable flow region represents free traffic with relatively high speed and low density; whereas the unstable flow region signifies interrupted traffic flow with low speed and high density. Figure 6.2 shows when the MPR is at 10% and 20%, unstable flow occurs at DL and DLA, due to the lane use imbalance: less than 20% of the total traffic volume was assigned to the managed lane. In comparison, UML and MML kept the traffic flow in the stable region. With the introduction of CACC vehicles, the unstable flow observed in the BASE was even eliminated. When the MPR reaches 30% or above, the DLA started to produce stable flow at a higher speed, with its data points concentrating at the upper right corner of the speed-flow curve. As the MPR grows from 30% to 50%, only DLA maintains the same performance, whereas the observations of the remaining three strategies shift downward. The observations from the RTMS 2 reveal a similar pattern. When MPR is less than 30%, UML and MML yield better performance. The unstable flow region shown in the BASE is eliminated by the introduction of CACC even at 10% MPR. The DLA shows its benefits when MPR reaches 30% and above. As an overall trend, the traffic flow in RTMS 2 does not show as much of degradation as the one in RTMS 1, when the MPR reaches above 30%. Such phenomenon indicates that,

at high traffic demand, the DLA is able to accommodate more traffic, consequently increasing the carrying capacity of the roadway. In comparison, UML and MML do not yield homogenous traffic flow for CACC platooning. Admittedly, DL generates a homogenous CACC traffic flow, but the disruptions of CACC weaving into the managed lane decrease the capacity of CACC lane. Hence DL does not successfully avert the degradation occurred in UML and MML.

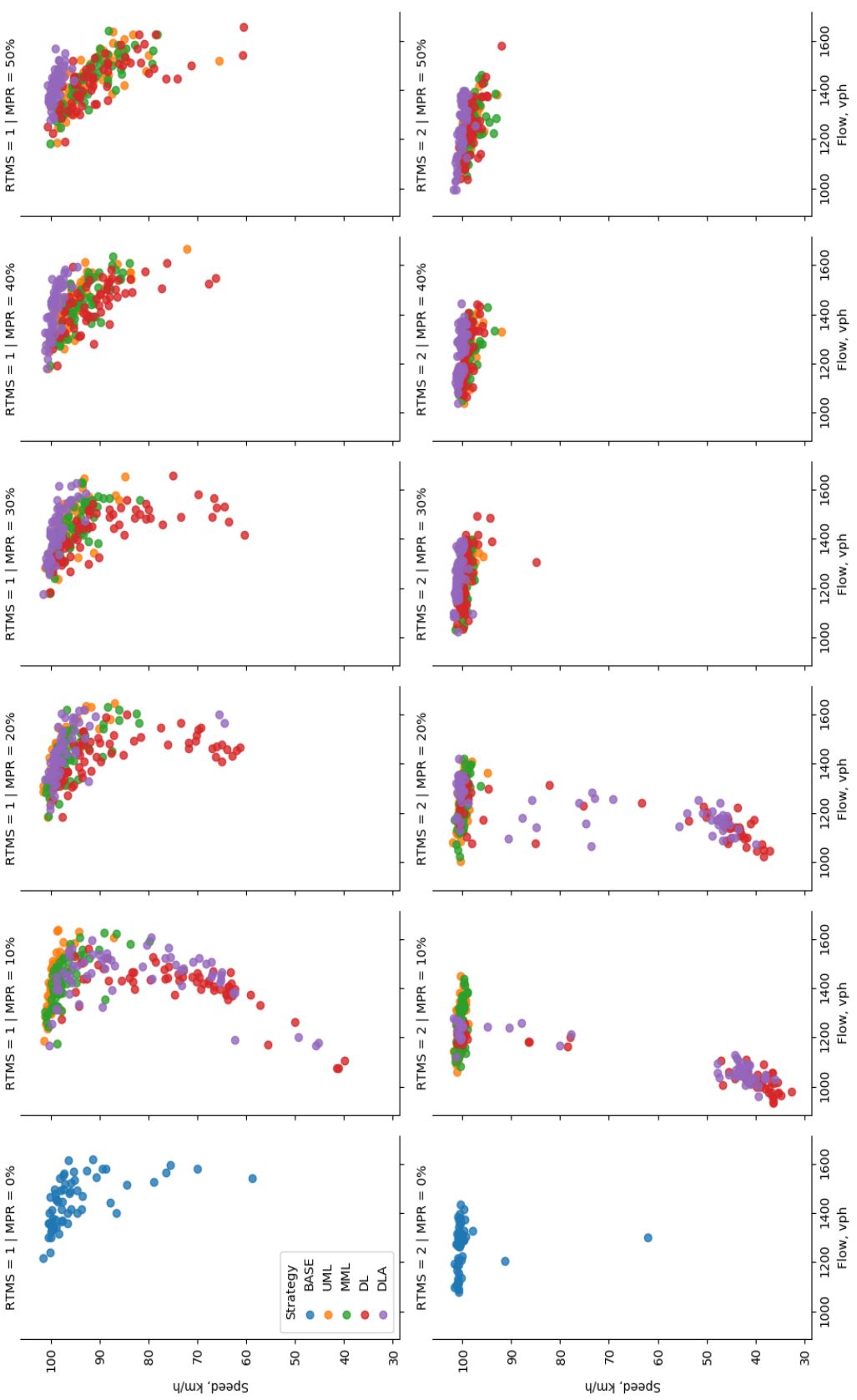

Figure 6.2 Observed speed-flow diagram.

Compared to spot performance measure obtained by RTMS, network performance measures offer a more comprehensive view in assessing the potential benefits brought by CACC. The network throughput shown in Figure 6.3(a) represents the total amount of vehicles that have reached their destination during the simulation. The original network is able to serve approximately 7900 vph. With the introduction of 10% MPR of CACC, the network throughput is increased by 550 vph and 300 vph for UML and MML, respectively. The improvement reaches the highest level-8450 vph and 8400 vph-at 20% MPR for UML and at 40% MPR for MML respectively. By comparing the O-D demand of each traffic generation zone of the network, it is concluded that all the demand within the simulation has been met and as such, the vehicle arrived levels off at 8450 vph. DL and DLA both have a negative impact on the overall throughputs when MPR is below 30%. The two dedicated lane deployment strategies appear undesirable for CACC deployment on freeways under low MPRs, because such implementation would likely degrade the system performance by assigning more GP vehicles to the rest of the GP lanes. At the 40% MPR, the demand of the network is met as well in DL and DLA.

Another commonly-used network performance measure is vehicle hour traveled (VHT), which represents the accumulated amount of time that all the vehicle spent on a certain section of a highway over a period. Judging from Figure 6.3(b) , the VHT decreases to 60.1 vehicle-hour at 10% MPR with MML from 67.8 vehicle-hour observed at the base case. UML achieves the best

improvement in reducing VHT to 60 vehicle-hour. When the MPR reaches 40%, the VHT of DLA reaches the lowest value-60.5 vehicle-hour.

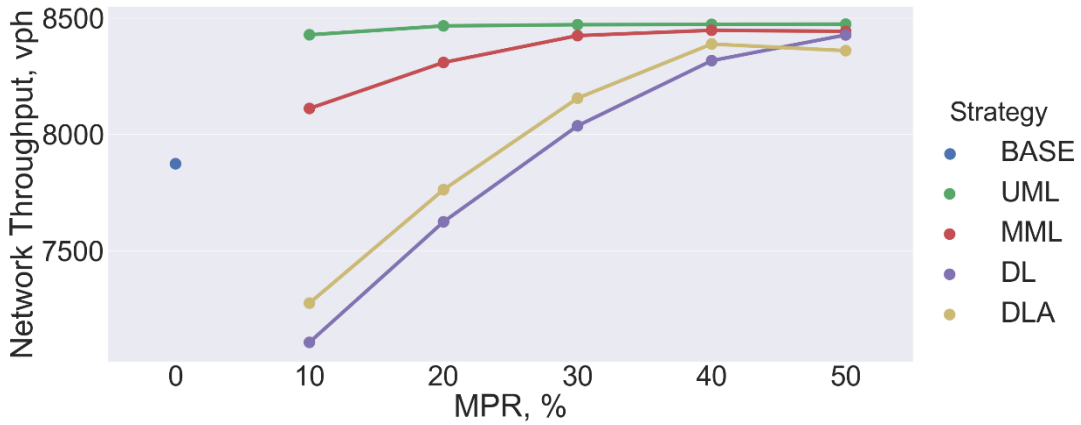

(a) Network throughput

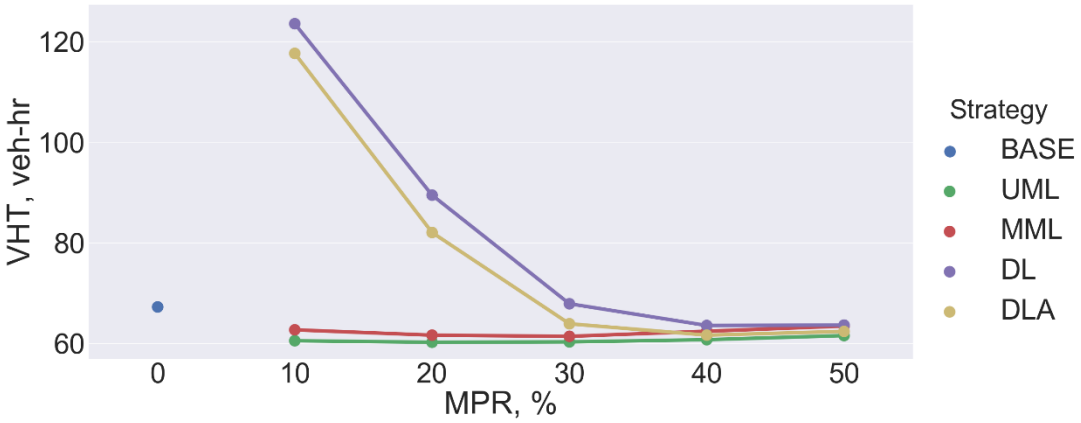

(b) Vehicle hour traveled

Figure 6.3 Network-wide performance measure.

The travel time for the mainline of the I-66 is observed and displayed in Figure 6.4. The mainline travel time represents the amount of time it takes for a

vehicle to traverse from the entry point on the east of the mainline to the exiting point of the mainline in the west. UML and MML produce lower and more consistent travel times among all the MPRs for both GP and CACC vehicles. The travel time decreases from 440 seconds to 400 seconds, a 9% reduction at 10% MPR. The break-even MPR for DL and DLA in comparison to the BASE is 30% MPR. The lowest mainline travel time, 410 seconds, is observed at 30% MPR for DL. The travel time for GP vehicle reaches the same level of the base case when MPR is 40% and above, which indicates that DL is able to accommodate up to 50% of the original traffic demand. Observing the ranges of mainline travel times under the UML and MML in Figure 6.5, CACC vehicles achieve more reliable mainline travel time as not only the median of the travel time but also the variance of the travel time decrease. DLA systematically performs better than DL among all levels of MPR by yielding a lower median. The lowest median is observed at 50% MPR when DLA is implemented.

Figure 6.4 Network mainline travel time.

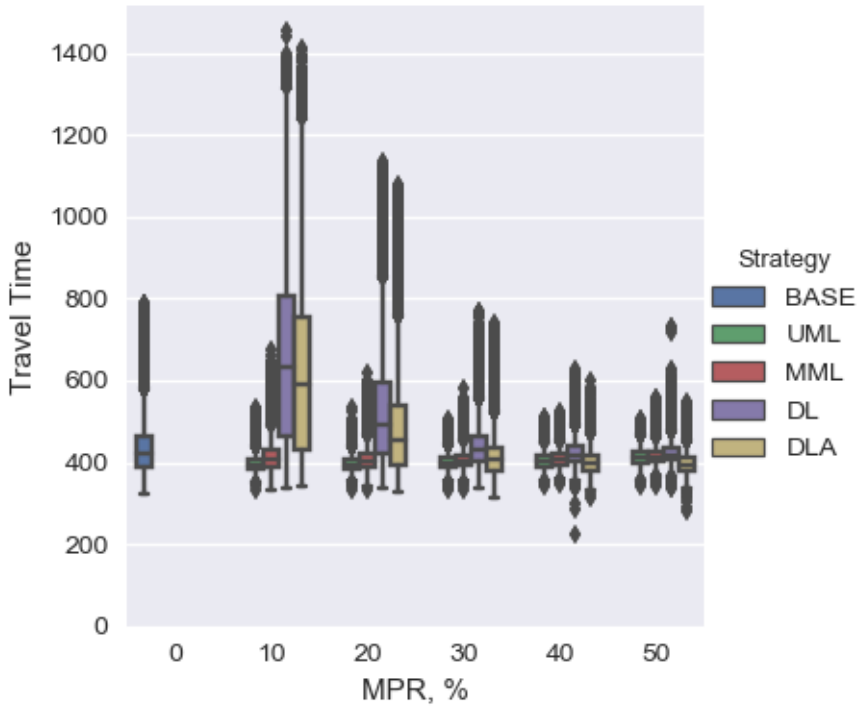

Figure 6.5 Mainline travel time for all vehicles.

Speed variance, related to the crash frequency [114], is used as an SSAM to evaluate the segment level safety performance. It has been found that roads with a higher speed variance had a higher crash rate than the roads with a lower speed variance [115]. The boxplot shown in Figure 6.6 exhibit the speed variance. It shows that the traffic flow is smoothed by the reduction of veribility at low MPR (i.e., 20% or less) in UML and MML. It was also observed that at mid-range MPRs, the speed variances are slightly increased, but they are still lower than BASE. The speed variances were increased at low-range MPRs for DL and DLA. DLA produces more consistent speed than DL at mid-range MPR and it shows a higher median value, compared to the remaining three managed lane strategies.

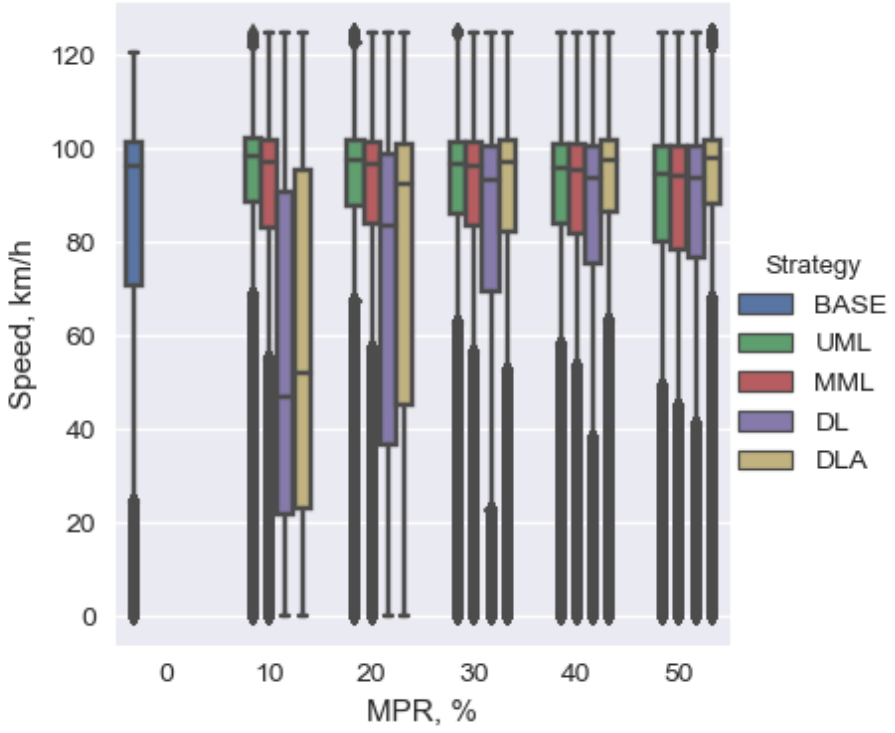

Figure 6.6 Speed variance.

6.2.2 Platoon Performance Measure

In this section, a set of rarely-examined MOEs is introduced. They are related to CACC platoon and made possible by the high customizability of Vissim. One of the major benefits of CACC is the vehicular platoon with short intra-platoon following distance enabled by V2V communication. Thus, the number of vehicles for forming platoons is crucial. As exhibited in Figure 6.7, providing exclusive use of a managed lane such as DL and DLA, shows a positive effect on the growth of platooned CACC vehicles. At 10% MPR, the percentage of platooned CACC vehicle in DL is only 24%, which is significantly lower than the rest of the strategies. This is mainly because of the disruption to platoons from CACC vehicles trying to get onto the CACC lane. That is, once an unregistered vehicle merges into an existing platoon, the platoon will be dissolved into two sub platoons or dissolved entirely, depending on the initial size. With access control for the DL, the potential disruptions to the CACC platoons on the CACC lane was minimized, as displayed in Figure 6.7. As the MPR increases, the percentage of platooned CACC vehicles starts to decrease in UML and MML strategies. Consistent improvements among all MPRs for DLA were demonstrated, indicating the effectiveness of DLA strategy. The highest percentage for platooned CACC is 51% at 50% MPR. At 30% MPR, the percentage of platoon CACC vehicles in DLA starts to exceed that of MML. Regardless of the platoon size and platoon number, the more CACC vehicles are in a platoon, the higher the percentage of short-distance intra-platooning car-following occurs. When MPR is below 30%, UML and MML seem to be suitable choices. Between UML and MML, however, the latter produces a higher

percentage of platooned CACC vehicles, as grouping CACC vehicle as much as possible in one lane could increase the likelihood of platoon formation. The low percentage of platooned CACC vehicles observed in DL is because of the aforementioned weaving activity of CACC vehicles into the managed lane at any locations.

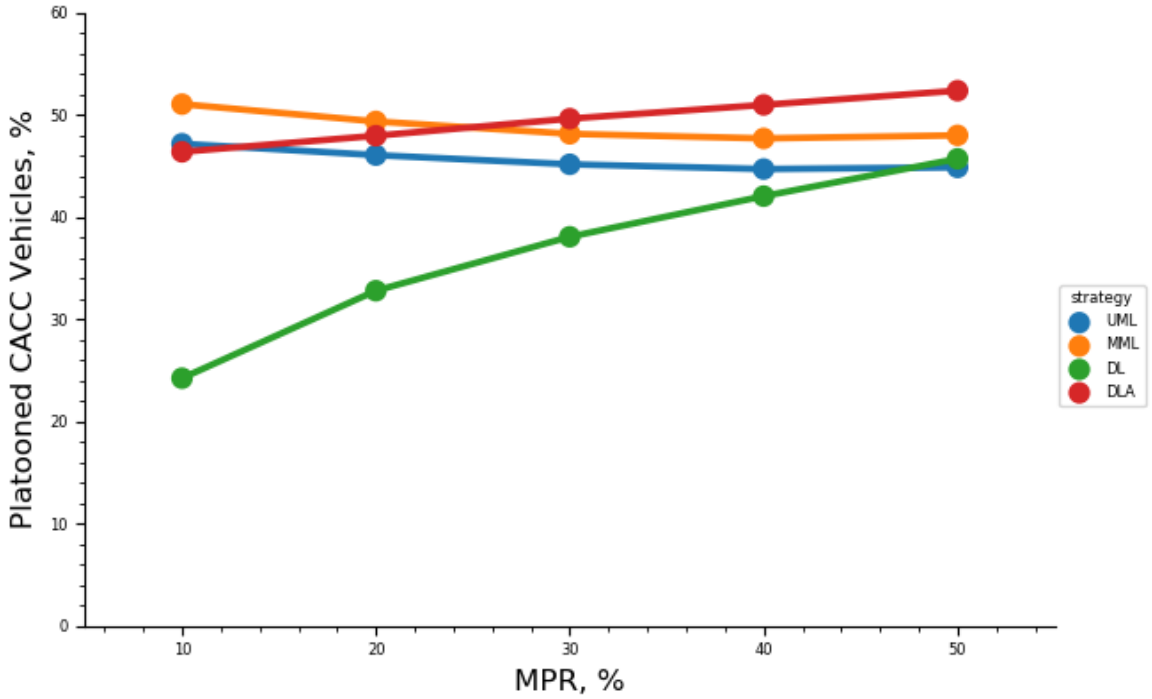

Figure 6.7 Percentage of CACC vehicles in platoons.

Figure 6.8(a) represents the average number of platoons (with vehicle no less than three) at any given simulation second. Figure 6.8(b) exhibits the mean position of a CACC vehicle. When a CACC platoon is formed, each vehicle of the platoon is assigned an ordinal number to identify its position within a platoon. The leader of a platoon is assigned as one. The mean position factors in all active CACC vehicles in the network. As shown in Table 6.3, the total number of platoons

as well as the mean platoon position decrease as more and more CACC vehicles being added into the network in UML and MML. It indicates that the benefits of these two strategies diminish as the MPR increases. They provide a better opportunity for CACC vehicles to form platoons when the MPR is below 30%.

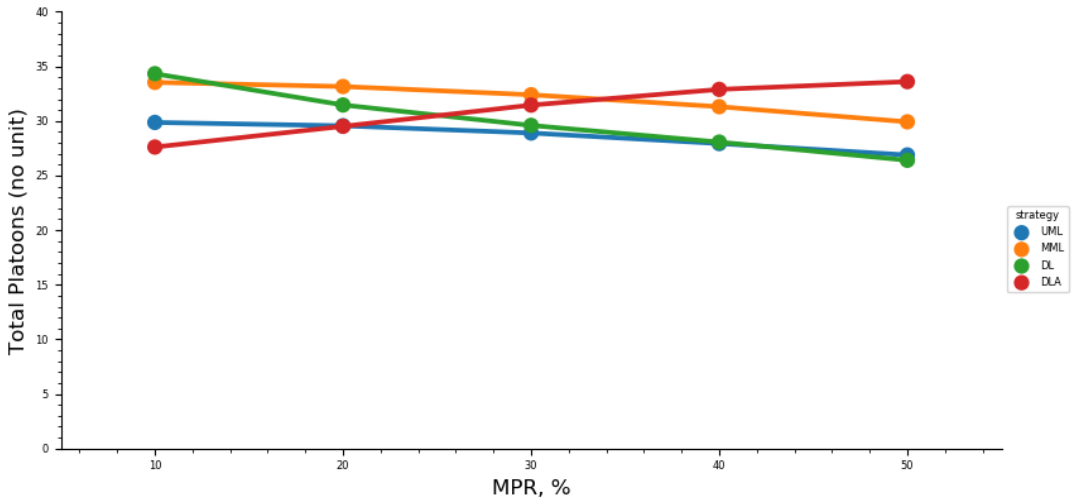

(a) Number of CACC platoons.

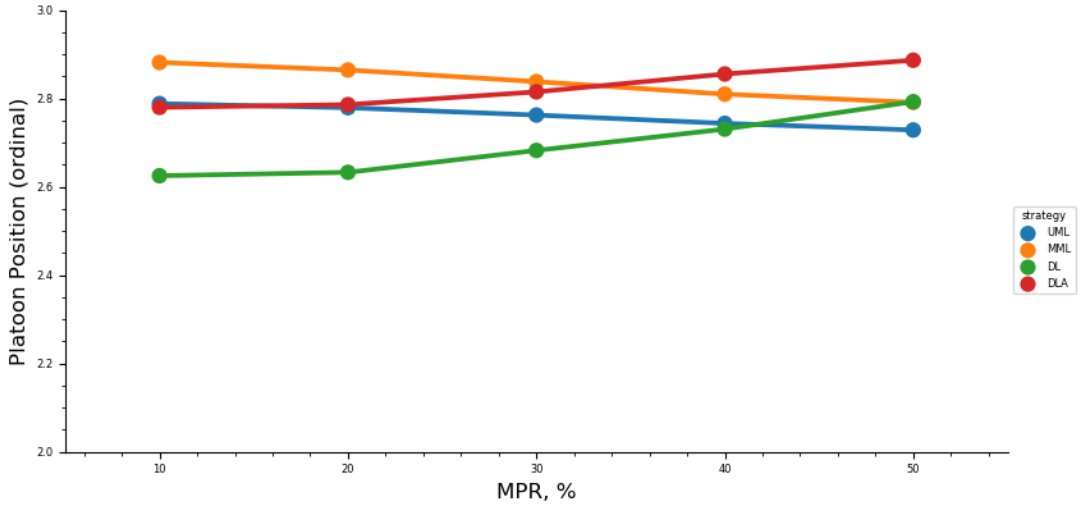

(b) Average platoon position of CACC vehicles.

Figure 6.8 Average total number of platoons in the network.

In DL, the total platoons and the mean platoon position have opposite trends as the MPR increases. With higher the MPR, total platoons become lesser, while the mean platoon position becomes greater in DL, which indicates that larger platoons are able to form in DL, and the number of platoons becomes lesser as a result. This is a sight that the performance of DL does not degrade due to high MPRs, which is suitable for implementation when the MPR raises above 30%. The DLA exhibits an ideal case for deploying CACC in mid- or high-range MPR. Unlike UML and MML, both of the total platoon and mean platoon position increase along with the MPR. This is an indicator that, by the implementation of DLA, not only the platoon size but also the number of platoon increase. The break-even point of the dedicated lane and the non-dedicated lane is 30% MPR.

Table 6.3 Relationship of Platoon Variables

	MPR	Total Platoon	Avg. Platoon Position	Correlation	Note
UML	↑	↓	↓	positive	less and smaller platoons
MML	↑	↓	↓	positive	less and smaller platoons
DA	↑	↓	↑	negative	less but larger platoons
DLA	↑	↑	↑	positive	more and larger platoons

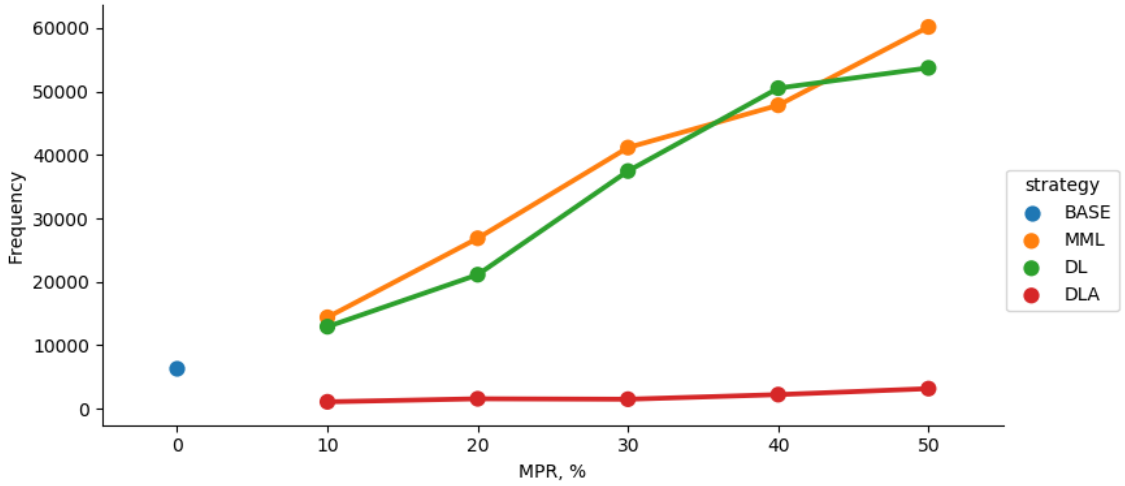

Figure 6.9 Weaving activity of leftmost/managed lane.

The induced weaving activity for CACC vehicles that actively seek for platooning opportunity is seldom discussed, as most of the previous CACC evaluations do not factor in the local coordination among CACC vehicles in forming platooning. Since the leftmost lane is used as a candidate lane for managed lane purpose, the weaving activity between the 3rd and the 4th lane has an impact on the performance of CACC vehicles that operate on the leftmost lane (4th lane). Figure 6.9 shows the total number of lane changes made to merge into the managed lane. By comparing the lane change frequencies among strategies, the potential weaving impact to the managed lane can be gauged. Without access control, an eligible vehicle is able to merge into the managed lane at any location of the roadway, which can be disruptive to the already-formed CACC platoons on the managed lane. With demands remain constant, the increase in weaving activity that is induced by CACC vehicles actively seeking for platooning

opportunity could be counterproductive. The reduction in weaving activity can be treated as an indirect indicator of the disruption to the managed lane traffic that would have been prevented. The merging movements of DL have been significantly limited owing to access control as indicated. The potential drawback of active platooning is shown as an important factor when it comes to designing CACC operational strategy. As known, access control is more efficient when paired with physical barriers. However, the cost of creating such physical barriers sometime may be hard to justify economically. Automated lateral control may become necessary as the adaptation of CACC progresses. By implementing an effective lateral control for un-platooned CACC vehicles, the platoon seeking of CACC vehicles then is able to take into account the potential disruption to CACC platoons. Hence, similar CACC performance could be achieved even without the infrastructure cost of the physical barriers of DLA.

6.2.3 Wireless Communication Performance Measure

The impact of wireless communication for CACC is typically assumed to be perfect in the previous simulation study, and its impact is rarely taken into consideration when deploying CACC in mixed traffic. The transmission density shown in Figure 6.10 represents the number of vehicles (transmission nodes) per km. It is an approximation of the channel load for communication of adjacent CACC vehicles. According to Equation (5.1), the transmission density is inversely related to the probability of success packet reception. Thus, a lower value in transmission density typically represents a more reliable communication environment.

The overall trend observed is that the transmission density kept pace with the MPR for all four strategies. UML and MML generated the very similar transmission density among all MPRs. At 20% and 30% MPR, the transmission density for DL was higher than the rest of the strategies. It is also noticeable that the transmission density in DLA was lower than the rest of the strategies at any given MPR, which is a good sign for alleviating the communication burden of the DSRC channel. Such difference in transmission density was caused by CACC traffic flow pattern. When a CACC vehicle with a lower speed merges into the CACC lane, the speed difference between incoming CACC vehicle and those that are cruising at high-speed on the managed lane could force the platoon to slow down; and consequently, the CACC string was compressed, resulting in a higher transmission density. The highest median of transmission density observed is 35 veh/km at 50% MPR for UML, MML, and DL. DLA yielded the highest median transmission density, 30 veh/km, at 50% MPR as well. The DLA boxplots exhibit less variance at all MPRs.

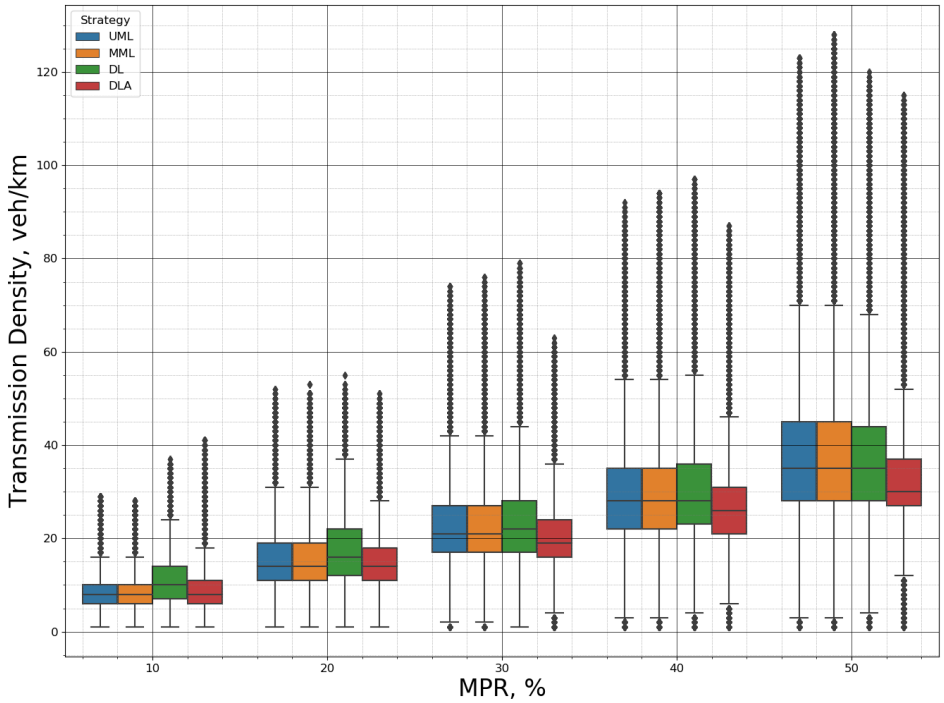

Figure 6.10 Transmission density for CACC vehicle.

The probability of successful reception of a packet is shown in Figure 6.11. While the reception probability is above 0.9 for all cases, DL has the lowest probability among all strategies at any given MPR. Such observation reflects the relatively higher transmission density in Figure 6.11. Admittedly, this study only provides a basic glimpse of V2V communication performance under different managed lane strategies. The routing of the packages, which influence the reliability and performance of the V2V communication, has not been fully taken into account. From the pure perspective of wireless communication, the higher the packet reception rate, the more reliable of the communication among platooned CACC vehicles. However, when the reception rate is above 92.5% in the cases in this study, the reception ratio becomes a less impactful factor in choosing

strategies. The diminishing return of packet reception ratio may not be justifiable among other factors (e.g., platoon size, total platoons, or the percentage of platooned CACC vehicles). In another word, when the packet reception ratio of certain managed lane strategies is out of the acceptable range, the reliability of wireless communication has to be weighted in.

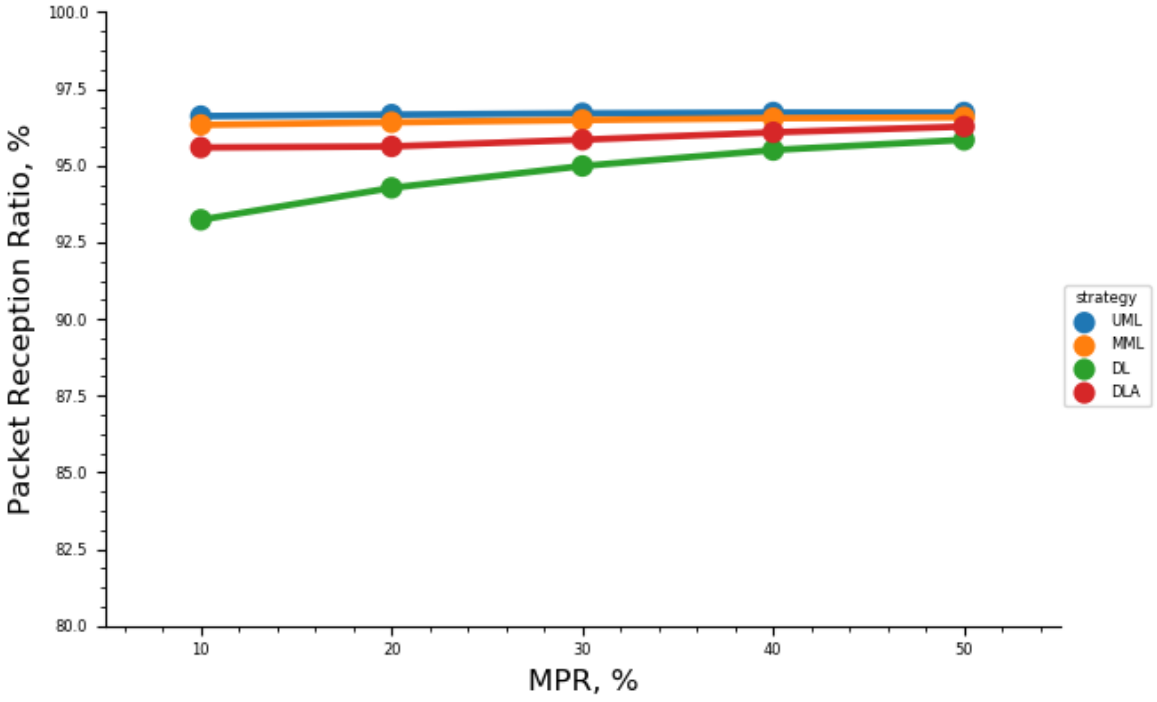

Figure 6.11 Packet reception ratio of V2V packet.

6.2.4 Optimization Performance Measure

Figure 6.12 shows the probability of obtaining feasible solutions among all the optimization conducted for CACC platoons. The likelihood of obtaining a feasible solution for MOOP is in an inverse relationship with the platoon size along with

traffic dynamics. As more vehicles are introduced to a platoon, additional dimensions in the search space and constraints are imposed, resulting in a more complex searching in a smaller feasible solution space. As seen, the probabilities of obtaining feasible solutions for UML, MML, and DL are patently higher than that of DLA. The trends for these three strategies are the feasibility decrease as the MPR increase, with the exception of 20% MPR and 30% MPR where the feasibility values stay at the same level. For the feasibility of DLA, it starts at 0.63 at 10% MPR, then decreases to 0.58 at 20% MPR. When the MPR raises above 20%, the feasibility begins to increase and eventually reaches the highest value of 0.64 at 50% MPR.

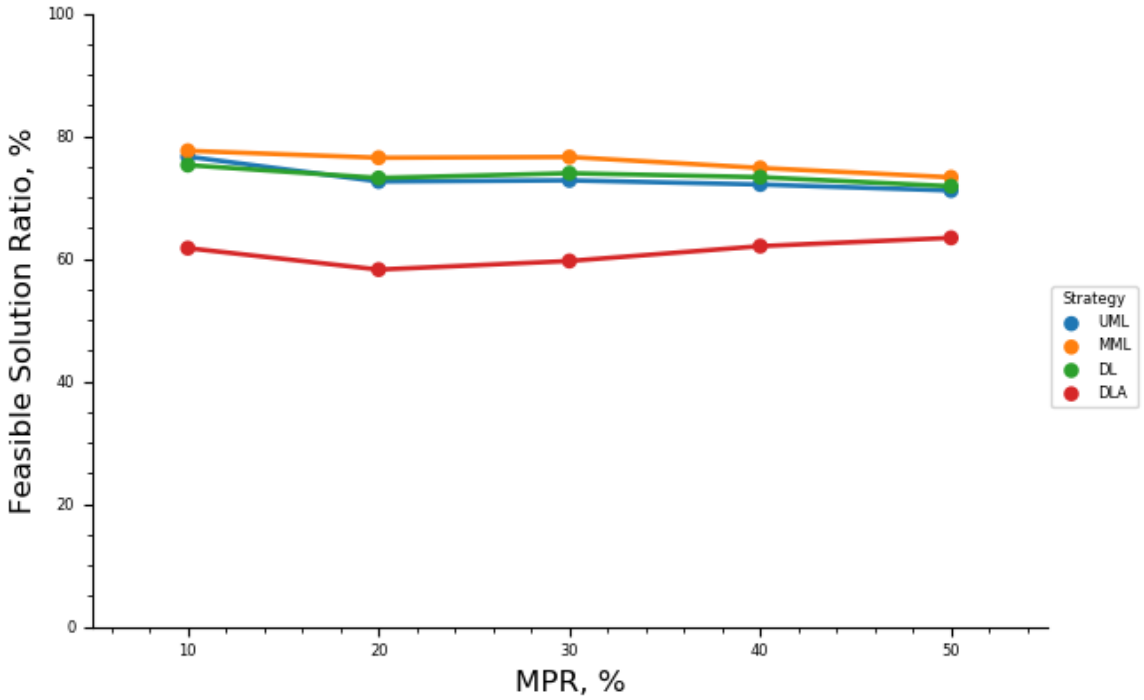

Figure 6.12 Feasible solution ratios among strategies.

Four objective functions concerning mobility, comfort and emission and fuel consumption are incorporated into the MOOP framework. The E-IDM based longitudinal control is designed to obtain the desired time gap, which essentially minimizes the difference between the actual headway and the desired headway. Therefore, it can be considered as a SOOP-based control algorithm. Since the four objectives all share different units as well as magnitude, normalization for each of them to the range [0, 1] is performed. The objective function values obtained for individual CACC vehicle are presented in Figure 6.13. For UML, MML, and DL, MOOP achieves more balanced objective values by the indication of the smaller area of the MOOP polygon in blue. In DLA, however, the average objective function values in MOOP are higher than those of the E-IDM, except in Headway objective. As discussed in section 6.3.2, the size of the platoon grows with the aid of DLA. With bigger platoon size, the search for a feasible solution becomes more complex and challenging. The low rate of feasible solution and the switching on and off of MOOP driving causes the increase in objective values in Jitter, Emission, and Fuel Consumption. However, GA can be fine-tuned for specific application to maximize feasibility of solutions. A potential improvement for deploying MOOP with DLA is to study the optimal platoon size. Additionally, certain constraints may be relaxed. For instance, the speed limit of the dedicate lane could set higher than that of the GP lanes, since CACC vehicles are able to conduct high-performance driving by reducing or even eliminating human error. By doing so, the feasible region for the MOOP could potentially be enlarged.

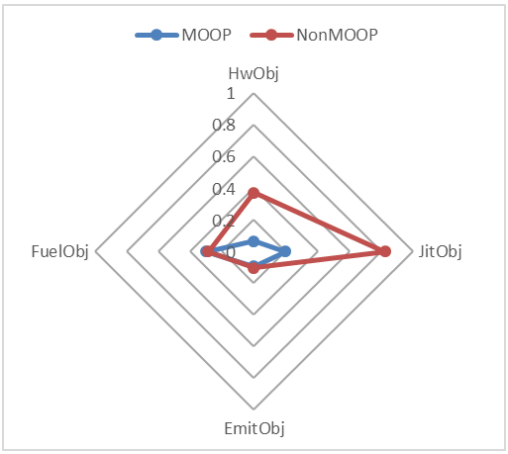

(a) UML

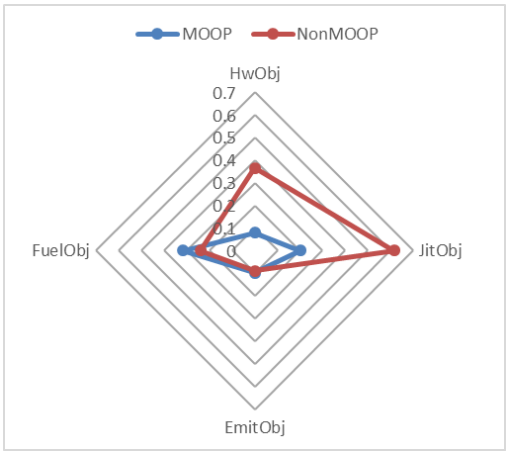

(b) MML

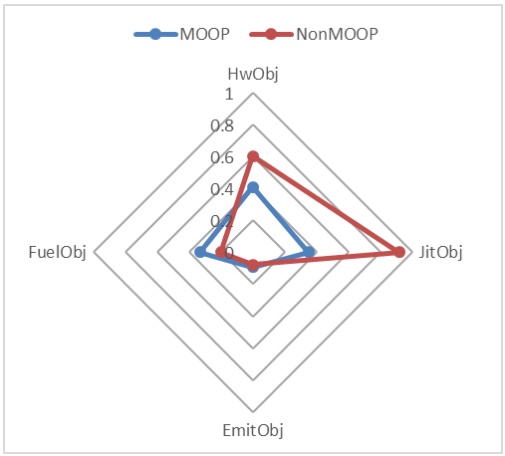

(c) DL

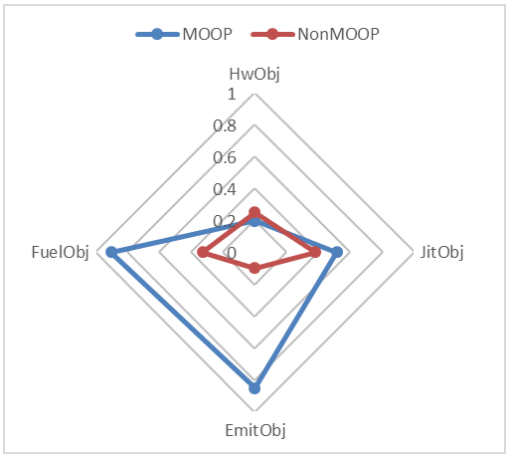

(d) DLA

Figure 6.13 Objective values for each vehicle between SOOP and MOOP.

6.3 Discussion

The performance of CACC and its impacts on the mixed traffic flow have been evaluated from four categories of performance measures. Readers should be informed that the type of the managed lanes tested in this study is not intended to be exhaustive. The simulations have revealed several important aspects of deploying CACC in mixed traffic, most of which have rarely been discussed and yet the stakeholders have to take into account.

The performance measures in the above section are aggregated based on mobility, safety, equity, and CACC platooning. The score assignment rule is shown in Table 6.4. The first three performance measures are determined based on the comparison with the base case, whereas the CACC platooning is determined the sole comparison among four tested strategies at each level of MPR. A color scaling is assigned to Figure 6.14 at each type of performance measures with green being the desirable outcome and red being the undesirable ones.

Table 6.4 Evaluation Score Assignment

Performance measure	**Evaluation score determination**
Mobility, safety, and equity	• Improvement: 1 • Neural: 0 • Degradation: -1

CACC platooning	• Rank from the best to the worst
	  • 1st: 4
	  • 2nd: 3
	  • 3rd: 2
	  • 4th: 1

	10%	20%	30%	40%	50%
UML	4	4	4	3	3
MML	4	4	4	4	3
DL	-4	-4	1	4	4
DLA	-4	-4	1	4	4

(a) Mobility scores

	10%	20%	30%	40%	50%
UML	1	1	1	1	1
MML	1	1	1	1	1
DL	-1	-1	0	1	1
DLA	-1	-1	0	1	1

(b) Equity scores

	10%	20%	30%	40%	50%
UML	1	1	1	1	1
MML	1	1	1	1	1
DL	-1	-1	0	1	1
DLA	-1	-1	1	1	1

(c) Safety scores

	10%	20%	30%	40%	50%
UML	10	8	6	7	7
MML	10	10	10	9	9
DL	7	4	3	4	6
DLA	4	8	10	9	10

(d) CACC scores

Figure 6.14 Evaluation scores.

At the mid-range MPR (equal or above 30% MPR), a dedicated CACC lane should be considered. Starting from 30%, the congestion on GP lanes incurred by dedicated CACC lane starts to subside. The throughput of the network keeps increasing as the CACC demand increases, which indicates that a CACC dedicated lane is able to provide additional carrying capacity. Furthermore, at mid-range MPR, short intra-platoon headway can be implemented on the dedicated lane, something that may raise safety concerns when CACC vehicles are mixed with non-CACC ones. Homogenous CACC traffic not only provides more platooning opportunity but also allow CACC vehicles to conduct high-performance driving (e.g., with higher speed limits, closer following distance).

The platoon dissolution resulted from weaving activity is also a crucial aspect of CACC deployment, when access control of dedicated CACC lane is not provided or when CACC traffic is mixed with human traffic. Again, at low-range of MPR, the intra-platoon headway of CACC vehicles is expected to be longer, which may not prevent human drivers from inadvertently merging into CACC platoons. Additional signage on a CACC vehicle may be required to inform the adjacent human drivers of the platoon status and discourage lane change into a CACC platoon. Alternatively, a dedicated CACC lane could solve the problem by concentrating the CACC platoons in one lane and prevent potential disruption for human drivers by erecting physical barriers. However, the infrastructure investment should be carefully considered and economically justified.

In light of the weaving activity induced by CACC vehicles that actively seek for platooning opportunity, global coordination of CACC vehicle from similar origin-destination is another alternative. Global coordination can minimize the weaving activity and consequently provide smoother operation of CACC vehicles in mixed traffic. The technical aspect of the global coordination, which primarily includes an extensive communication network for management, may be ready by the time when the MPR of CACC reaches mid-range. Lastly, the V2V communication is a vital aspect of the success of CACC. However, the policymakers have little influence in the communication standard or protocol, which may be subject to change in the future in anticipant of the next-generation of wireless communication technology (e.g., 5G wireless communication).

The selection of the managed lane strategy for near-term deployment is summarized in Figure 6.15. The two main decision-making factors are 1) the existence of a managed lane on a roadway and 2) the MPR of CACC. As the budgetary constraint has always been an important factor, the infrastructure investment of a managed lane should be taken into consideration. Utilization of the existing managed lane could save the costly infrastructure investment. The priority usage of the existing managed manage could be implemented even when the MPR is less than 20%. For the roadways that do not have existing managed lane infrastructure, it is hard to justify the instrumentation of a managed lane for CACC vehicles which is a small portion of the overall traffic demand. As such, the mixed traffic strategy without managed lane is somehow more viable until MPR raises to a certain level. When the MPR is at 30% or above, the existing managed lane can be converted to a dedicated CACC lane. Additionally, physical barriers could be added for access control for the managed lane. As the simulation data shows, the access control can greatly enhance the performance of CACC.

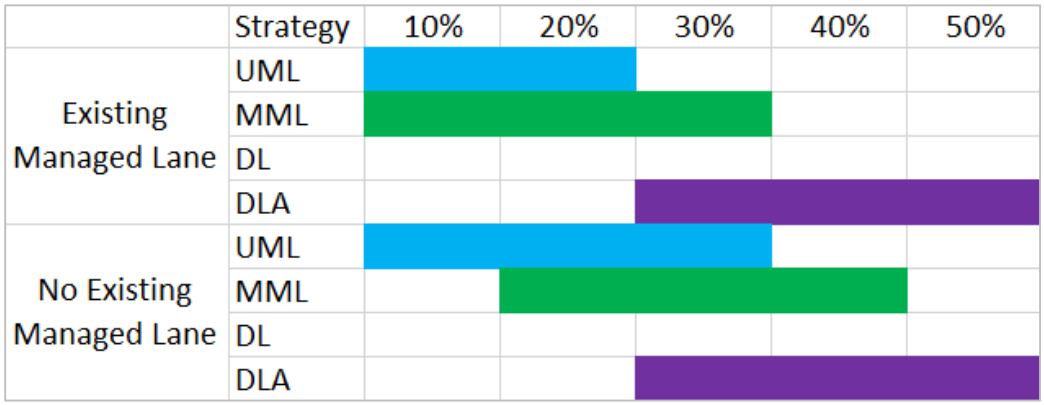

Figure 6.15 Managed lane strategies recommendations.

CHAPTER 7

CONCLUSIONS AND FUTURE RESEARCH

7.1 Conclusions

In this dissertation, an integrated simulation testbed for CACC, along with other C/AV application has been developed. The testbed takes into account granular longitudinal and lateral control of CACC vehicles and is able to test the performance of CACC under various managed lane strategies with mixed traffics. In addition, a DSRC-based analytical wireless simulation model is integrated into the testbed, which enables the assessment of communication impact during the traffic simulation. The scalability of the analytical approach for V2V communication has been tested. Furthermore, a MOOP-based control algorithm is proposed, where all platooned CACC vehicles are able to perform cooperative driving based on quantifiable platoon-wide objectives. Efforts have been spent on the scalability and the computational efficiency of implementing the MOOP-based control algorithm in simulation as well. A data-exchanging module based on the user-defined attributes (e.g., platoon position, C/AV density, and platoon number) in Vissim has developed to enable the seamless communication between Vissim COM interface and Driver Model API.

With the calibrated 8-km I-66 freeway network, four different managed lane strategies were evaluated for the MOOP-based CACC platooning. The four objectives for a CACC platoon cover 1) mobility, 2) comfortability, 3) emission, and

4) fuel consumption. The simulation result shows that the introduction of CACC even at low MPR (i.e., 10%) helps the network to eliminate bottlenecks. UML and MML yield better performances when it comes to improving the overall performance of the network. The network throughput increases by 7% (i.e., 600 vph) for UML and 3.8% (i.e., 300vph) for MML; and the VHT decreases by approximately 11.3 % (i.e., 7.7 vehicle-hour) and 10.7% (i.e., 7.3 vehicle-hour) at 10% MPR for MML and UML, respectively. Travel time also shows that the introduction of CACC decreases the mainline travel time for both CACC and GP vehicle for UML and MML strategies. Dedicated CACC lane strategies (i.e., DL and DLA) appear to be suitable when the MPR is higher than 30%. The speed-flow diagram on two observation locations shows DLA is able to produce a more stable traffic flow.

Considering platooning capability of CACC, a new set of performance measure aiming to evaluate CACC behaviors in traffic flow is proposed and used. There are the percentage of CACC vehicle in a platoon, total platoon number, average platoon position, transmission density, and package reception probability. The result shows that CACC dedicated lane with access control facilitates platoon formation, and limits disruption for CACC platoons. With the help of DLA, the number of CACC vehicle that is able to form platoon increases linearly along with the increase of MPR. The percentage of platooned CACC vehicle reaches 53% at 50% MPR. In comparison, DL only obtains 45% platooned CACC at the same level of MPR. Additionally, the access control approach is able to generate larger platoon size, which is better for harnessing the benefits of CACC.

The MOOP-based optimization is able to provide a common platform for cooperative driving for each vehicle within a platoon. The control algorithm can achieve more balanced values among all given objectives, in comparison to E-IDM-based SOOP control algorithm except for the DLA case where the feasibility decreases due to the increase of search complexity as a result of larger platoon size.

7.2 Future Research

As tested, the proposed simulation testbed is able to provide a suitable platform for assessing the various scenarios of operation strategies of near-term CACC deployment. The following research is recommended:

- The induced weaving activity during the formation of a platoon could impact the traffic flow as well. Optimization-based lateral control could also be integrated into to the CACC model. For instance, use MOBIL model to minimize the overall deceleration of the adjacent vehicles.
- More efficient search techniques (e.g., NSGA-III, Grid-based EA, MOEA/ decomposition - penalty boundary intersection (PBI)) could be adopted for the multi-objective optimization
- Alternative objective functions can be tailored to specific operational goals that may vary by locales and agencies.
- As the rapid advancement of information and communication technology, the analytical wireless communication module may need to be calibrated accordingly to reflect the latest specifications of DSRC-based V2V communication.
- Packet routing has not been fully taken into account in this study. This aspect of the wireless communication could be added to the analytical model for more realistic simulation.
- Vehicle dynamics and low-level controller could be integrated into to the Vissim EDM to increase the degree of realism of the simulation.

APPENDIX A

NUMERICAL SIMULATION RESUTLS

The results of all ten trajectories in the numerical simulation in Chapter 4 is shown in this appendix in Figure A.1.

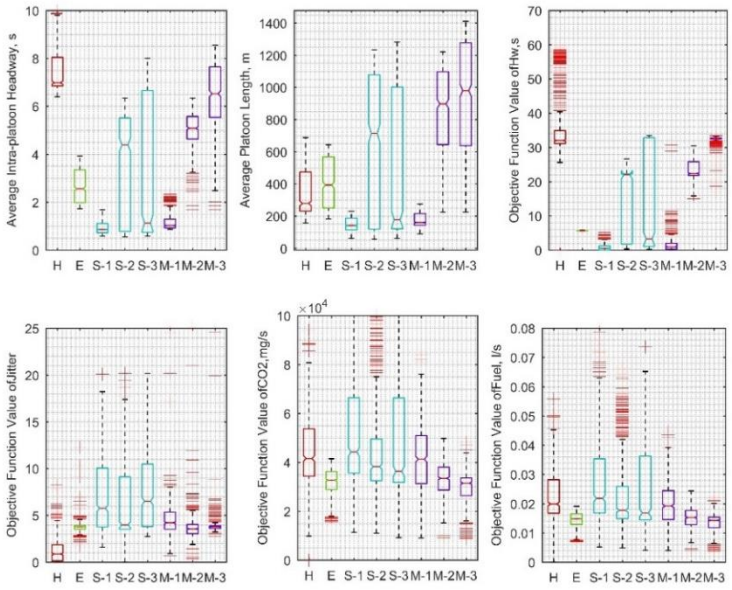

(a) trajectory #1

Figure A.1 Comparisons of ten trajectories. (Continued)

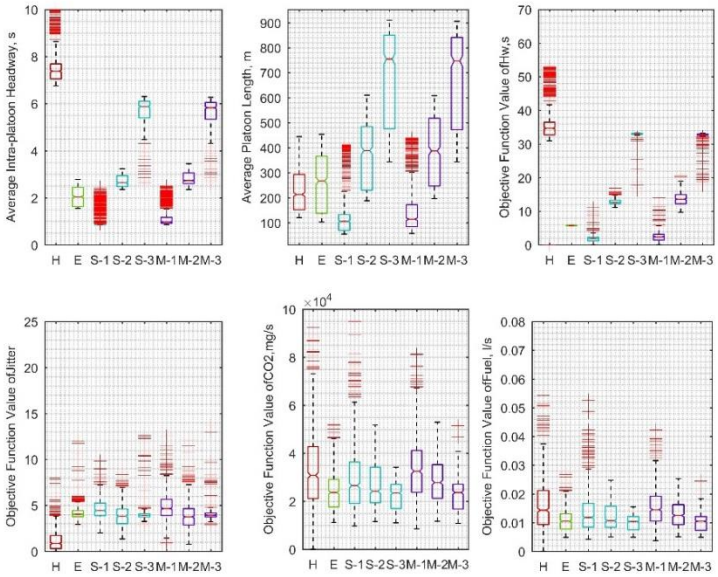

(b) trajectory #2

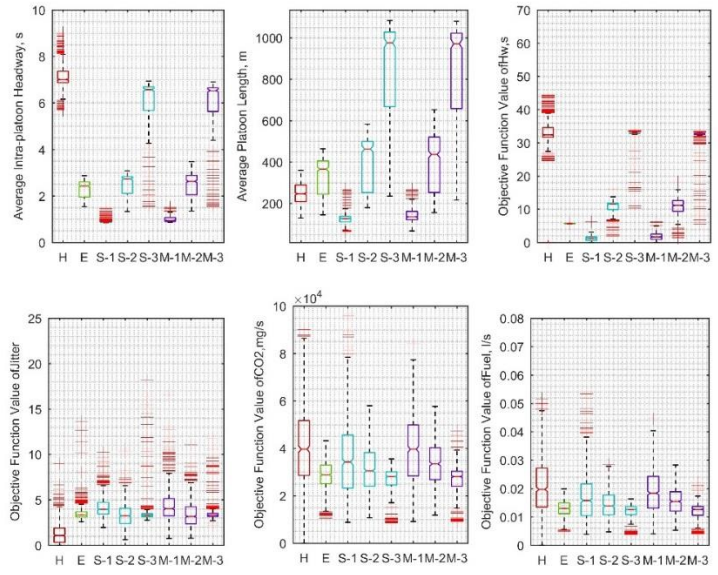

(c) trajectory #3

Figure A.1 (Continued) Comparisons of ten trajectories.

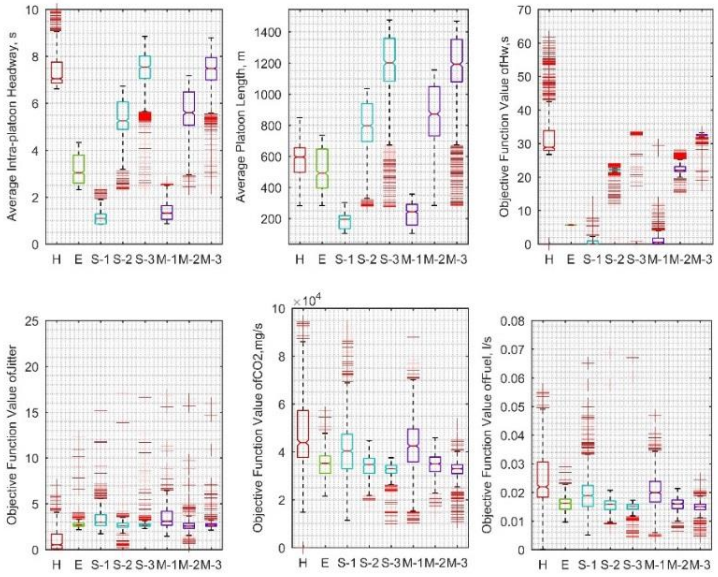

(d) trajectory #4

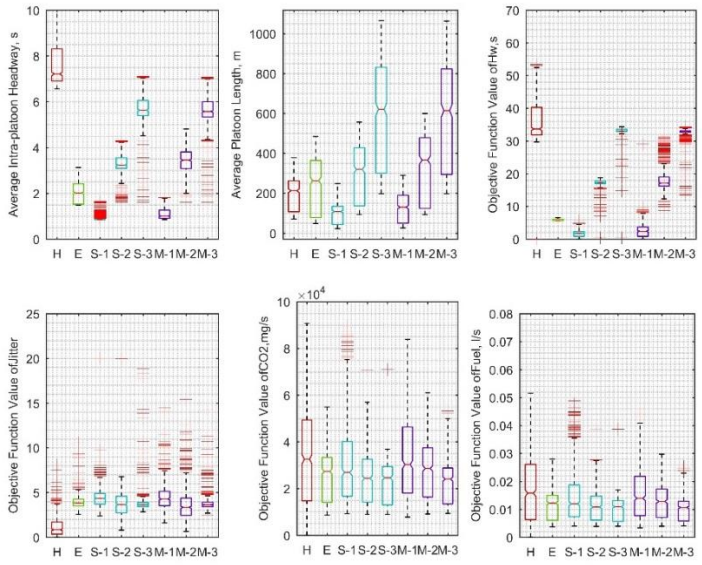

(e) trajectory #5

Figure A.1 (Continued) Comparisons of ten trajectories.

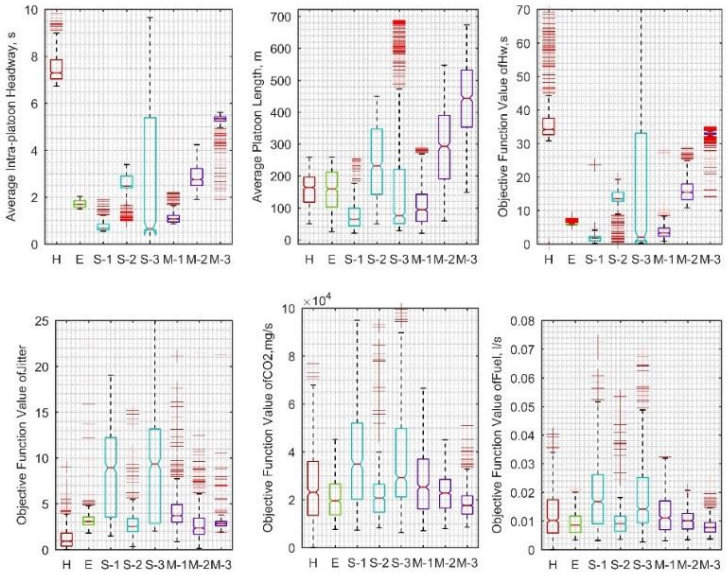

(f) trajectory #6

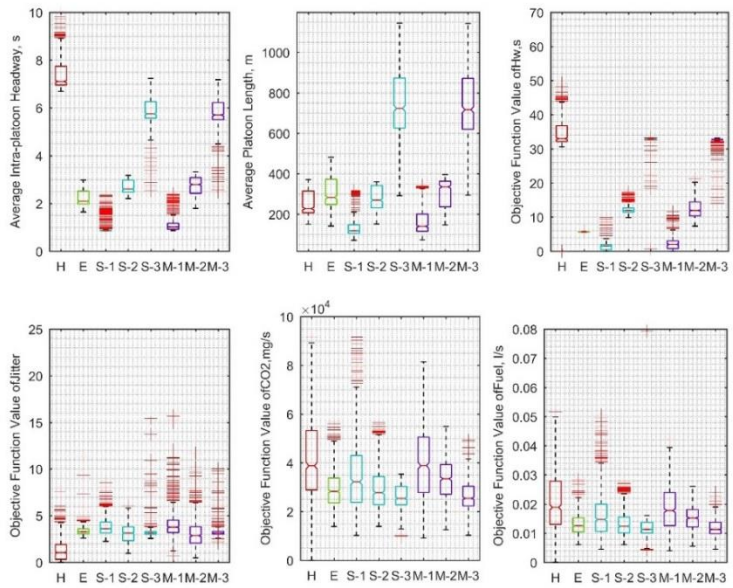

(g) trajectory #7

Figure A.1 (Continued) Comparisons of ten trajectories.

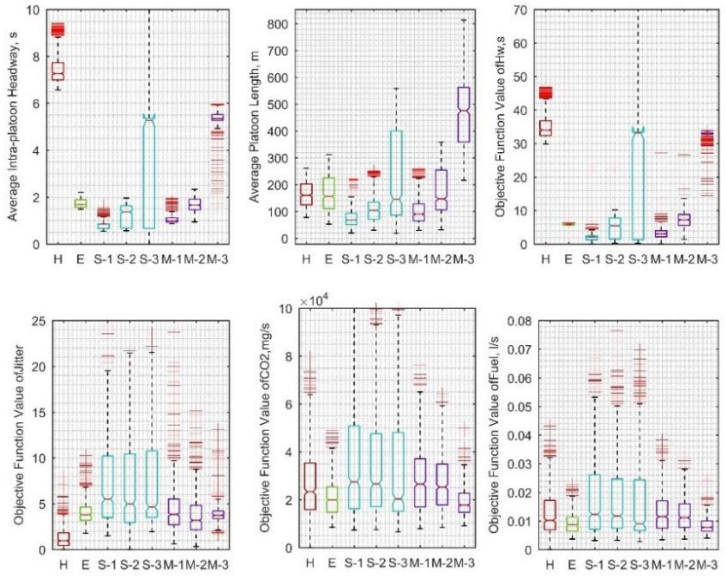

(h) trajectory #8

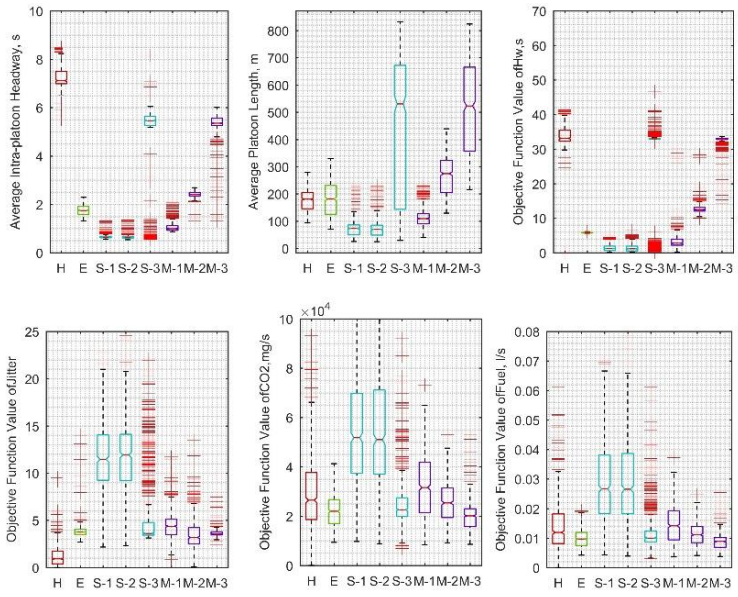

(i) trajectory #9

Figure A.1 (Continued) Comparisons of ten trajectories.

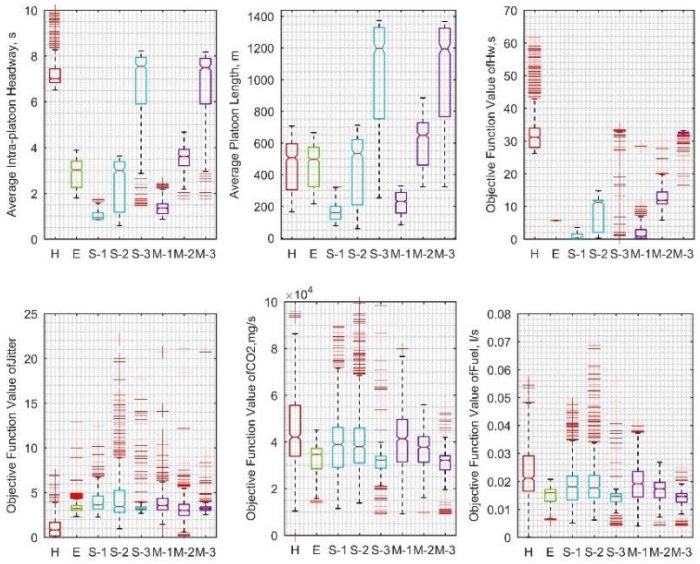

(j) trajectory #10

Figure A.1 (Continued) Comparisons of ten trajectories.

APPENDIX B

I-66 SIMULATION NETWORK CALIBRATION

As mentioned in Chapter 6, a segmented of I-66 in Virginia (shown in Figure B.1) was selected for the simulation. Before conducting any experiment, the simulation network constructed in Vissim has to be calibrated in order to produce valid results. The calibration involves two critical tasks: 1) estimating origin-destination (O-D) matrix and route choice and 2) adjusting driving behavior parameters in the Vissim's car-following models.

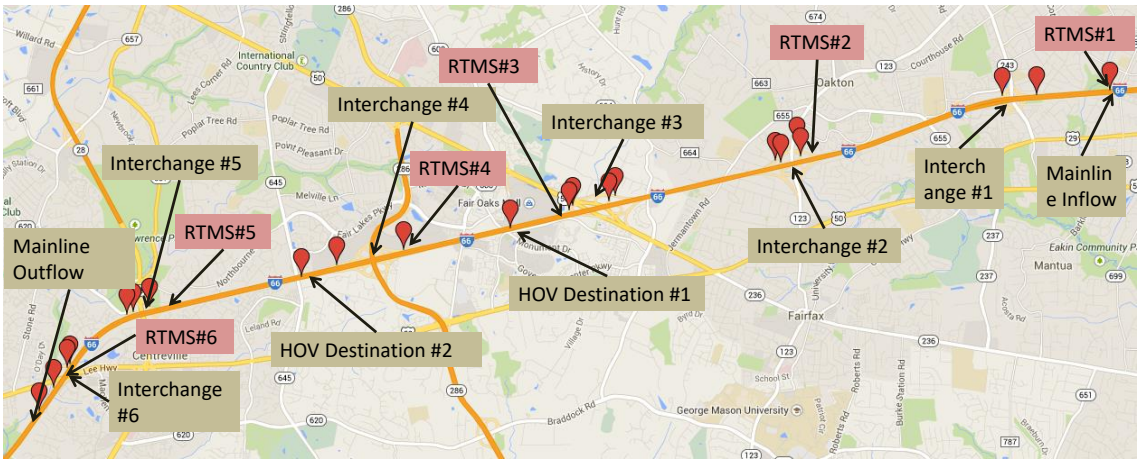

Figure B.1 I-66 network.

The O-D matrix for the I-66 simulation was calibrated by the QUEENSOD software based on the field observed link volume counts which were collected by

cameras and RTMSs. Twenty-six O-D demands with 15-minute intervals were generated. Six RTMSs were strategically placed in the vicinity of each interchange to capture both mainline and, on- or off-ramp volume and speed. Probe vehicle travel time data from INRIX (Traffic Management Channel (TMC)) was also used as the secondary data source.

The Latin Hypercube Sampling (LHS), a stochastic sampling method, was used to generate the parameter set candidates. The best candidate was selected from 500-scenario pool after running five replications of simulation for each with the priorities of matching volume, flow-speed curve, and TMC travel time in descending order. Then the selected candidate was fine-tuned to obtain the final simulation model. The locations of the RTMS trailers are shown in Table B.1, the circles represent the traffic data collected in the field being used as ground truth; whereas the crosses represent the data collected in the simulation in Figure B.2. The greater the overlapping area of the two type of the data point, the higher the resemblance of the simulation. Additionally, the simulation travel times of the selected TMC with relative long length are presented in Table B.2. The calibration results for the selected TMC are shown in Figure B.3.

Table B.1 RTMS Trailer Locations

Interchange ID	Nearest Exit	Nearest Crossing St	Mile Marker	Lat.	Long.
IC 1	62	Rt. 243/ Nutley St.	61.6	38.879646	-77.250504
IC 2	60	Rt. 123	60.0	38.8705306	-77.3009333
IC 3	57	Rt. 50	58.0	38.861246	-77.352807
IC 4	55	Rt. 286	55.5	38.856415	-77.378025
IC 5	53	Rt. 28/ Sully Rd.	53.0	38.847060	-77.429654
IC 6	52	Rt. 29	51.8	38.8386833	-77.4462111

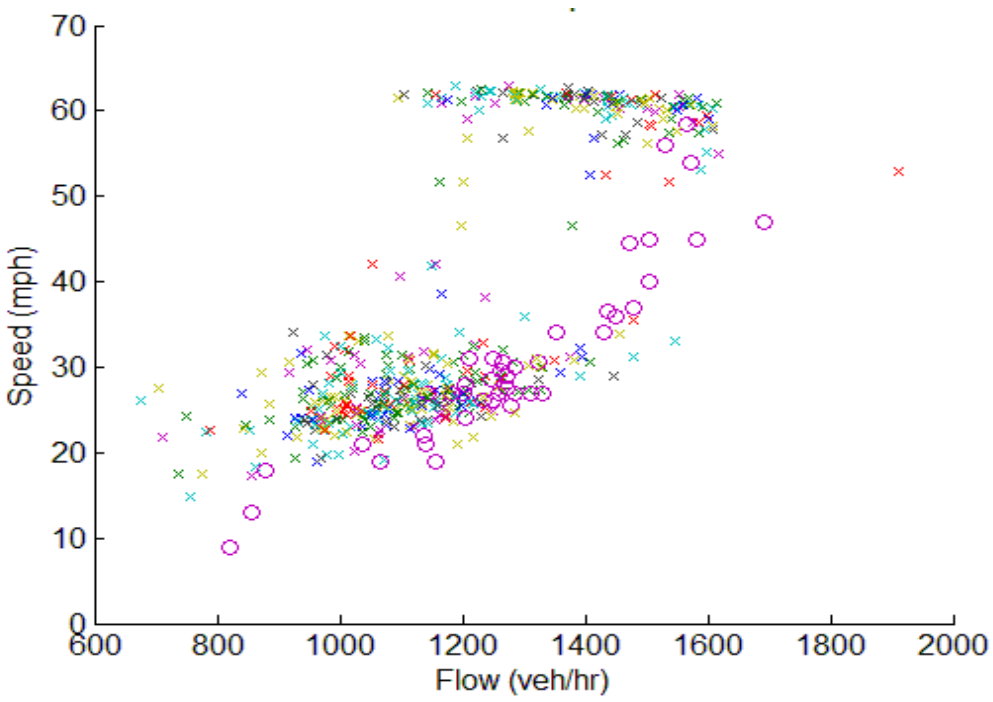

(a) Speed-flow Diagram for Interchange 1

Figure B.2 Flow-speed diagram comparison. (Continued)

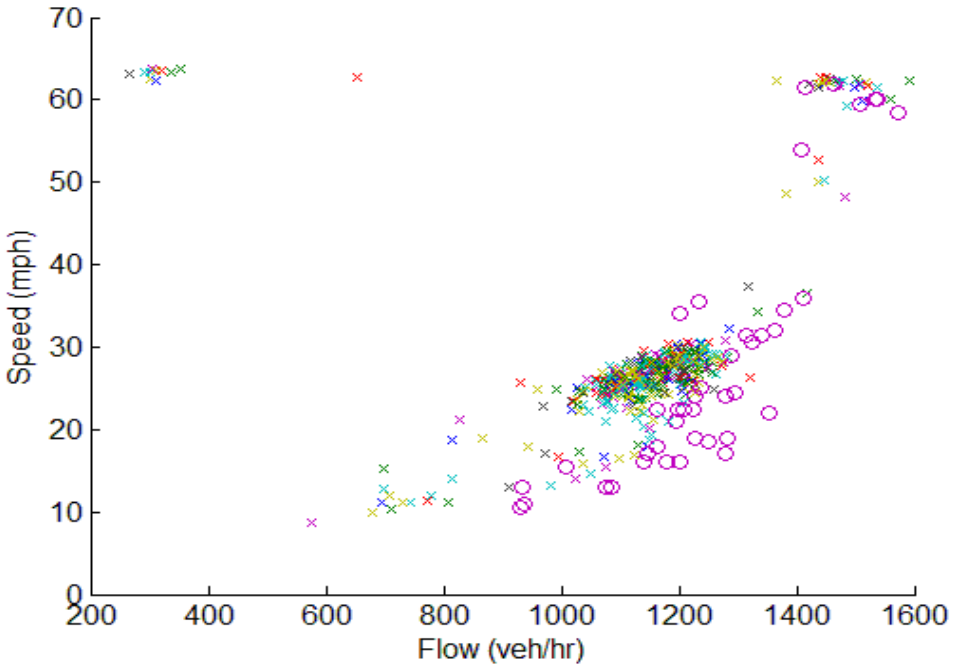

(b) Speed-flow Diagram for Interchange 2

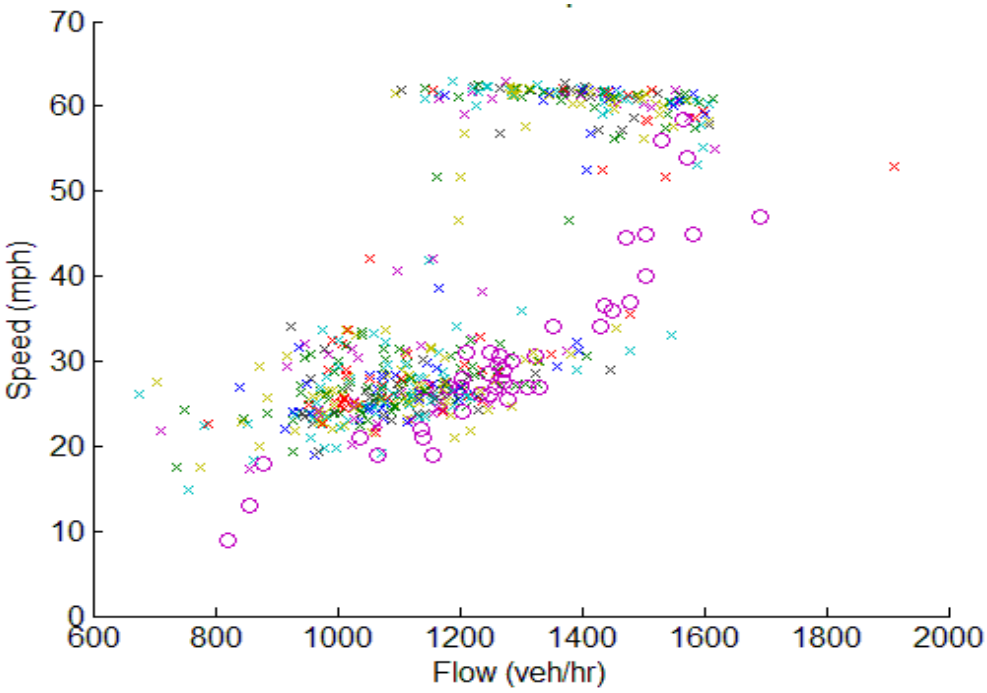

(c) Speed-flow Diagram for Interchange 3

Figure B.2 Flow-speed diagram comparison. (Continued)

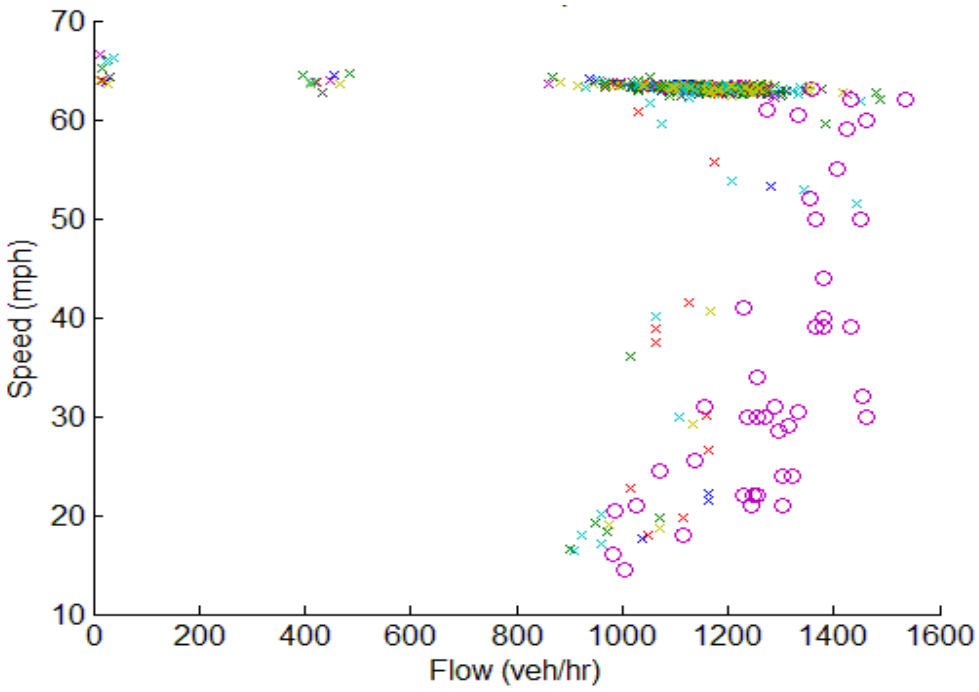

(d) Speed-flow Diagram for Interchange 4

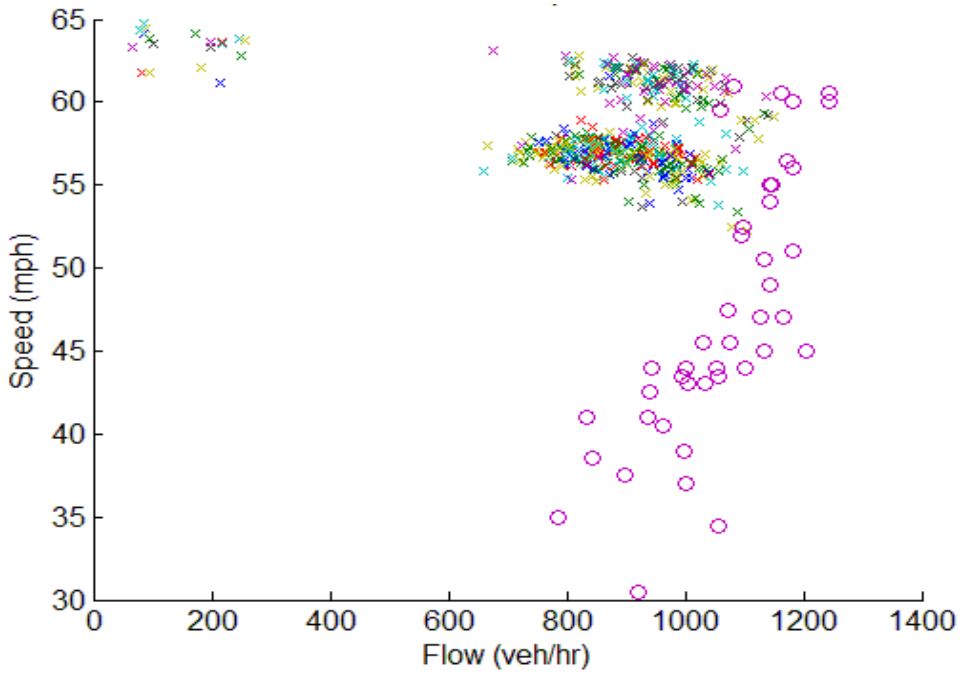

(e) Speed-flow Diagram for Interchange 5

Figure B.2 (Continued) Flow-speed diagram comparison.

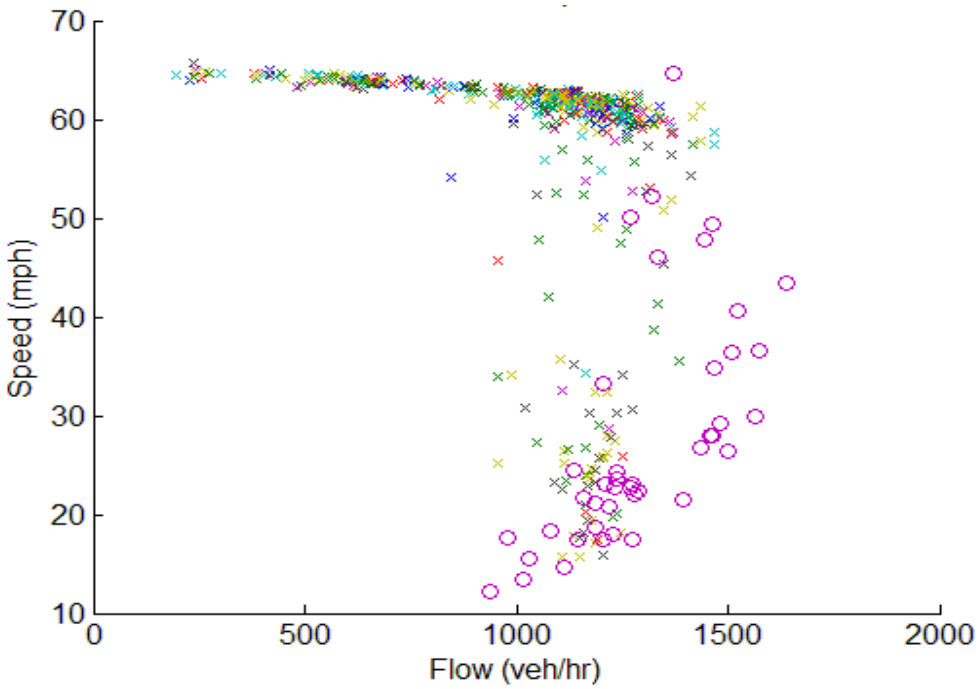

(f) Speed-flow Diagram for Interchange 6

Figure B.2 (Continued) Flow-speed diagram comparison.

Table B.2 TMC Information

TMC Code	Beginning Exit	Ending Exit	Mileage
110+04176	I-495/Exit 64	Va-243/Nutley St/Exit 62	1.8
110P04176	I-495/Exit 64	Va-243/Nutley St/Exit 62	0.4
110+04177	Vaden Dr/Exit 62	Va-123/Exit 60	0.3
110+04178	Va-243/Nutley St/Exit 62	Va-123/Exit 60	1.4
110P04178	Va-123/Exit 60	Us-50/Exit 57	0.9

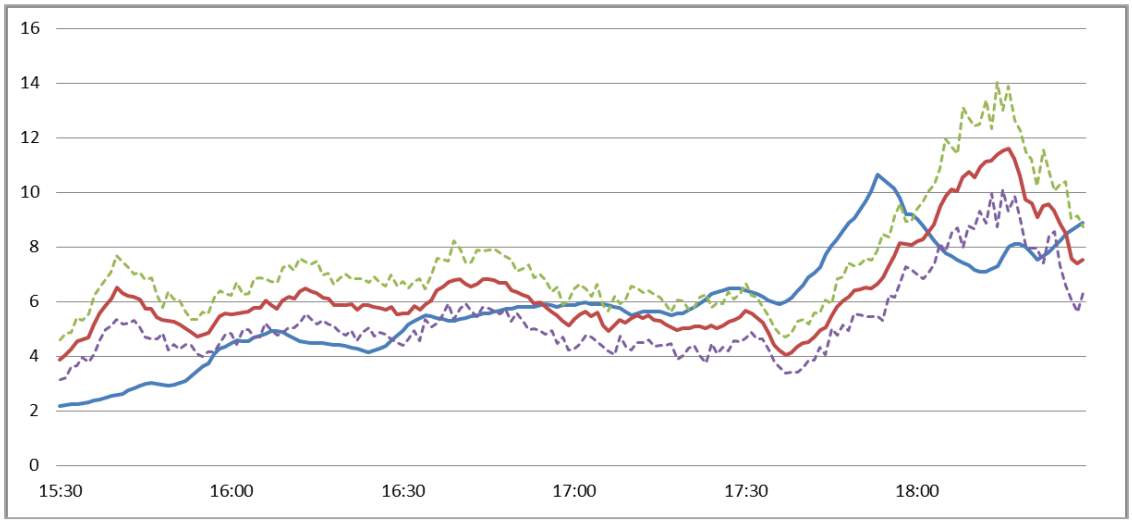

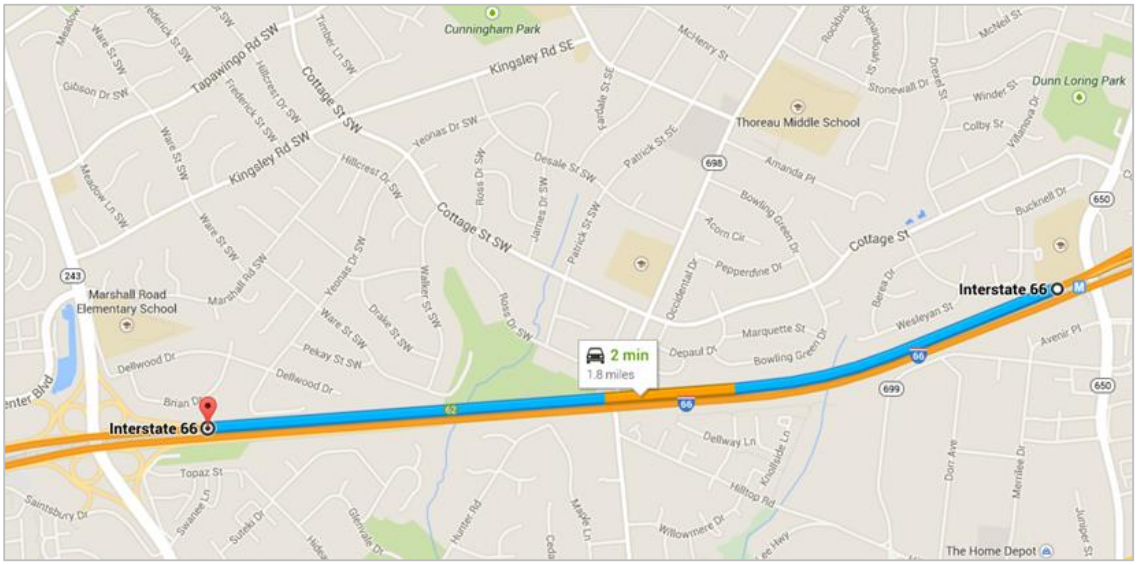

(a) TMC 110+01476 (unit minute)

Figure B.3 TMC travel time calibration. (Continued)

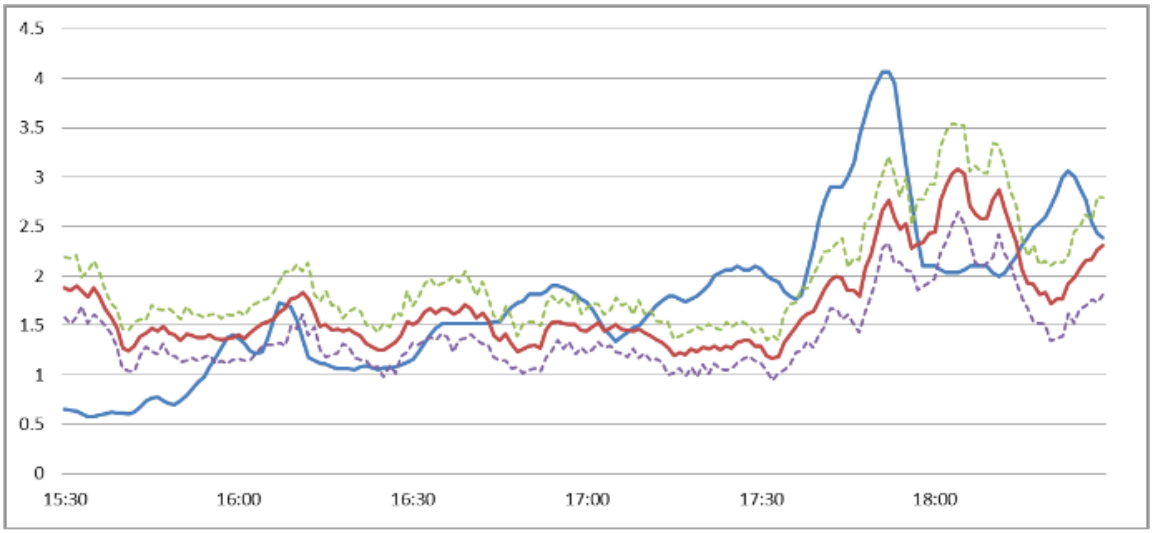

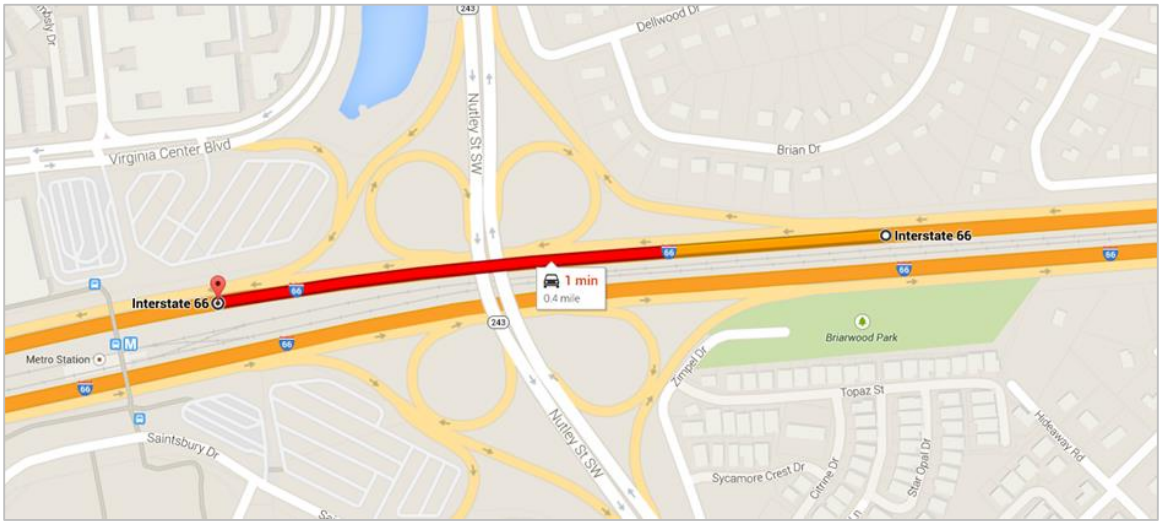

(b) TMC 110P01476(unit minute)

Figure B.3 (Continued) TMC travel time calibration.

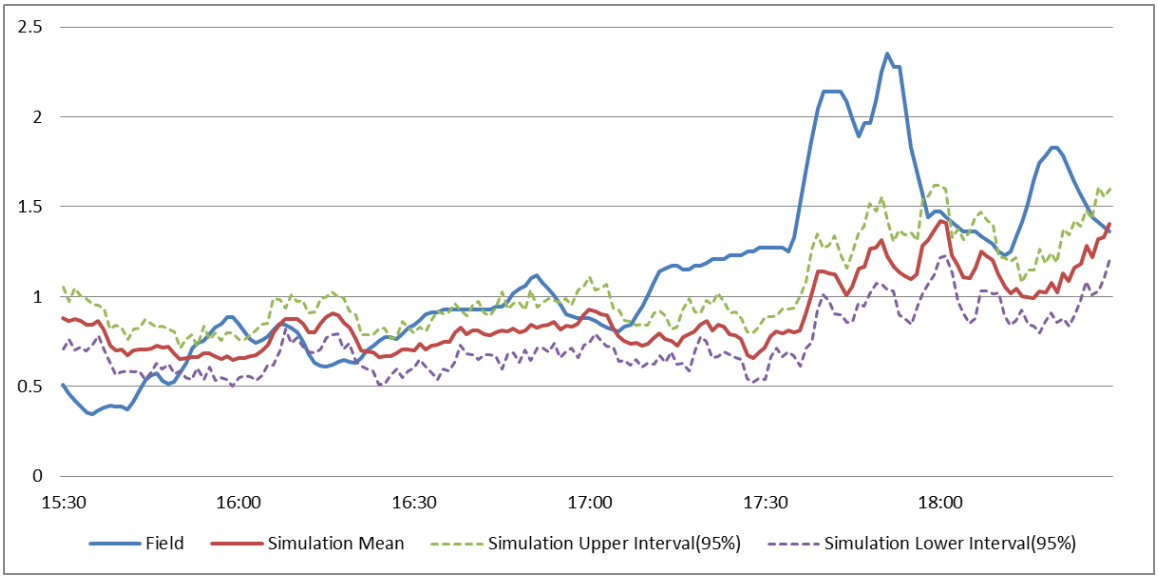

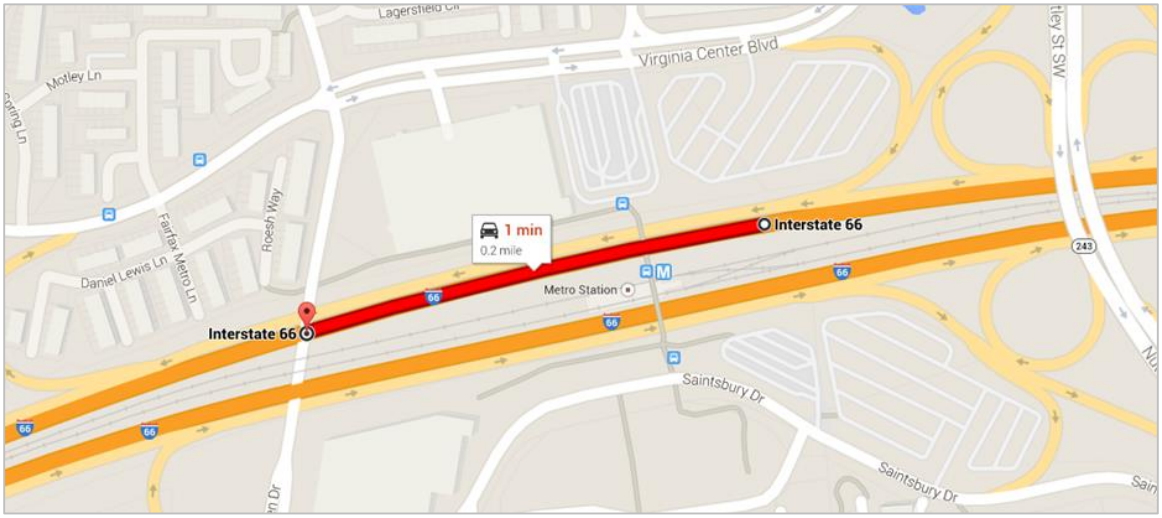

(c) TMC 110+01477

Figure B.3 (Continued) TMC travel time calibration.

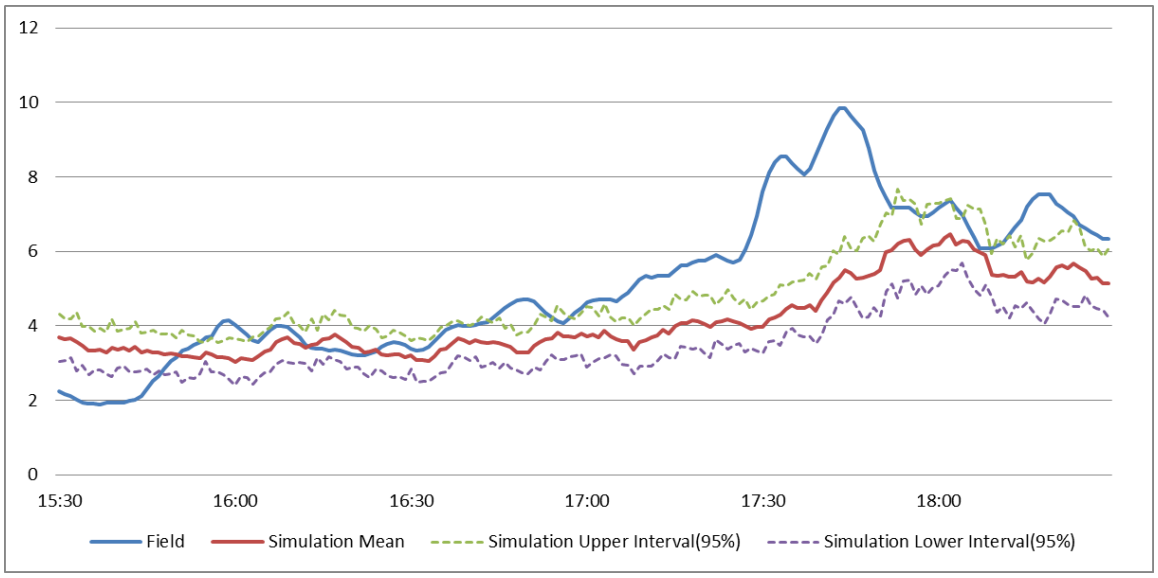

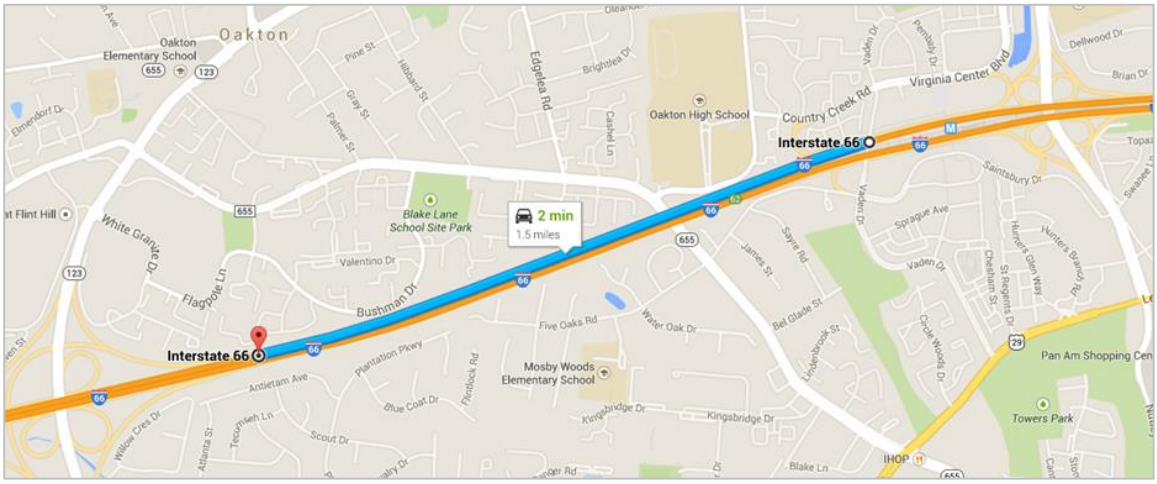

(d) TMC 110+01478

Figure B.3 (Continued) TMC travel time calibration.

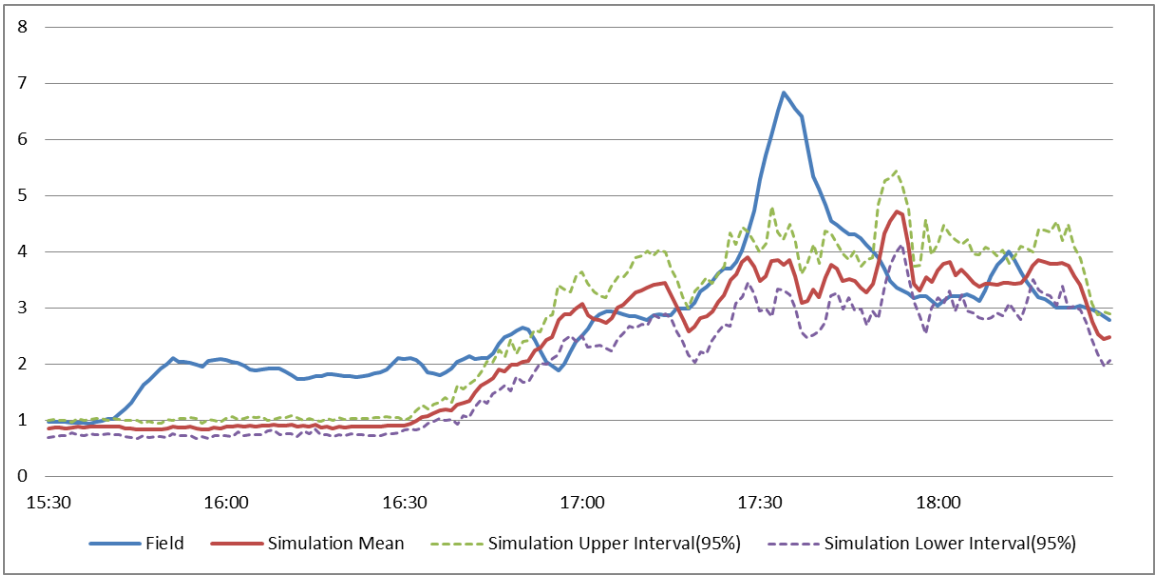

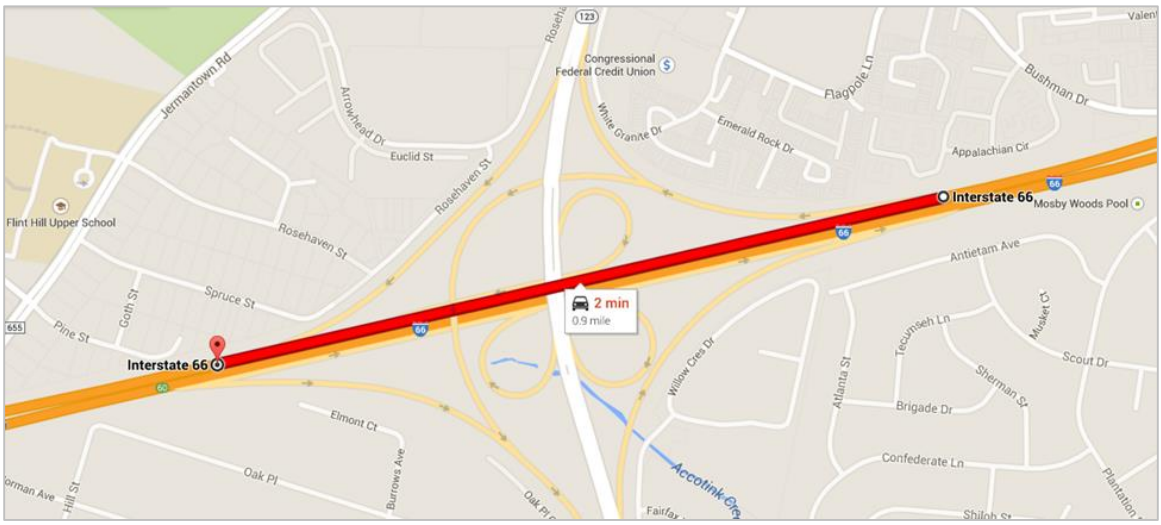

(e) TMC 110P01478

Figure B.3 (Continued) TMC travel time calibration.

Based on the comparison of speed-flow diagrams, along with travel time and volume measure at each interchange, the simulation network is believed to preserve a high fidelity of the selected I-66 segment.

REFERENCES

[1] D. Schrank, B. Eisele, T. Lomax, and J. Bak, “2015 urban mobility scorecard,” Texas A&M Transportation Institute, College Station, TX, 2015.

[2] Federal Highway Administration. “Facts and statistics - work zone delay,” 2013. [Online]. Available: http://www.ops.fhwa.dot.gov/wz/resources/facts_stats/delay.htm. Accessed on: Mar. 6, 2018

[3] International Traffic Safety Data and Analysis Group,” Road safety annual report 2014 summary,” International Traffic Safety Data and Analysis Group, 2014. [Online] Available: http://www.oecd-ilibrary.org/docserver/download/7514011e.pdf?expires=1520489954&id=id&accname=guest&checksum=AEC9CA3255E6581AD981E5BB8F55B281

[4] K. Kim and K. Choi, *Algorithm & SoC design for automotive vision systems*. Netherlands: Springer, 2014.

[5] W. G. Najm, J. D. Smith, and M. Yanagisawa, “Pre-crash scenario typology for crash avoidance research,” National Highway Traffic Safety Administration, Washington, DC, 2007.

[6] A. Mehra, W.-L. Ma, F. Berg, P. Tabuada, J. W. Grizzle, and A. D. Ames, “Adaptive cruise control: experimental validation of advanced controllers on scale-model cars,” in *2015 Amer. Control Conf. (ACC)*, 2015, pp. 1411–1418.

[7] Ford Motor Co. (2015, Jan) “Ford at CES announces smart mobility plan and 25 global experiments designed to change the way the world moves.” Ford Motor Co., Dearborn, MI, 2016, [Online] Available: https://media.ford.com/content/fordmedia/fna/us/en/news/2015/01/06/ford-at-ces-announces-smart-mobility-plan.html. Accessed on: Mar. 6, 2018

[8] H. Furlong. (2016, Jan.) “Treading: GM, FORD launch new partnership to drive the future of mobility.” 2016. [Online] Available: http://www.sustainablebrands.com/news_and_views/ict_big_data/hannah_furlong/trending_gm_ford_launch_new_partnerships_driving_future_m. Accessed on: Mar. 6, 2018

[9] R. Resendes. (2010, Jul.) “Vehicle-to-vehicle and safety pilot.” The United State Department of Transportation, 2010. [Online] Available: https://its.dot.gov/presentations/Safety_workshop2010/Vehicle-toVehicle%20and%20Safety%20Pilot%20--%20R%20Resendes.pdf

[10] S. Soper. (2016, Sept.) “Seattle tech vets to propose driverless stretch of Interstate 5,” 2016. [Online] Available: https://www.bloomberg.com/news/articles/2016-09-19/seattle-tech-vets-to-propose-driverless-stretch-of-interstate-5. Accessed on: Mar. 6, 2018

[11] R. Rajamani and S. E. Shladover, “An experimental comparative study of autonomous and co-operative vehicle-follower control systems,” *Transp. Res. Part C Emerg. Technol.*, vol. 9, no. 1, pp. 15–31, 2001.

[12] F. Bu, H.-S. Tan, and J. Huang, “Design and field testing of a cooperative adaptive cruise control system,” *2010 Amer. Control Conf*. Baltimore, MD USA, 2010.

[13] V. Milanes, S. E. Shladover, J. Spring, C. Nowakowski, H. Kawazoe, and M. Nakamura, “Cooperative adaptive cruise control in real traffic situations,” *Intell. Transp. Syst. IEEE Trans*., vol. 15, no. 1, pp. 296–305, 2014.

[14] S. E. Shladover, “Recent international activity in cooperative vehicle-highway automation systems,” Federal Highway Administration, McLean, VA, 2012.

[15] W. van Willigen, E. Haasdijk, and L. Kester, “A multi-objective approach to evolving platooning strategies in intelligent transportation systems,” in *15th annu. Conf Genetic and Evol. Comput.*, 2013, pp. 1397–1404.

[16] M. Wille, M. Röwenstrunk, and G. Debus, “Konvoi: electronically coupled truck-convoy,” *Hum. Factors Assist. Autom*., Maastricht, the Netherlands, pp. 243, 2007.

[17] J. van Dijke and M. van Schijndel, “CityMobil, advanced transport for the urban environment: update,” *Transp. Res. Rec. J. Transp. Res. Board*, no. 2324, pp. 29–36, 2012.

[18] S. E. Shladover, “Review of the state of development of advanced vehicle control systems (AVCS),” *Veh. Syst. Dyn.*, vol. 24, no. 6, pp. 551–595, 1995.

[19] D. Sivaraj, A. Kandaswamy, V. Rajasekar, P. B. Sankarganesh, and G. Manikandan, “Implementation of AVCS using Kalman filter and PID controller in autonomous self-guided vehicle,” *Int. J. Comput. Appl.*, vol. 27, no. 2, pp. 1–8, 2011.

[20] Y. Li, H. Wang, W. Wang, L. Xing, S. Liu, and X. Wei, “Evaluation of the impacts of cooperative adaptive cruise control on reducing rear-end collision risks on freeways,” *Accid. Anal. Prev.*, vol. 98, pp. 87–95, 2017.

[21] H. Peng and M. Tomizuka, “Vehicle lateral control for highway automation,” in *Amer. Control Conf.*, 1990, pp. 788–794.

[22] B. van Arem et al., “Design and evaluation of an integrated full-range speed assistant,” TNO, 2007. [Online] Available: publications.tno.nl/publication/34623299/0wxA9h/D-R0280-B.pdf Accessed on: Mar. 6, 2018

[23] S. Yu and Z. Shi, “The effects of vehicular gap changes with memory on traffic flow in cooperative adaptive cruise control strategy,” *Phys. A Stat. Mech. Its Appl.*, vol. 428, no. 0, pp. 206–223, 2015.

[24] H. M. Zhang, “A mathematical theory of traffic hysteresis,” *Transp. Res. Part B Methodol*., vol. 33, no. 1, pp. 1–23, 1999.

[25] M. Wang, W. Daamen, S. P. Hoogendoorn, and B. van Arem, “Rolling horizon control framework for driver assistance systems. part ii: cooperative sensing and cooperative control,” *Transp. Res. Part C Emerg. Technol.*, vol. 40, no. 0, pp. 290–311, 2014.

[26] M. Wang, W. Daamen, S. P. Hoogendoorn, and B. van Arem, “Rolling horizon control framework for driver assistance systems. part i: mathematical formulation and non-cooperative systems,” *Transp. Res. Part C Emerg. Technol.*, vol. 40, no. 0, pp. 271–289, 2014.

[27] W. Helly, “Simulation of bottlenecks in single lane traffic flow,” in *Sypo. on Theory of Traffic Flow*, 1959.

[28] M. Treiber, A. Hennecke, and D. Helbing, “Congested traffic states in empirical observations and microscopic simulations,” *Phys. Rev. E*, vol. 62, no. 2, p. 1805, 2000.

[29] Z. Li, W. Li, S. Xu, and Y. Qian, “Stability analysis of an extended intelligent driver model and its simulations under open boundary condition,” *Phys. A: Stat. Mech. its Appl.*, vol. 419, no. 0, pp. 526–536, 2015.

[30] U. Montanaro, M. Tufo, G. Fiengo, M. di Bernardo, A. Salvi, and S. Santini, “Extended cooperative adaptive cruise control,” in *2014 IEEE Intell. Veh. Symp.*, 2014, pp. 605–610.

[31] J. I. Ge and G. Orosz, “Dynamics of connected vehicle systems with delayed acceleration feedback,” *Transp. Res. Part C Emerg. Technol.*, vol. 46, no. 0, pp. 46–64, 2014.

[32] J. Lee, J. Bared, and B. (Brain) Park, “Mobility impact of cooperative adaptive cruise control (CACC) under mixed traffic conditions,” in *93rd Transp. Res. Board Annu. Meeting*, 2014.

[33] Z. Wang, G. Wu, and M. Barth, “Developing a distributed consensus-based cooperative adaptive cruise control (CACC) system,” in *96th Transp. Res. Board Annu. Meeting*, 2017.

[34] G. M. Arnaout and S. Bowling, “A progressive deployment strategy for cooperative adaptive cruise control to improve traffic dynamics,” *Int. J. Autom. Comput.*, vol. 11, no. 1, pp. 10–18, 2014.

[35] “Surface vehicle recommended practice, Taxonomy and Definitions for Terms Related to Driving Automation Systems for On-Road Motor Vehicles”. Society of Automotive Engineering International, 2016.

[36] National Highway Traffic Safety Administration. “Federal automated vehicles policy,” National Highway Traffic Safety Administration, 2016. [Online]. Available: https://www.transportation.gov/sites/dot.gov/files/docs/AV%20policy%20guidance%20PDF.pdf

[37] C. Diakaki, M. Papageorgiou, I. Papamichail, and I. Nikolos, “Overview and analysis of vehicle automation and communication systems from a motorway traffic management perspective*,” Transp. Res. Part A Policy Pract.*, vol. 75, pp. 147–165, 2015.

[38] S. E. Shladover, “The california PATH program of IVHS research and its approach to vehicle-highway automation,” in *Intell. Veh. `92 Symp.*, 1992, pp. 347–352.

[39] M. Omae, R. Fukuda, T. Ogitsu, and W.-P. Chiang, “Control procedures and exchanged information for cooperative adaptive cruise control of heavy-duty vehicles using broadcast inter-vehicle communication*,” Int. J. Intell. Transp. Syst. Res.,* vol. 12, no. 3, pp. 84–97, 2014.

[40] A. Alam, A. Gattami, K. H. Johansson, and C. J. Tomlin, “Guaranteeing safety for heavy duty vehicle platooning: safe set computations and experimental evaluations,” *Control Eng. Pract.*, vol. 24, no. 0, pp. 33–41, 2014.

[41] E. van Nunen, R. Kwakkernaat, J. Ploeg, and B. D. Netten, “Cooperative competition for future mobility,” *Intell. Transp. Syst. IEEE Trans.,* vol. 13, no. 3, pp. 1018–1025, 2012.

[42] M. R. I. Nieuwenhuijze, T. van Keulen, S. Oncu, B. Bonsen, and H. Nijmeijer, “Cooperative driving with a heavy-duty truck in mixed traffic: experimental results,” *Intell. Transp. Syst. IEEE Trans.*, vol. 13, no. 3, pp. 1026–1032, 2012.

[43] C. Bergenhem, E. Hedin, and D. Skarin, “Vehicle-to-vehicle communication for a platooning system,” *Procedia - Soc. Behav. Sci.,* vol. 48, no. 0, pp. 1222–1233, 2012.

[44] J. Ploeg, A. A. Serrarens, and G. Heijenk, “Connect & drive: design and evaluation of cooperative adaptive cruise control for congestion reduction,” *J. Mod. Transp.,* vol. 19, no. 3, pp. 207–213, 2011.

[45] WS Atkins plc. “Research on the impacts of connected and autonomous vehicles (CAVS) on traffic flow,” United Kingdom Department for Transport, 2016.

[46] M. Gouy, K. Wiedemann, A. Stevens, G. Brunett, and N. Reed, “Driving next to automated vehicle platoons: how do short time headways influence non-platoon drivers’ longitudinal control?,” *Transp. Res. Part F Traffic Psychol. Behav.*, vol. 27, no. PB, pp. 264–273, 2014.

[47] R. Wiedemann, “Modelling of RTI-elements on multi-lane roads,” in *Advanced Telematics Road Transport: Proc. Drive Conf.*, 1991.

[48] P. G. Gipps, “A behavioural car-following model for computer simulation,” *Transp. Res. Part B Methodol.*, vol. 15, no. 2, pp. 105–11, 1981.

[49] M. Behrisch, L. Bieker, J. Erdmann, and D. Krajzewicz, “Sumo – simulation of urban mobility,” *3rd Int. Conf. Adv. Syst. Simul.*, 2011.

[50] S. Krauß, “Microscopic modeling of traffic flow: investigation of collision free vehicle dynamics,” D L R - Forschungsberichte, no. 8, 1998.

[51] D. Krajzewicz, “Kombination von taktischen und strategischen einflüssen in einer mikroskopischen verkehrsflusssimulation.” VDI-Verlag, 2009.

[52] D. Krajzewicz, J. Erdmann, M. Behrisch, and Bieker Laura, “Recent development and applications of sumo - simulation of urban mobility,” *Int. J. Adv. Syst. Meas.*, vol. 5, no. 3–4, pp. 128–138, 2012.

[53] I. K. Nikolos, A. I. Delis, and M. Papageorgiou, “Macroscopic modelling and simulation of acc and cacc traffic,” in *2015 IEEE 18th Int. Conf. on Transp. Syst. (ITSC)*, 2015, pp. 2129–2134.

[54] D. Ngoduy, “Instability of cooperative adaptive cruise control traffic flow: a macroscopic approach,” *Commun. Nonlinear Sci. Numer. Simul.*, vol. 18, no. 10, pp. 2838–2851, 2013.

[55] S. Smith et al., “Benefits estimation framework for automated vehicle operations,” Federal Highway Administration, Rep. FHWA-JPO-16-229, 2018.

[56] H. Yeo, “Asymmetric microscopic driving behavior theory,” Ph.D. dissertation, University of California Transportation Center, UC Berkeley, 2008.

[57] H. Yeo, A. Skabardonis, J. Halkias, J. Colyar, and V. Alexiadis, “Oversaturated freeway flow algorithm for use in next generation simulation,” *Transp. Res. Rec. J. Transp. Res. Board*, vol. 2088, no. 1, pp. 68–79, 2009.

[58] G. F. Newell, “A simplified car-following theory: a lower order model,” *Transp. Res. Part B Methodol.*, vol. 36, no. 3, pp. 195–205, 2002.

[59] B. van Arem, A. P. de Vos, and M. J. Vanderschuren, “The microscopic traffic simulation model MIXIC 1.3,” TNO, Delft, Netherlands, Rep. INRO-VVG 1997-02b 1997.

[60] T. P. Alkim, H. Schuurman, and C. M. J. Tampere, “Effects of external cruise control and co-operative following on highways: an analysis with the MIXIC traffic simulation model,” in *IEEE Intell. Veh. Symp.*, 2000, pp. 474–479.

[61] M. Treiber and A. Kesting, “An open-source microscopic traffic simulator,” *IEEE Intell. Transp. Syst. Mag.*, vol. 2, no. 3, pp. 6–13, 2010.

[62] J. Lee, “VEDM-CAV 1.0,” 2014. [Online]. Available: https:// www.itsforge.net/index.php/community/explore-applications/ for-search-results#/31/75.

[63] PTV Group. (2017) *PTV Vissim introduction to the COM API*. Karlsruhe, Germany: PTV Group, 2017.

[64] PTV Group. (2017) PTV Vissim Drivermodel DLL interface documentation. Karlsruhe, Germany: PTV Group, 2017.

[65] Z. Zhong, L. Joyoung, and L. Zhao, “Evaluations of managed lane strategies for arterial deployment of cooperative adaptive cruise control,” in *96th Transp. Res. Board Annu. Meeting*, 2017.

[66] Z. Zhong, L. Joyoung, and L. Zhao, “Multiobjective optimization framework for cooperative adaptive cruise control vehicles in the automated vehicle platooning environment,” *Transp. Res. Rec. J. Transp. Res. Board*, vol. 2625, pp. 32–42, 2017.

[67] P. Songchitruksa, A. Bibeka, L. (Irene) Lin, and Y. Zhang, “Incorporating driver behaviors into connected and automated vehicle simulation,” Texas A&M Transportation Institute, College Station, TX, Rep. ATLAS-2016-13, 2016.

[68] H. Rakha, K. Ahn, and A. Trani, “Development of VT-micro model for estimating hot stabilized light duty vehicle and truck emissions,” *Transp. Res. Part D Transp. Environ.*, vol. 9, no. 1, pp. 49–74, 2004.

[69] J. Koupal, H. Michaels, M. Cumberworth, C. Bailey, and D. Brzezinski, “EPA’s plan for moves: a comprehensive mobile source emissions model,” in *12th CRC On-Road Veh. Emissions Workshop*, 2002, pp. 15–17.

[70] M. Barth et al., “The development of a comprehensive modal emissions model,” National Cooperative Highway Research Program, Washington, DC, 2000. [Online]. Available: http://onlinepubs.trb.org/ onlinepubs/nchrp/nchrp_w122.pdf Accessed on: Mar. 6, 2018

[71] D. Jiang, V. Taliwal, A. Meier, W. Holfelder, and R. Herrtwich, “Design of 5.9 GHz DSRC-based vehicular safety communication,” *IEEE Wireless Commun*., vol. 13, no. 5, 2006.

[72] S. Eichler, B. Ostermaier, C. Schroth, and T. Kosch, “Simulation of car-to-car messaging: analyzing the impact on road traffic,” in *13th IEEE Int. Symp. Modeling, Anal., and Simulation of Comput. and Telecommum. Syst.*, 2005, pp. 507–510.

[73] A. ur Rehman Khan, S. M. Bilal, and M. Othman, “A performance comparison of network simulators for wireless networks,” in *2012 IEEE Int. Conf. Control Syst. Computing Eng.*, no. November, pp. 34–38, 2012.

[74] M. Segata, S. Joerer, B. Bloessl, C. Sommer, F. Dressler, and R. Lo Cigno, “Plexe: a platooning extension for veins,” *IEEE Veh. Netw. Conf. VNC*, vol. 2015, January, pp. 53–60, 2015.

[75] C. Sommer, R. German, and F. Dressler, “Bidirectionally coupled network and road traffic simulation for improved IVC analysis,” *IEEE Trans. Mob. Comput.,* vol. 10, no. 1, pp. 3–15, 2011.

[76] A. Varga, “Omnet++,” in *Modeling and Tools for Netw. Simulation*, 2010.

[77] D. Jiang, Q. Chen, and L. Delgrossi, “Communication density: a channel load metric for vehicular communications research,” in *2007 IEEE Int. Conf. on Mobile Adhoc and Sensor Syst.*, 2007, pp. 1–8.

[78] M. Killat et al., “Enabling efficient and accurate large-scale simulations of VANETS for vehicular traffic management,” in *4th ACM Int. Workshop on Veh. ad hoc Netw.*, 2007, pp. 29–38.

[79] V. Taliwal, D. Jiang, H. Mangold, C. Chen, and R. Sengupta, “Empirical determination of channel characteristics for DSRC vehicle-to-vehicle communication,” in *1st ACM Int. Workshop on Veh. ad hoc Netw.*, 2004, p. 88.

[80] W. Weisstein, Eric, “Levenberg-marquardt method,” MathWorld--A Wolfram Web Resource, 2014. [Online] Available: http://mathworld.wolfram.com/Levenberg-MarquardtMethod.html. Accessed on: Mar. 6, 2018

[81] X. Weidong, *Wireless access in vehicular environments technology*. Verlag New York: Springer, 2009.

[82] Federal Highway Administration. “Managed lanes: a primer,” Federal Highway Administration, Washington DC, United States, 2008. [Online] Available: https://ops.fhwa.dot.gov/publications/managelanes_primer/managed_lanes_primer.pdf, Accessed on: Mar. 6, 2018

[83] “High-occupancy vehicle lane.” [Online]. Available: https://en.wikipedia.org/wiki/High-occupancy_vehicle_lane. Accessed on: Mar. 6, 2018

[84] K. F. Turnbull, “Impact of exempt vehicles on managed lanes,” Texas A&M Transportation Institute, College Station, TX, USA, Rep. FHWA-HOP-14-006, 2014. [Online] Available: https://ops.fhwa.dot.gov/publications/fhwahop14006/fhwahop14006.pdf. Accessed on: Mar. 6, 2018

[85] *Clean air vehicle decal. (n.d.)* California Department of Motor Vehicles [Online]. Available: https://www.dmv.ca.gov/portal/dmv/?1dmy&urile=wcm:path:/dmv_content_en/dmv/vr/cav_decal. Assessed on: Mar. 6, 2018

[86] D. Brownstone, A. Ghosh, T. F. Golob, C. Kazimi, and D. Van Amelsfort, “Drivers’ willingness-to-pay to reduce travel time: evidence from the san diego I-15 congestion pricing project,” *Transp. Res. Part A Policy Pract.*, vol. 37, no. 4, pp. 373–387, 2003.

[87] M. W. Burris and B. R. Stockton, “HOT lanes in Houston-six years of experience,” *J. Public Transp.,* vol. 7, no. 3, p. 1, 2004.

[88] J. Dahlgren, “High-occupancy/toll lanes: where should they be implemented?,” *Transp. Res. Part A Policy Pract.*, vol. 36, no. 3, pp. 239–255, 2002.

[89] T. Collier and G. Coodin, “Managed lanes: a cross-cutting study,” Texas A&M Transportation Institute, College Station, TX, USA, 2004. [Online]. Available: https://ops.fhwa.dot.gov/freewaymgmt/publications/managed_lanes/crosscuttingstudy/final3_05.pdf. Accessed Mar. 6, 2018

[90] R. W. Poole and C. K. Orski. (1999, Apr.) “Building a case for hot lanes: a new approach to reducing urban highway congestion,” [Online]. Available: https://reason.org/policy_study/building-a-case-for-hot-lanes/. Accessed on: Mar. 6, 2018

[91] S. E. Shladover, C. Nowakowski, X.-Y. Lu, and R. Ferlis, “Cooperative adaptive cruise control,” *Transp. Res. Rec. J. Transp. Res. Board*, vol. 2489, pp. 145–152, 2015.

[92] A. Al Alam, A. Gattami, K. H. Johansson, and C. J. Tomlin, “When is it fuel efficient for heavy duty vehicles to catch up with a platoon,” in *Proc. IFAC world congress*, 2013.

[93] A. Dávila, (2010, Sept.) “*SARTRE report on infrastructure and environment*,” [Online]. Available: https://www.princeton.edu/~alaink/Orf467F10/PRT@LHR10_Conf/Arturo_Davila_prez_SafeTrains.pdf. Accessed Mar. 6, 2018.

[94] J. Larson, C. Kammer, K. Liang, and K. H. Johansson, “Coordinated route optimization for heavy duty vehicle platoons,” *IEEE Annu. Conf. Intell. Transp. Syst.,* 2013.

[95] J. Larson, K. Y. Liang, and K. H. Johansson, “A distributed framework for coordinated heavy-duty vehicle platooning,” *IEEE Trans. Intell. Transp. Syst.*, 2015.

[96] T. Litman, “Autonmous vehicle implementation predictions,” in *94th Transp. Res. Board Annu. Meeting*. Washington DC, 2014.

[97] T. Litman. “Evaluating transportation equity: guidance for incorporating distributional impacts in transportation planning,” Victoria Transportation Policy Institute, Victoria, Canada. vol. 8, no. 2, pp. 50–65, 2005.

[98] Z. Wu, G. Flintsch, A. Ferreira, and L. Picado-Santos, “Framework for multiobjective optimization of physical highway assets investments,” *J. Transp. Eng.*, vol. 138, no. 12, pp. 1411–1421, 2012.

[99] W. Wu, A. Gan, F. Cevallos, and M. Hadi, “Multiobjective optimization model for prioritizing transit stops for ADA improvements,” *J. Transp. Eng.*, vol. 137, no. 8, pp. 580–588, 2011.

[100] Q. Meng and H. L. Khoo, “A Pareto-optimization approach for a fair ramp metering,” *Transp. Res. Part C Emerg. Technol.*, vol. 18, no. 4, pp. 489–506, 2010.

[101] H. Abdelgawad, B. Abdulhai, and M. Wahba, “Multiobjective optimization for multimodal evacuation,” *Transp. Res. Rec. J. Transp. Res. Board*, vol. 2196, no. 1, pp. 21–33, 2010.

[102] K. Deb, *Multi-objective optimization using evolutionary algorithms*. Delhi, India: Sharda Offset Press, 2010.

[103] K. Deb, A. Pratap, S. Agarwal, and T. Meyarivan, “A fast and elitist multiobjective genetic algorithm: nsga-ii,” *IEEE Trans. Evol. Comput.,* vol. 6, no. 2, pp. 182–197, 2002.

[104] A. Kesting, M. Treiber, and D. Helbing, “Enhanced intelligent driver model to access the impact of driving strategies on traffic capacity,” *Philos. Trans. R. Soc. A Math. Physical Eng. Sci.*, vol. 368, no. 1928, pp. 4585–4605, 2010.

[105] MatchWorks, “Optimization toolbox,” 2018. [Online]. Available: https://www.mathworks.com/help/optim/index.html. Accessed on: Mar. 6, 2018

[106] PTV *Vissim 10 user manual*. Karlsruhe, Germany: PTV AG, 2017.

[107] R. M. Michaels, “Perceptual factors in car following,” in *2nd Int. Symp. Theory Road Traffic Flow*, 1963.

[108] R. Herman, E. W. Montroll, R. B. Potts, and R. W. Rothery, “Traffic dynamics: analysis of stability in car following,” *Oper. Res.*, vol. 7, no. 1, pp. 86–106, 1959.

[109] W. Leutzbach, *Introduction to the theory of traffic flow*, vol. 47. Verlag Berlin Heidelberg : Springer, 1988.

[110] PTV Vissim 5.30 user manual. Karlsruhe, Germany: PTV AG, 2011.

[111] “Joblib: runnning python functions as pipeline jobs.” [Online]. Available: https://pythonhosted.org/joblib/. Accessed on: Mar. 6, 2018

[112] M. Killat and H. Hartenstein, “An empirical model for probability of packet reception in vehicular ad hoc networks,” *EURASIP J. Wirel. Commun. Netw.* vol. 2009, pp. 1–12, 2009.

[113] M. K. Simon and M.-S. Alouini, *Digital communication over fading channels*, vol. 95. New York: John Wiley & Sons, 2000.

[114] M.C. Taylor, D.A. Lynam, and A. Baruya, “The effects of drivers’ speed on the frequency of road accidents,” TRL Report, No. 421.Transport Research Laboratory TRL, Crowthorne, Berkshire, UK. [Online] Available: http://www.20splenty.org/UsefulReports/TRLREports/trl421SpeedAccidents.pdf. Accessed Mar. 6, 2018

[115] N. J. Garber and R. Gadiraju, “Factors affecting speed variance and its influence on accidents,” *Transp. Res. Rec. vol. 1213,* pp. 64-71, 1990